Monitoring of Incremental Rotary Forming

Engineering Doctorate Thesis

Andrew Appleby

Advanced Forming Research Centre

Department of Design, Manufacture and Engineering Management

School of Engineering

University of Strathclyde

Glasgow

October 30, 2019

This thesis is the result of the author's original research. It has been composed by the author and has not been previously submitted for examination which has led to the award of a degree.

The copyright of this thesis belongs to the author under the terms of the United Kingdom Copyright Acts as qualified by University of Strathclyde Regulation 3.50. Due acknowledgement must always be made of the use of any material contained in, or derived from, this thesis.

Signed: Andrew Appleby October 30, 2019

Abstract

As manufacturing processes move toward full automation, reliable instrumentation is vital for improved process control. This work examines new applications of non-disruptive monitoring techniques for incremental rotary forming (IRF) processes.

IRF processes such as flow forming (FF) and spinning make rotationally symmetric components. These cold, incremental processes produce parts to near net shape with improved mechanical properties and high material utilisation. The design and operation of these processes is limited by an incomplete understanding of forming mechanics and process design.

Monitoring is used in many industries to improve process understanding, control and operation. The relevance of existing monitoring technologies to IRF was assessed and three were selected. Acoustic and vibration monitoring were both investigated for detecting fracture during FF. An ultrasonic (US) monitoring system was developed to scan the contact area between the tool and the material during FF and spinning.

The results showed that acoustic monitoring can detect major fracture events in FF. Vibration monitoring did not show useful results. Testing of the US system showed that it is possible to record changes in the tool-workpiece contact area, detect internal fractures in the part, and measure the thickness of parts spun in free air. Fracture, contact area and thickness have never before been measured in-process.

This work demonstrates for the first time the ability to monitor IRF contact properties, thickness and fracture in real time. Monitoring of these could be used in industry to refine the design of tooling and processes, validate modelling, and avoid unexpected failures. In the medium term, improved monitoring will allow improved process control and automation with reduced risk.

Acknowledgements

This document has just one name on the title page, but it is a collaborative effort, and I would have got nowhere without the support of many people.

Thanks go to Alastair and Bill who administered an invaluable mixture of critique, advice and encouragement. The members of the Forging and Incremental Technologies team took time out of their schedules to help me when they really had more important things to do - thanks Jill, Gerry, May, Kadir, Kyle, Bhaskaran, Gordon and Aurik for answering my sensible questions, and pointing out why the silly questions were silly. The workshop technicians, Stevie, Thomas and Helge, were particularly generous with their time and advice. Thanks also to Thomas McMaster, who gave crucial help with the Abaqus modelling, and Dad for his astute commentary on a late draft.

And - last but most important - Corinne, Mum, Dad, Duncan, Gran and friends too many to name. You kept me from going daft, even when you didn't know you were doing it. Thank you.

Contents

List of Figures

List of Tables

Terms and abbreviations

AE acoustic emission 38

AFRC Advanced Forming Research Centre 5

AU arbitrary units 109

CNC computer numerical controlled 7

DAQ data acquisition system 60

DOE design of experiments xvi

DZ deformation zone x

FE finite element 5

FF flow forming x

IR-0508-R-RU transducer from Olympus Scientific Solutions 88

IRF incremental rotary forming x

SF shear forming 9

SNR signal-to-noise ratio 39

SSF shear-spin-flow forming xiv

TCM tool condition monitoring 35

US ultrasonic xi

UT ultrasonic transducer xii

STR600 WF Maschinenbau STR600 shear, spin and flow forming machine x

Chapter 1

Introduction

1.1 Overview

This work is an exploration of the opportunities to use monitoring to improve incremental rotary forming (IRF). Chapter 2 contains an examination of the IRF literature, carried out to establish the challenges in the area. Chapter 3 contains a review of work on monitoring, conducted to assess its applicability to IRF. Several approaches for monitoring IRF were considered. Developmental work on these different systems was carried out in an exploratory fashion. Vibration and then acoustic monitoring approaches were explored in Chapter 5. Ultimately, the evidence pointed to the value of ultrasonic (US) monitoring, so a US system was developed (Chapter 6). Testing showed the potential benefits and limitations of the various monitoring methods (Chapter 7). The results are then discussed in Chapter8.

1.2 Introduction and problem statement

IRF is a family of forming technologies for making rotationally symmetric parts. They use small, cyclical deformations which cause large flows of material in aggregate, at low temperatures. Figure 1.1 shows an example process, where 3 rollers shape a stepped cylindrical part. These processes are useful because they can create complex, near-net shape components with little material wastage while improving mechanical properties.

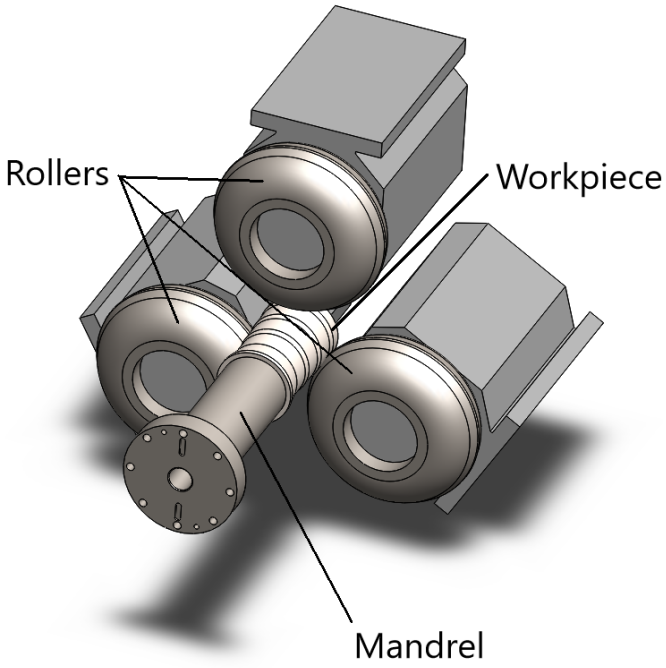

Figure 1.1: Flow forming

IRF is used in many industries, but its mechanics are not yet fully understood. Chapter 2 explains the limitations on the understanding of IRF mechanics. Modelling and process design are limited. While they can be accurate for specific combinations of geometry and material, they are generally not effective at predicting where there is a major change in the process. Indeed, there are no generalised guidelines for process selection (Podder et al., 2018). This means that, if a new process differs significantly from previous processes, significant 'run-in' may be required. That is, a number of parts are needed to fine-tune the process parameters before production starts in a trial-and-error approach.

Problem statement: *The mechanics of IRF are poorly understood. Research based around modelling and simplified experimentation cannot answer fundamental questions about the process behaviour during forming.*

Other processes, e.g. machining, are much better understood. In such cases, the mechanics of the process are so well characterised that the machining of any material or geometry can be planned and predicted. The current process modelling and process

understanding in the IRF literature cannot yet generate this degree of insight. Given the limitations of these approaches, new techniques are needed that help our understanding of incremental deformation in rotary processes. One possible approach is to utilise process monitoring. If the mechanics of the process can be instrumented, then the deformation mechanics and behaviour can be linked to process outcomes, allowing a general understanding of behaviour to develop.

Chapter 3 examines how other forming and machining processes have been instrumented. Instrumentation and monitoring have been carried out effectively on a range of relevant processes using a range of technologies. The potential to gather useful information is clear - as is the power to improve control in the long term. These examples are mined for insight to benefit monitoring of IRF.

1.3 Aims and approach

The findings from Chapters 2 and 3 aim to establish the existence of a problem - poor process understanding - and a potential solution - process monitoring. The work of the remainder of the thesis is to find and test implementations of monitoring for IRF. The aims can therefore be laid out as the following:

- To broadly explore IRF and process monitoring
- To choose the most appropriate approaches for monitoring IRF
- To examine what capabilities these have for monitoring IRF

Taking each in turn, the aims each represent a critical strand of the research. A wide approach is necessary to find relevant technologies and applications which may be relevant to IRF. Selecting the most appropriate of these is a logical narrowing which will allow a deeper focus on the areas with the greatest potential. Once selected, the monitoring technologies were tested. This testing should show in a reliable manner which features of the process can be detected and monitored. Figure 1.2 shows the how the work was carried out.

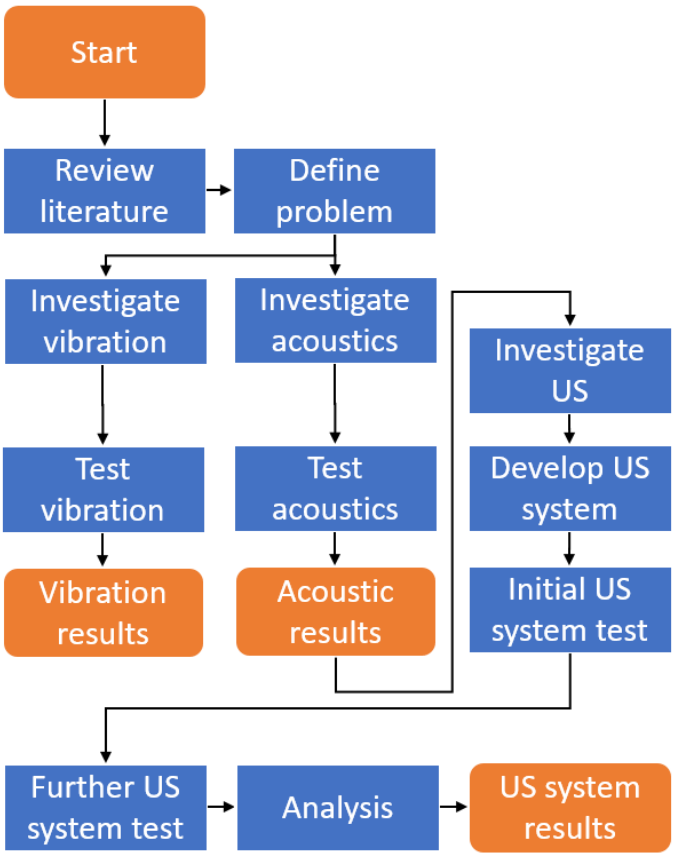

Figure 1.2: Flowchart of the project execution

To fulfill these aims, a systematic approach was taken. Research questions were set (see Section 1.5) and then developed through the process. Literature addressing both IRF and monitoring was examined for lessons from previous approaches. The literature and context is examined in two separate Chapters (2 and 3) because of the minimal overlap existing between the fields. The results from the literature are incorporated into the research questions in Sections 2.5 and 3.6. These developing questions plot the course of the research.

The essential objective of the methodology was to observe the function of the process without interference - (see constraints in Chapter 6). The methodology for testing the monitoring options is set out in Section 4. This methodology was kept under review during the work and further details of the testing were developed as appropriate.

1.4 Scope

The general area of research encompasses the whole fields of IRF and process monitoring. The goal is to review these separate disciplines and explore their potential cross-over. Exploration of this new territory could easily be hampered by getting bogged down in details. The aim is therefore to achieve broad, inter-disciplinary levels of expertise, and avoid getting deep into specialist sub-areas of the topics. This means that it is important to define the scope of the project. Table 1.1 shows this.

Table 1.1: Scope for the project

In scope	**Out of scope**
Assessment of the knowledge gaps in IRF	Design/fabrication of bespoke sensors
Development of new monitoring approaches	Finite element modelling of IRF
Prototyping and proof-of-concept	In-depth work on the physics of IRF
Assessment of potential for these approaches	Industry-ready systems
Insight into IRF process	Fabrication of scale testing rig

There are constraints that drive these scope choices. The research was carried out at the Advanced Forming Research Centre (AFRC) - a part of the University of Strathclyde. The AFRC has a large workshop facility, including several IRF machines, of which one was available for use on this project. The available machine - the STR600 - defined the scope in terms of which processes and geometries were possible in its operational envelope. The STR600 is a typical example of IRF machines used in industry. The specifications of the STR600 are discussed in Section 2.2. Some lines of enquiry which would clearly be useful and interesting are simply not possible due to the constrained nature of a single-person project. These include finite element (FE) modelling of the process, production of bespoke transducers, rigs to test the monitoring systems in a simplified, scaled down environment and more advanced signal processing. Recommendations for how these areas could be developed are given in Chapter 8.

1.5 Research questions

The research questions in this project were continually evolved through the process. The initial research question is:

What insights can monitoring provide into an industrial IRF process?

As the later chapters examine the nature of IRF, the applications of process monitoring and the details of specific monitoring options, more questions emerge. The questions are:

- **How can IRF processes be monitored?**
- **What monitoring technologies would be appropriate?**
- **What lessons can be learned from the use of monitoring in other industries?**
- **What process changes in IRF can be detected with vibration and acoustic monitoring?**
- **What insight can US monitoring provide into an industrial IRF process? Specifically:**
  - What insight into forming forces in IRF can US monitoring provide?
  - What insight into contact area in IRF can US monitoring provide?
  - What insight into fracture in IRF can US monitoring provide?
  - What insight into part thickness in IRF can US monitoring provide?

These arise though the research process. Sections 2.5, 3.6, 5.4.3 and 7.6 show this development. The research questions are answered in Section 8.1.

Chapter 2

Incremental rotary forming

2.1 Introduction

This chapter explains the origins and types of incremental rotary forming. It addresses their advantages and disadvantages, and the use of the processes.

The following pages will describe IRF processes, especially FF, discuss their mechanics and associated challenges. They will assess the opportunities for development and examine how the control, feedback and instrumentation could be improved.

2.2 The STR-600 machine

The AFRC has a shear, spin and flow forming machine which is used for industrial research - the STR600. This will be used for any experimental work and is described here to give an overview of an industrial IRF machine. Figure 2.1 shows an overview of the machine, with three rollers fitted for FF. The rollers and mandrel are made from AISI D2 tool steel (see Appendix B.7).

The STR600 is computer numerical controlled (CNC) for position. Figure 2.2 shows how the three rollers are configured. They are referred to as the X1, X2 and X3 roller, and can be controlled in the X and Z dimensions. The spindle is driven and the rollers are free rolling. Forming is carried out by plotting a forming path with G codes

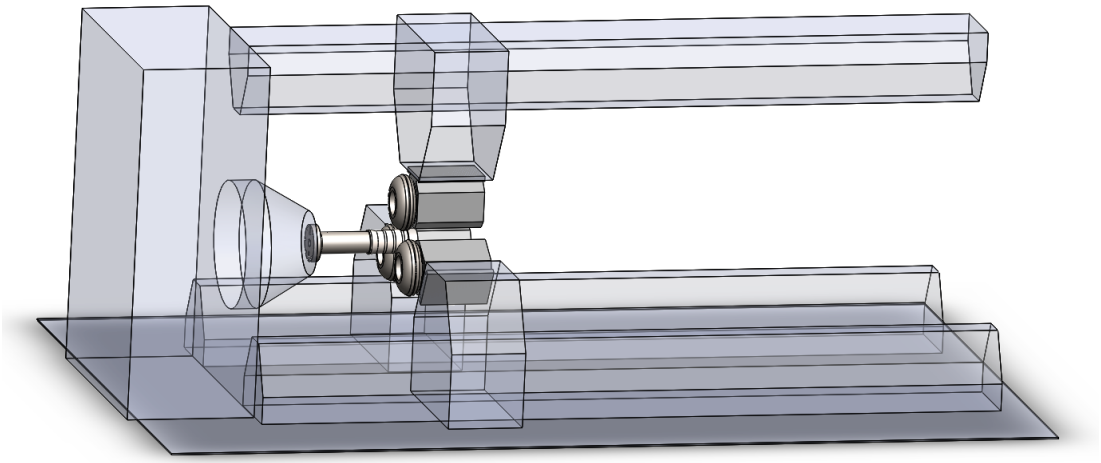

Figure 2.1: The STR600 machine set up for FF (author's figure).

controlling the machine.

The machine is feedback-controlled with regards to position, but not force controlled (except for a cut-out if the maximum rated force is exceeded). The key variables that can be controlled are the spindle speed, roller feed rate and tool path. Usually, the tool path is written for the leading (X1) roller and the other rollers are slaved to it with gaps in the X and Z dimensions, such that the rollers progressively engage the material.

Typically, the X gaps are set such that each of the rollers make a third of the pass depth. For example, in a reduction from 12 to 6 mm (6 mm total reduction, or 50%) the X1 roller would pass at 2 mm depth (below the starting surface), the X2 roller at 4 mm and the X3 roller at 6 mm. The Z gaps are set to distribute the load between the rollers, with X1 (the X1 roller) passing over the material first, then X2, then X3. The trailing gaps in the Z dimension are dependent on the roller geometry.

The acstr can be considered a good general example of a FF machine, reperesentative of industrial use. This is evidenced by the significan financial investment by the AFRC's industrial partners in commercial process research on the machine.

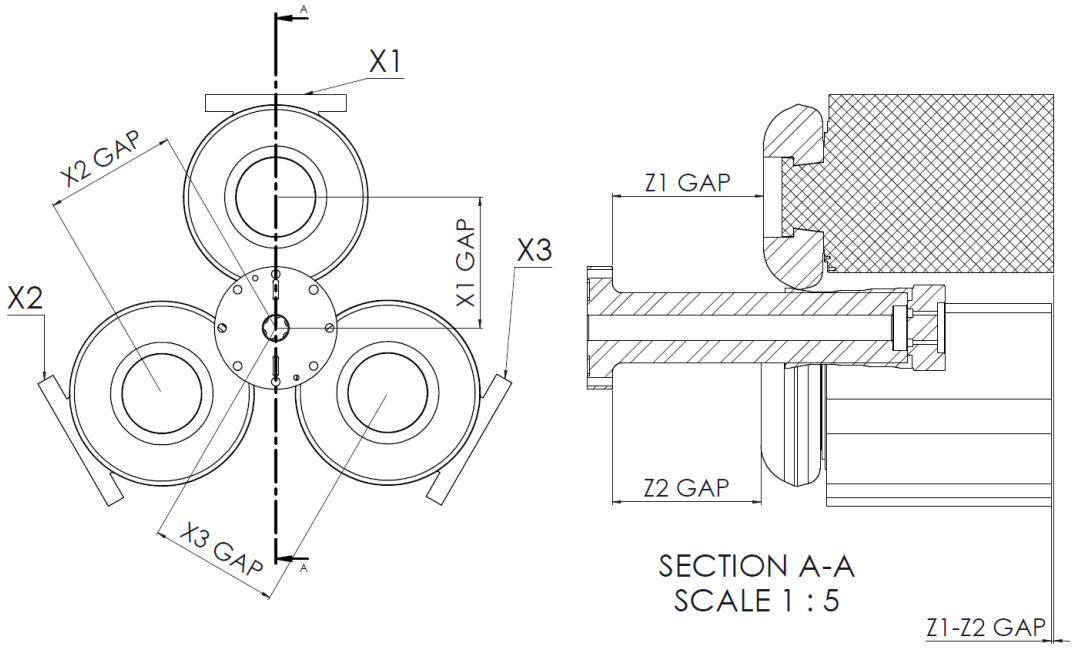

Figure 2.2: The STR600 roller setup for FF.

2.3 IRF processes

The term incremental rotary forming (IRF) is used here to refer to a set of technologies that share some similar mechanics. These include: flow forming (FF), shear forming (SF), spinning, ring rolling, radial forging and rotary forging. These processes share many common elements in their mechanics, but principally the method of deformation. The workpiece is rotated and deformed a small (incremental) amount during each tool pass. This allows the shaping of rotationally symmetrical parts with large deformations. The incremental nature of the process allows much greater deformation than in a process which uses fewer larger deformations, such as deep drawing or cupping.

For the purposes of this document, the term IRF will refer to three distinct but related processes - FF, SF and spinning.

2.3.1 Spinning

Spinning is the oldest form of IRF. It was first practised by hand on a lathe and hand spinning is still carried out. Spinning at its simplest fabricates rotationally symmetric

components from flat disc preforms by applying force with a blunt handheld tool. The tool gradually smooths the metal over the spinning mandrel with minimal reduction from the initial thickness (T_0) to the final thickness (T_1). Figure 2.3 shows this process.

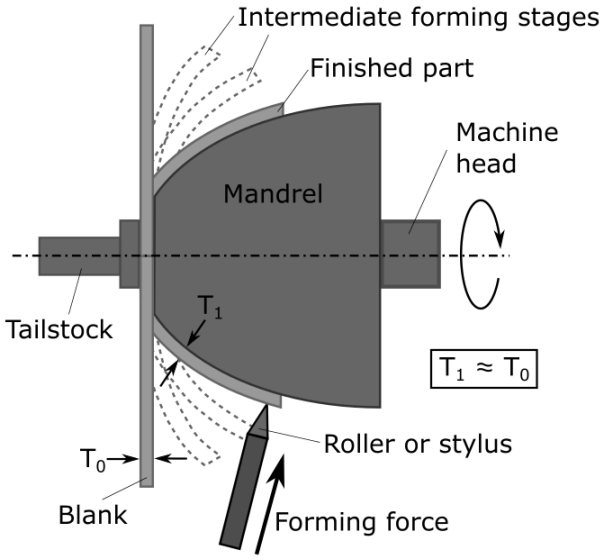

Figure 2.3: Spinning schematic. The force can be applied by hand for the simplest, smallest applications, or by computer numerical controlled hydraulics or electrical actuation for modern, large-scale spinning.

These early techniques required skilled operators and were largely used to produce cookware and similar low-precision items (Lloyd, 1986). These features along with low load capacity made spinning effectively a handicraft.

Later developments introduced machine-powered spindles and tools which increased load capacity. This was driven by interest in manufacturing aerospace components such as nose cones and heat shields. These parts required thicker walls and more deformation which led to the use of hand-controlled hydraulic spinning lathes (Wong et al., 2003).

Along with the wider machining and metal-forming industry, spinning processes moved steadily towards automation. Modern spinning is computer numerical control operated, which reduces the former problems of tool clash and poor process consistency (Quigley and Monaghan, 2000). However the process is controlled in an open feedback loop. This means that much more modernisation is possible - consider state of the art machining or forging, where temperature, force and position

measurement are in use to assess the performance of the process. This sort of feedback could provide deep and valuable insight into IRF. At present, tool force and position are measured, but due to the complex effects of plastic flow and springback these are hard to interpret with reference to the part and process properties.

The development towards heavier, faster processes that came alongside improved control led to a diversification in spinning into the category of techniques now termed IRF. These new techniques used thicker materials and much increased deformation and began to form separate specialities with their own machines and approaches. Modern spinning is classified (somewhat simplistically) under DIN (2003b) as a process where triaxial compressive and tensile forces cause plastic deformations.

Spinning is normally categorised as a sheet metal process with minimal thickness reduction to the part (Wong et al., 2003). It is generally carried out against a form or mandrel by a single roller.

Spinning has the advantage of making huge geometric changes in a part very quickly for low cost. Forming a tube, dome or cone shape by spinning requires relatively little outlay. A single toolset can be used for different processes with adjusted toolpaths, and adjustments can be made while refining the spinning process. Disc blanks are cost-effective to produce and the machining costs can be vastly reduced when compared to machining hollow shapes from solid bar or cast preforms.

2.3.2 Shear forming

Shear forming (SF) is a method of bulk incremental rotary forming.[1] SF developed out of spinning and has some similarities, but it is a distinct process - better described as a bulk metal forming than sheet metal forming process. It is normally carried out by a single roller and forms flat plates into conical sections with significant thickness reduction. These are typically used for oil and gas or aerospace applications because of the requirements for good material properties and the use of expensive materials.

[1]The project scope is to work with the machine tools available for intervention/modification. The shear tooling is not because of IP/ownership issues. For this reason SF will not be examined for monitoring but is included here for completeness.

As with other IRF processes, SF offers good material utilisation, improved material properties and reduced machining for many parts.

Figure 2.4 shows the process schematically. Starting from a disc blank, the thickness reduction in SF is generally given by

$$T_1 = T_0 sin(\alpha) \tag{2.1}$$

where T_0 and T_1 are the initial and final thicknesses, and α is the angle of the formed cone.

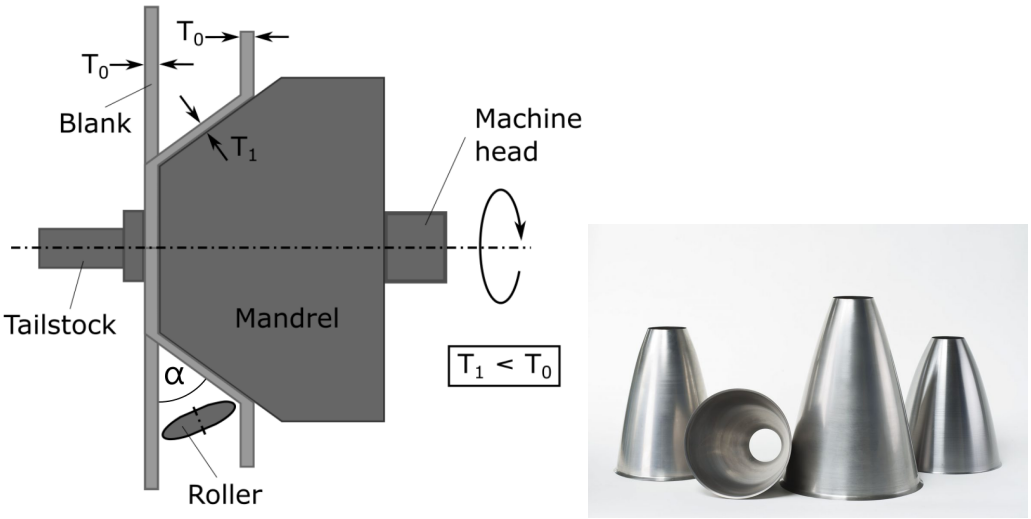

Figure 2.4: Shear forming machine schematic (left) and example parts (right).

2.3.3 Flow forming

Flow forming (FF) is another form of IRF that, like SF, is more properly considered a bulk process. FF starts with a cup or cylinder preform and deforms it longitudinally. This is accomplished by two, three or four rollers which deform the material in the radial direction, causing longitudinal (axial) extension. Major reductions in thickness are possible - typically 20 to 80%. This is accompanied by significant extension in the part length.

The FF process has the ability for the rollers to transition inward and outward (radially) during the process. This stands in contrast to spun parts with a constant

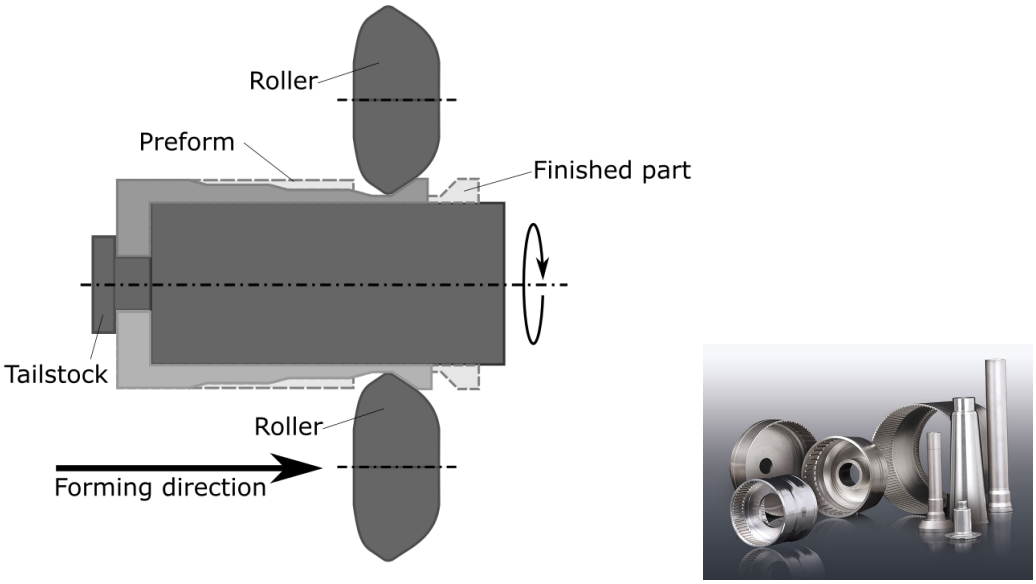

Figure 2.5: Flow forming schematic (left) and example parts (right).

wall thickness or SF parts with a constant thickness change per angle. This means that FF can be used to make complex stepped parts like driveshafts and landing gear with significant savings in machining costs. In addition, simpler parts like pressure vessels or tube components can be formed from small preforms due to the extension in length during the process. FF is classified under DIN (2003a) as a purely compressive process of plastic deformations.

FF has significant potential because of its capacity to improve material properties. Bedekar et al. (2014) found "dramatic" increases in strength and hardness. But Birosca et al. (2015) found that the microstructure was complex and hard to categorise. It can be seen that these increases are appealing to the supply chain. However, where the process is poorly optimised or understood it is hard to control the microstructure changes. This stands in the way of uptake of IRF processes.

Flow formed parts

FF parts generally start as a tubular preform and end as a stepped cylinder. Figure 2.6 shows an example preform and part. This example part is a standard test part with a reduction of 25, 50 and 75 %. These areas of constant thickness are referred to as

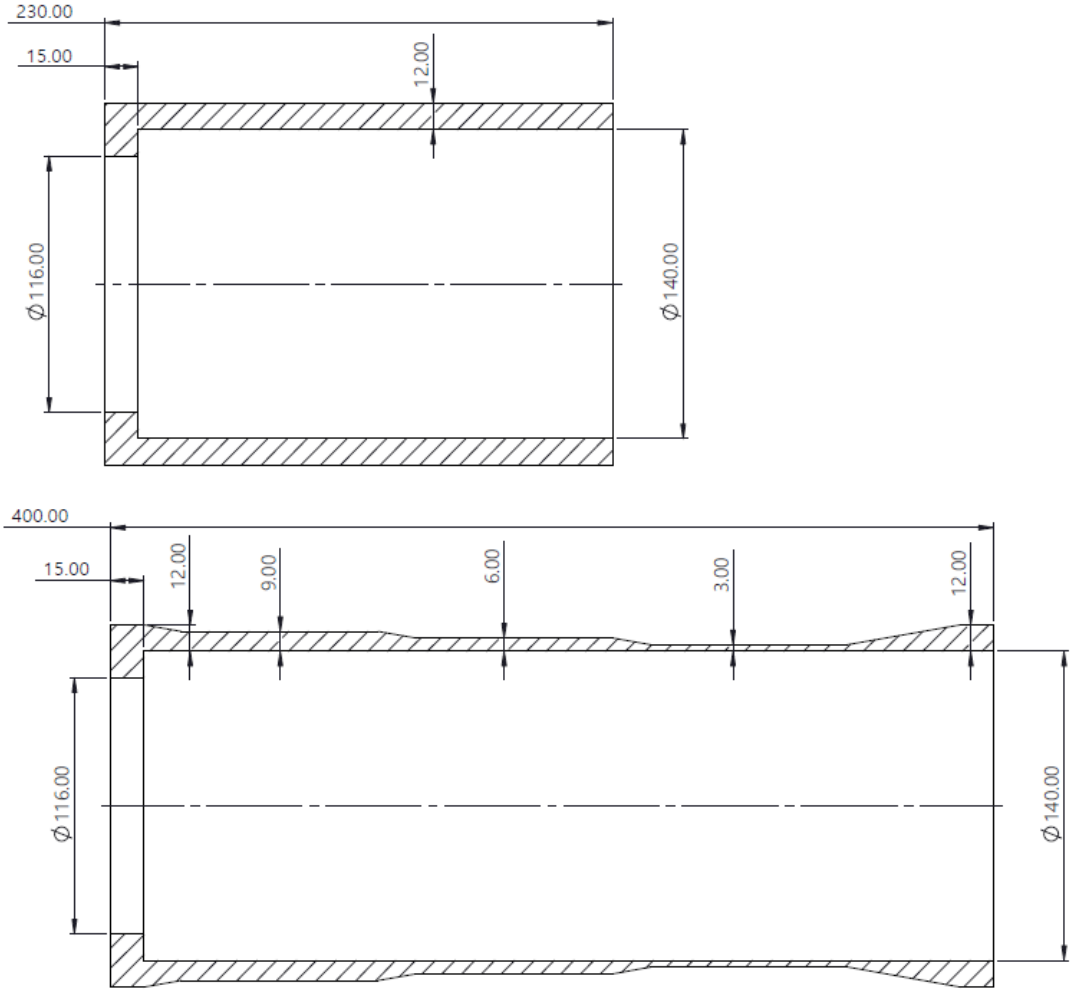

Figure 2.6: A FF preform and part

"lands" and the angled areas between them are termed transitions. Note the significant elongation in the formed part. Both parts have the same volume as there is no material wastage in the process.

2.3.4 Shear-spin-flow forming

Compound processes have also seen interest and development. Pollitt (1995) describes the interest in forming more complex parts, especially alloy wheels. This can be accomplished with multi-pass processes that combine the benefits of the component processes.

AFRC uses a shear-spin-flow forming (SSF) process that starts with a flat disc and produces a conical-tubular component. Figure 2.7 shows how the shear, spin and flow forming produces a complex part shape from a simple preform.

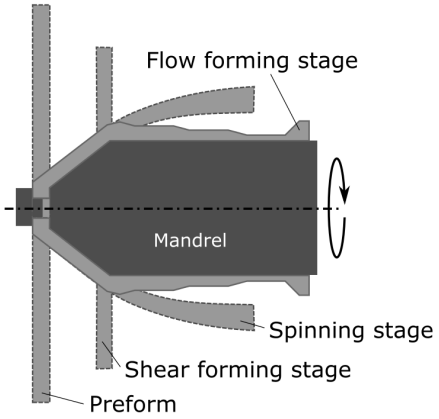

Figure 2.7: Shear-spin-flow forming schematic

One of the challenges of multi-stage processes like this is the difficulty of knowing what the part will look like during and after each stage. For example, Makhdum et al. (2016) found that a multi-stage process suffered circumferential and axial fracture, which required iterative process development to rectify. Without good predictive modelling or monitoring, the process design must be an operation of trial and error.

2.3.5 Conclusions on IRF processes

These processes have significant potential. They can reliably produce high quality parts. They can make complex shapes from simple preforms. They can give material enhanced properties and good surface finish.

But they also have challenges. Modelling and process design are lacking. Solutions are needed to improve the useability of these processes. This is addressed below.

2.4 Challenges of IRF

IRF processes work by incremental cold-working. This section will summarise the current understanding of the physical mechanics of that process. It will explain how

and where that understanding is limited and how that impacts on the use of IRF. In addition, the efforts to understand the impact of process parameters and the causes of defects will be reviewed.

2.4.1 Deformation mechanics

There is a major challenge facing any expansion in the use of IRF. The fundamental mechanics of deformation and tool-part interface are poorly understood. Research has gone some way to rectifying this gap but more effort is needed to gain a fuller understanding.

Fundamentally, all IRF processes use the same approach. By deforming the workpiece a small amount on a cyclical basis, it is possible to create large amounts of deformation. However the specific mechanics of how the material is deformed are inherently complex. The complex deformation is considered by Xu et al. (2001), who divide the zone of plastic deformation, or deformation zone (DZ) into five areas under three regimes (Figure 2.8).

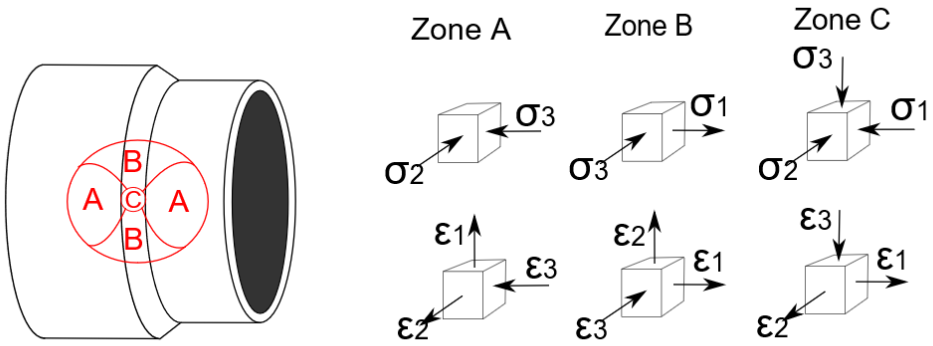

Figure 2.8: Stress-strain states surrounding the DZ, adapted from Xu et al. (2001).

It is notable that, seventeen years on, little progress has been made on a general understanding of the stress state. Bylya et al. (2018) describe an interplay of non-uniaxial and non-uniform stress state with large changes in strain and stress across the forming area. This, combined with the continuous movement of the DZ make it

a difficult process to understand. A hard process to understand is a hard process to operate and optimise.

Despite being complex, the benefits of this forming approach are significant. Molladavoudi and Djavanroodi (2011) describes a significant increase in strength and hardness under higher levels of deformation. This is supported by Wang et al. (2017) who used a multiple-pass process to increase grain refinement. Haghshenas and Klassen (2015) also found hardening and strength increase but noted that the strength increases are larger in the axial than the radial direction. This agrees with their examination of the grain flow.

IRF processes offer significant benefits for forming large deformations. They can also make material savings in some geometries. Unfortunately, the forming mechanics are complex and not fully understood. This means that the processes are hard to understand and hard to use. These difficulties limit the possibilities to reap the benefits of IRF.

2.4.2 The deformation zone

As mentioned above, the deformation zone is where the roller meets the part. In this area, the material is deformed (see Figure 2.8). Figure 2.9 shows a simple FF process with one roller (shown as transparent). The shape of the DZ will vary under different combinations of feed, speed and toolpath. It may grow larger or smaller and move around on the surface of the roller. Material may buildup in front of the roller, making it unevenly distributed.

The DZ is important because it is where the incremental forming is carried out. The size and shape of the DZ affect the process in important ways. Roy et al. (2010) states: "To properly understand the distribution of this intense local plastic deformation it is essential to be able to calculate the roller/workpiece contact area ... the roller/workpiece contact area is critical to coupling other experimental findings."

In many IRF processes there are multiple DZs (one for each roller) which each may be different in size, shape and tribological properties. The nature of these in real industrial forming is hard to gauge because they are constantly moving and covered in

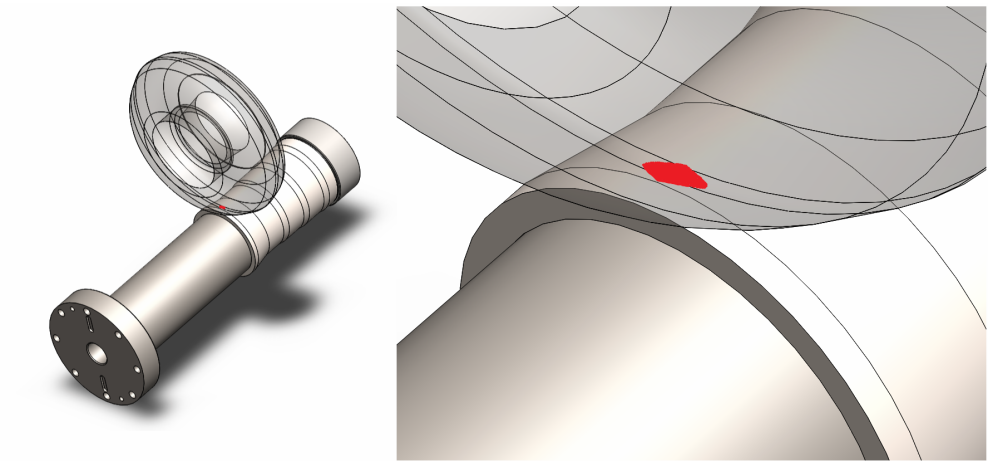

Figure 2.9: Simplified visualisation of the DZ.

coolant. It is not possible to turn off the coolant because of the problems of overheating. I.e., it is challenging to examine the DZ without altering the process substantially.

2.4.3 IRF development work

Throughout the history of IRF as a technology, researchers have attempted to improve their understanding of the process setup and parameters. Research has looked at several areas, particularly the influence of cut depth, feed rate, speed, roller angles, thickness reduction and material properties. This is a natural part of a broad movement towards a fully realised understanding of IRF, which will allow improved process design and operation. There are issues with work in the field, however. Each trial looks at a specific process and specific parameters, and draws a relatively narrow conclusion. Thus it has been difficult to develop a more general understanding of the principles that govern this kind of forming.

Parameter research

A number of studies have looked at forming forces in relation to process parameters or outputs. For example, Hayama and Kudo (1979), and Shinde et al. (2016) looked at diametral growth in FF and its relation to forming forces in flow forming. Diametral growth is the tendency for the internal diameter of the part to exceed the mandrel

diameter, leading to ovality in the part. The literature suggests that this mainly affects softer materials - indeed Singhal et al. (1990) considers it negligible in hard materials. But work at AFRC has shown this effect in some high-hardness aerospace alloys (Miscandlon et al., 2018). This may be considered an example of the limited depth of understanding that exists around IRF forming mechanics.

Out-of-roundness is also studied, with Razani et al. (2011) finding it to decrease with increased depth of cut and increased feed rate and roller angle. These parameters also influenced wrinkling and fracture - the authors suggest a minimum feed rate and maximum depth of cut in AISI 321 stainless steel. However it is unclear how broadly applicable these results are.

Jolly and Bedi (2010) modelled the effect of changing thicknesses on forces. Forces increase with reduction, as expected. This result is found widely (Hayama and Kudo, 1979; Singhal et al., 1990).

D'Annibale et al. (2017) used a thermo-mechanical finite element model analysis to examine the heating effects of varying feed rate. Physical validation was done with a simplified, single-roller process on an adapted lathe.

Bhatt and Raval (2016, 2018b) examined the effects of the main operating parameters (feed, speed, forming depth, attack angle) on forming forces. They followed simulations with experiments and found speed, feed and fricton coefficient to be the most important factors in force. In most industrial processes, the process is flood cooled by a combined coolant/lubricant.

Surface finish can be excellent in IRF parts, although they generally require a machine finish for high precision applications. Bhatt and Raval (2018a) found that the surface finish was most strongly affected by the speed and feed.

The S/L ratio was first considered by Jahazi and Ebrahimi (2000), comparing the material flow in the axial (L) and circumferential (S) directions. The S/L ratio was later modelled by Parsa et al. (2009) as a predictor of formability.

The most important material aspects for avoiding defects are uniform microstructure high cleanliness and high formability (Rajan and Narasimhan, 2001; Jahazi and Ebrahimi, 2000).

Springback in IRF is found to be common. In this context springback means the elastic recovery of the material such that it is necessary to form to a higher deformation than the intended final deformation. For example, in FF parts from 2-10 mm thickness at AFRC, it is standard to form 0.5 mm more (so that the material is thinner) to achieve the desired end thickness.

In another example of the limited understanding of the process, Xu et al. (2016) saw major effects in mandrel deflection (in simulation and experiment) from the distribution of the rollers in FF. Most IRF processes with multiple rollers use regular angular distribution. But the authors propose non-standard distribution with three or four rollers with non-equal angular distribution to balance the effect on the mandrel. Roller distribution is a good example of an issue arising out of the inherent complexity of the process. Three rollers with differing nose angles, radial distributions and linear staggering will obviously experience very different loading. Tsivoulas et al. (2015) recommended lower contact angles for reducing stresses. The impact of this on the process is not well understood.

These challenges mean that there is not a rigorous general understanding of the mechanics of IRF processes. This makes it hard to design, implement and modify these processes in the industrial environment.

Numerical analysis

Complex systems are usually resistant to numerical analysis and better approached by finite element modelling. Nonetheless, some numerical analyses have been attempted. Changes in material properties have been examined. Some analytical work has been done, for example Roy et al. (2010) modelled the DZ numerically and Razani et al. (2014) used a polynomial-based response surface method to predict the hardness changes in steel. More studies have attempted to use finite element (FE) models. The effects of multiple forming parameters on IRF processes have been modelled with experimental validation (Wong, 2004; Song et al., 2014; Hwang et al., 2015; D'Annibale et al., 2017). Despite this, the models are a long way from being fully generalisable and robust. Indeed, although there are numerous studies they show a tendency to being

self-contained and lacking broader applicability outside of the specific materials and geometries studied. In a review of the field considering modelling and experimental approaches, Podder et al. (2018) stated that "there is no established guideline for the selection of process parameters." This matches the general impression of IRF process design and process modelling, that it is done by feel, or by trial-and-error, without a strong overarching theory.

The main challenge for FE modelling is that the processes are incremental, rather than discrete. At each cycle of deformation error will arise in any model. These errors relate to the changing material properties which themselves characterise the tool-part interaction. For example, an inaccuracy in the increase of hardness during cold working will affect the elasticity, which will affect the forming force. The many repeated iterations needed to model a cyclical-incremental process each introduce small errors. These cascade into large errors as each new stage of the calculation starts with incorrect inputs. In addition, this makes the modelling computationally expensive, as a typical IRF process can have multiple DZs and continuously altering geometry and material properties.

For modelling to contribute significantly to process design and industrial use, it needs to be robust and generalisable to new materials and geometries. This represents a potential contribution from monitoring. By expanding the information that can be collected from a process, the capacity to feed back into modelling development will be improved. This means that monitoring development could also contribute to modelling in the future.

Process failure in IRF

IRF processes suffer from a number of failure modes or defects. Failure modes are the set of ways in which the process can fail (Marini et al., 2015). A failure in this context is one where a part fractures or breaks down, or does not behave as expected. In general the failure starts as a small defect which can then lead to catastrophic fracture or process breakdown. Defects in IRF processes can be divided into three categories - geometric, surface and fracture. Each type has different causes and consequences.

Fracture occurs in IRF when the material reaches its forming limit. It is possible to describe the mechanics of fracture but hard to predict the onset of fracture. This is because of the issues raised above. Fracture defects can have serious consequences. While forming under high forces, fracture lead to tool damage. In one example at AFRC, a fracture in a FF part caused a roller to friction-weld onto the part surface. These failures can obviously incur significant costs.

Fracture is a common failure mode, where the high stresses present during these processes lead to rapid propagation. Hoop (circumferential) fractures can instigate because of high longitudinal tensile stress, and axial burst fractures due to high circumferential tensile stress. Other fractures can be caused by material impurities (Marini et al., 2015). The main factors influencing fracture are known to be feed rate, reduction ratio, and preform microstructure.

The surface defects possible include wrinkling, cracking (in various directions) and poor surface finish. Although it is known that, for example, cracking is caused by high deformation levels, it is hard to predict exactly how much deformation is too much. Marini et al. (2015) categorises the effects of parameters on defects. Figure 2.10 categorises the influences on IRF defects, collected from Marini et al. (2015); Wong et al. (2003). Many of these factors have interactions - for example, changes in part design require different forming parameters, and the parameters themselves are interrelated. Furthermore, the branch of material properties change through the process as the material hardens, which affects springback, which then affects the required tool path cut depth.

Conclusions

Studies have examined a large number of input parameters and output variables on IRF processes. Speed, feed, angle of attack, percentage reduction and roller geometry were the most commonly studied inputs. Surface finish and forming force were the most recorded outputs.

A common issue with these studies is the lack of broader applicability. Each study is tied to a specific model or experimental set-up, and results can vary from study

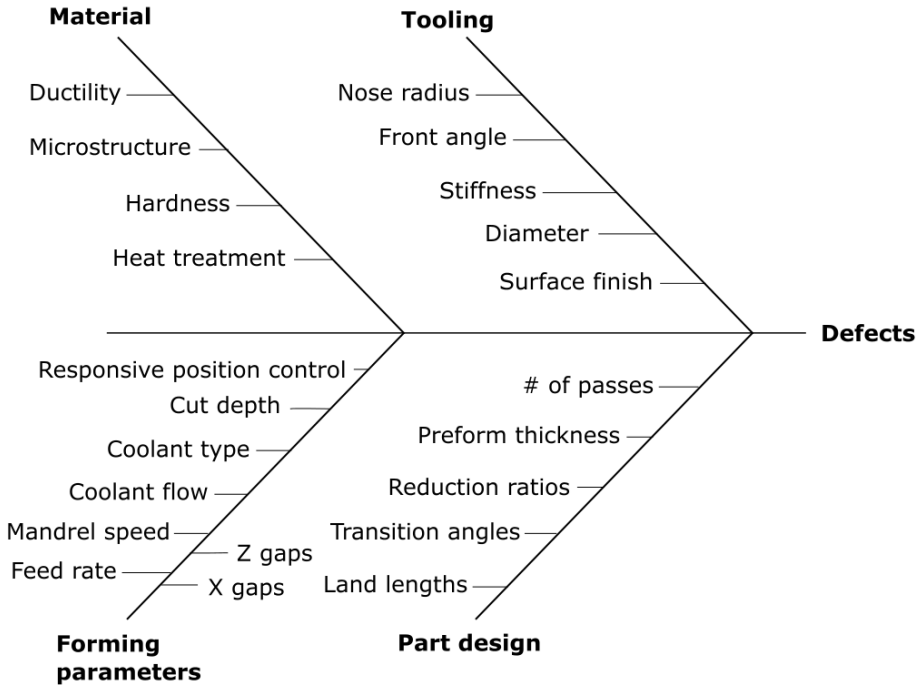

Figure 2.10: Fishbone diagram of inputs which affect defects

to study and from study to industry. Some of the studies discussed above carry out only simplified validation (e.g. D'Annibale et al. (2017)) which may not be valid in industrial machines. The work descibed above also tends to assess the accuracy of the outputs, without assessing if the models are describing the processes during operation.

These features mean that this type of work will always treat the deformation as something of a black box. It will therefore never produce a generalised, accurate understanding of IRF in operation.

2.4.4 Processes in operation

Much of industry is driving towards more feedback, closed-loop control and autonomy - so-called Industry 4.0. For high-value manufacturers (e.g. aerospace) and high-volume sectors (e.g. automotive), the investment in these technologies is particularly worthwhile. The ultimate aim is highly dynamic, responsive, and smart closed-loop control systems for all manufacturing technologies.

The current state of the art for IRF process operation is open-loop control. Open-

loop control is where the operational parameters are set independently from the outputs. This approach cannot adapt during the process - instead, each subsequent iteration must be manually adjusted. In closed-loop control, the process can sense the changing features of the part and use this information to adjust the process inputs - see Figure 2.11.

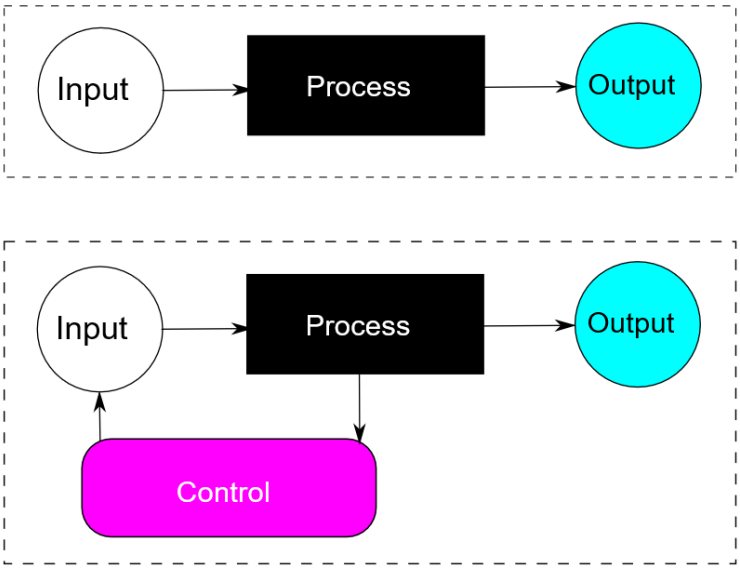

Figure 2.11: Open-loop control (above) and closed-loop control (below).

The work discussed above only considers these after the process is finished. But IRF processes feature changing properties of the geometry (thickness, roundness) and the material (hardness, ductility). Consider a FF process which had certain properties measured during forming. This information could provide a live feedback loop which controlled the machine operation. For example, the percentage reduction could be reduced as the part neared the forming limit. This would allow much easier measurement of forming limits and process capacity.

For this long-term goal of closed-loop control to be achieved, the processes need good methods of feedback. At present, the only in-process measurements carried out are roller position and loading. But load or force information cannot give the detailed, granular feedback that is needed for control. Consider work carried out by Roy et al. (2010), who modelled FF contact geometry in simulation and in a mock-up process.

The contact patch is the important interface between the process and the material (see Section 2.4.2). But it has never been examined on a real-world process. Similarly, no work exists attempting to measure, record or predict fracture in these processes. This is despite the fact that failure by fracture can happen without process operators noticing. If these process features can be instrumented, then control can be improved.

Existing instrumentation

For IRF to contribute its benefits to industry, it needs improved performance. Improved performance could be driven by improved control. For this to happen, better instrumentation is needed.

IRF instrumentation is very limited. Other manufacturing technologies routinely monitor many parameters - temperature, acoustic, vibration, and so on. They can leverage the information gathered to improve the process design, operation and control. IRF processes could also reap these benefits. See Chapter 3 for a more detailed discussion of this.

2.4.5 Summary of IRF capabilities and limitations

Challenges

Essentially, the challenges for IRF can be put into three categories.

1. The mechanics are inherently complex.
2. There is no overarching holistic model of the process.
3. The failure modes are unpredictable.

The first problem is the inherent complexity of the process mechanics. Unlike other processes, like machining or stamping, even the simplest IRF operation has multi-dimensional stresses with large changes across the forming area that are continuously evolving. This makes the processes hard to understand, and adds significant challenges to computational modelling.

The first problem tends to cause the second problem - it is hard to make a general rule for IRF performance, so work has focussed narrowly on specific systems and set-ups. This produces insight that is very process- and context-specific. It does not produce general process design guidelines or broad insights. There is little work attempting to assess the accuracy of the models in operation rather than in outputs.

Thirdly is the problem of process failure. This can mean poor quality of outputs (diametral growth, out-of-roundness, poor surface finish) or total failure (circumferential or axial fracture). Although the mechanics of individual process problems are understood, it is hard to predict when those conditions will occur because there is no information available on the process operation.

So what does all this mean for the use of IRF processes? A repeated thread in the literature, and in the industry, is that the processes must be refined by trial-and-error. This approach of empirical learning and development is not underpinned by a sound theoretical basis. Changing the process geometry or material often results in a "begin again" scenario where process development must start nearly from scratch. Even if it is possible to form some commercial part by IRF with great reductions in time and material cost, the process development will likely need significant investment. This is because the IRF process development approaches in use are not building a rule based understanding of the process. This fundamentally makes IRF processes unattractive in comparison with competing processes (e.g. machining, deep drawing).

In order to improve the useability and attractiveness of IRF, solutions are needed to improve process understanding and operation. Attempts to improve process operation by examining the inputs and outputs as described above are limited to specific examples. A new approach could offer new advantages.

Opportunity

There are major challenges for IRF, relating to the repeatability/reliability in wider industry. The broad aim of development in IRF is to make the processes more functional and more useable in industry. The evidence presented above suggests that the current development approach is not producing the desired result. The approaches

attempted (process design, modelling) have limited utility in solving these problems. By considering approaches used in other industries, it may be possible to make significant improvements in IRF process understanding and operation.

At present there is no way to evaluate the part or forming process or part during operation. The machine is feed-back position controlled during operation. The parts are evaluated after forming and the inputs are changed. This is off-line closed-loop control of the process. Many more mature manufacturing processes use online closed-loop process control of some sort - that is, they use feedback from the process to understand how it is operating and improve the process in real time. Figure 2.12 shows how IRF processes are currently controlled and how they could be with on-line process monitoring.

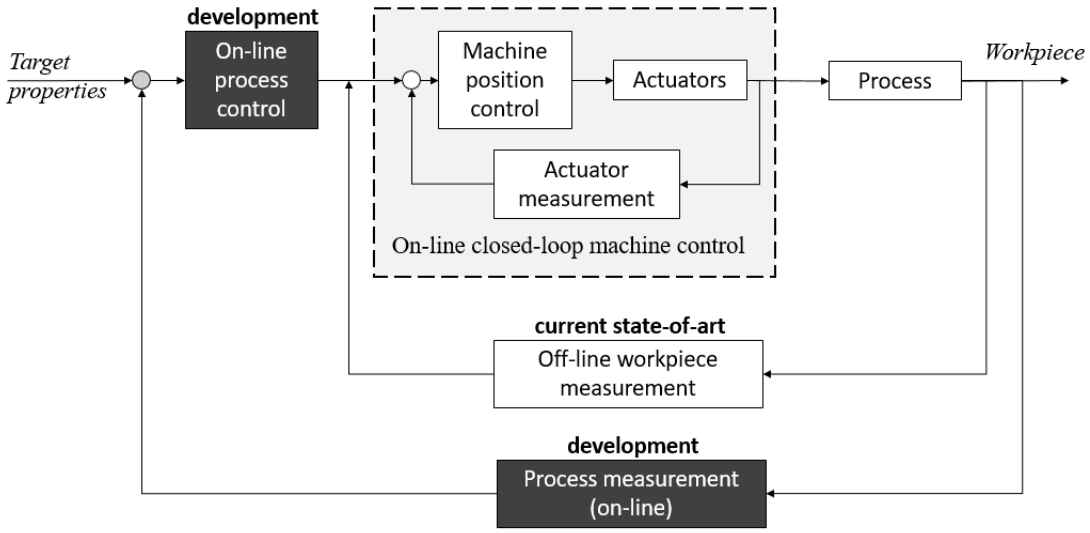

Figure 2.12: Current and desired machine and process control in IRF. Cf. Polyblank et al. (2014)

There are specific characteristics common to some IRF processes (flood cooling, forming in free air) that make the processes challenging to monitor. This is likely why there is little existing work looking at monitoring of IRF. Yet if it is possible to effectively extract data about the process, it would be possible to improve process control, design and understanding. Chapter 3 describes the principles of process monitoring, the use of monitoring in relevant applications and its potential for

application to IRF.

2.5 Research questions

IRF is in need of development to meet the challenges of complexity. Other manufacturing technologies have benefitted from monitoring and control. Note that this is not simply monitoring in the most general sense of observing outputs, but a systematic attempt to capture specific, numerical data which relate to the behaviour of the process. The broadest research question for the project is therefore simply:

Can monitoring provide insight into an industrial IRF process?

This essentially is attempting to combine two existing areas of research - IRF and process monitoring.

From this question arise a series of questions:

1. How can IRF processes be monitored?
2. What monitoring technologies would be appropriate?
3. What lessons can be learned from the use of monitoring in other industries?

Chapter 3 will attempt to answer the third question and refine the approach to the others. These questions will continue to develop through the work as avenues are explored or discarded.

2.6 Chapter conclusions

IRF processes offer a range of methods for producing rotationally symmetric components. They produce no swarf, and can allow much greater material utilisation and reduced machining against conventional production techniques. They give improved material characteristics and good surface finish. But the development of these processes is carried out though trial-and-error. Companies use large run-in phases when developing new geometries, even on an IRF process they may have used for years. The

principles that underlie the processes are grasped only dimly, and effective uses of the process are held, like recipes, in institutional memory.

So, if these processes provide such powerful tools for manufacturing, why are they so poorly understood? The answer to this question comes in two parts. Firstly, the inertia in an industry reluctant to change. Secondly, there are challenges for these processes - they are hard to model, predict, monitor and control. These challenges make it hard to carry out effective advanced process design and refinement.

To improve the utilisation of these technologies, both the inertia and the challenges must be addressed. This can only be done by improving the capacity of the processes to produce parts reliably and predictably.

The present situation in the IRF industry is that the processes are complex and poorly understood. Past research has focussed on open-loop control of the operational parameters. This has led to incremental improvements, and disagreement remains about optimising the processes. A more ambitious approach is needed to make more substantial improvements. Closed-loop control could provide this, but this would require feedback - and feedback requires instrumentation.

In short, incremental rotary forming processes have some properties which make them challenging to use: the complex and poorly understood interaction between tools and material is not illuminated by either detailed full-process models or deep operational understanding. Monitoring may offer the opportunity to better understand the processes and to better operate and control them. This approach will be challenging due to the hostile and inaccessible operating environment, but could use the benefits of process monitoring to unlock the benefits of IRF.

Chapter 3

Process monitoring

3.1 Chapter Introduction

As discussed in Chapter 2, the current state of IRF processes is one of limited understanding, instrumentation and control. The open-loop control is limiting for the design and operation of these processes. Closed-loop control requires instrumentation, which has seen vanishingly little development in IRF. For this advancement to happen, instrumentation must be developed for IRF processes.

This chapter explains the history and development of process monitoring, focussing on live and on-line approaches. This chapter is a continuation of the literature review.

It examines the available technologies and their uses in related processes and assesses the potential for these in IRF approaches.

Process monitoring is a wide field with many varieties and subspecialities. The aim of this chapter is to give a broad assessment of the field and its applicability to incremental rotary forming (IRF). The principles of monitoring are described. The available technologies and their applications are discussed with attention to their relevance to the problem at hand. The technologies considered most suitable for monitoring IRF are discussed. Special attention is given to the acoustic and ultrasonic technologies that underpin the work in Chapters 5, 6 and 7.

3.2 Principles of monitoring and fault detection

Process monitoring can be regarded as having two stages - instrumentation and processing. Instrumentation consists of the selection and implementation of an appropriate monitoring technology. The process for gathering data must be devised and improved so that it can operate reliably. Data processing is the final stage, which takes raw information and transforms it into process understanding.

Instrumentation is the process of applying a monitoring technology or technologies to a process. For this to be effective, the right technology must be chosen and correctly implemented.

3.2.1 Process instrumentation

Monitoring can be classed in two modes - direct and indirect (Kong and Nahavandi, 2002). Direct measurement records an outcome itself, such as tool wear. It is very accurate, but difficult to implement. Indirect monitoring records other system parameters that can be used to infer information about the outcome of interest parametrically. For example, force feedback or ultrasonic response might be used to infer some information about the process behaviour. This approach can be non-interrupting and continuous.

A direct approach in IRF would perhaps consist of manual measurement of material thickness and the presence of defects. This would require major interference in the process, which is counter-productive to the driver of process monitoring - improved process performance. Indirect methods can often avoid this issue because they are less invasive in the process.

The indirect approach works by extracting some signals from the process (data acquisition) and then processing the data to gain insight into process performance. This approach requires the use of a model to relate the signals to real-world behaviour - the important principles that underlie this are described in Section 3.2.

Without a systematic approach, any signal can be contrived to represent any result. In order to provide meaningful and comparable results, monitoring must be a formalised

process with a model which forms a testable hypothesis. The hypothesis is compared to the signal captured in the monitoring process and conclusions are drawn. This approach can be described as signal-based fault diagnosis

3.2.2 Signal-based fault diagnosis

Ding (2008) describes signal-based fault diagnosis as such: 'On the assumption that certain process signals carry information about the faults of interest and this information is presented in the form of symptoms, a fault diagnosis can be achieved by signal processing.' The symptoms can be thought of as deviations from normal behaviour; it is therefore necessary to establish what normal behaviour is and compare it to actual behaviour. This is done by creating a model that represents the behaviour of the process. Figure 3.1 shows how the model creates an expected output and compares it with the recorded output.

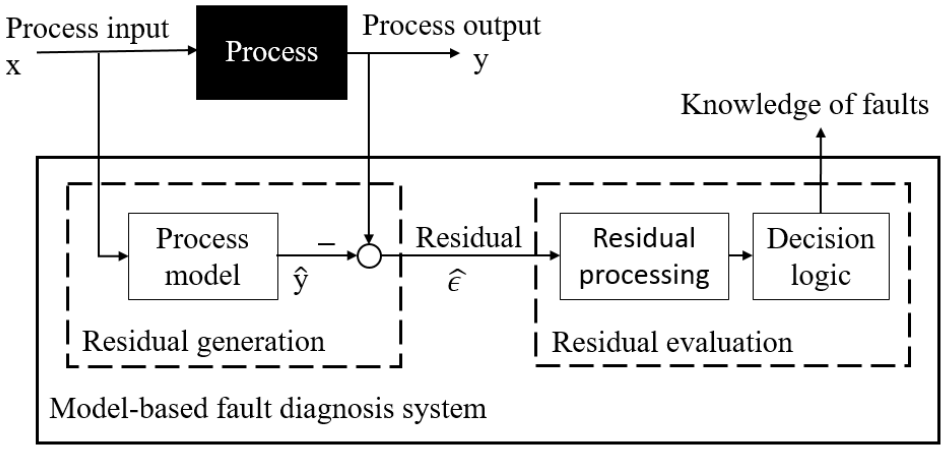

Figure 3.1: Fault diagnosis block diagram (adapted from Ding (2008))

So for a process which has output y the real behaviour is a function f_R of input x and parameter β with the error ϵ:

$$y = f_R(x; \beta) + \epsilon \tag{3.1}$$

The residual, $\hat{\epsilon}$, is an estimate of the error found from the difference between the real output y and the predicted output $\hat{y}$.

$$\hat{\epsilon} = y - \hat{y} \tag{3.2}$$

where the process is modelled as a function f_M of input x and estimated parameter $\hat{\beta}$

$$\hat{y} = f_M(x; \hat{\beta}) \tag{3.3}$$

Applying this in the real world works as follows. A process has some unknown feature of its behaviour (e.g. the forming force or contact area) given by y. In order to extract information from monitoring, two components are needed:

- A model of some part of the process which is being monitored (Equation 3.3).
- A signal from the process which contains information ($\hat{\epsilon}$).

This gives an estimate of the true process behaviour as:

$$y = f_M(x; \hat{\beta}) + \hat{\epsilon} \tag{3.4}$$

For a model which is representative of the process operation, the residual contains information about the process performance. Simply put:

- If $\hat{\epsilon} = 0$, then the process is behaving as expected.
- If $\hat{\epsilon} \neq 0$, then there is a fault or issue.

It can therefore be seen that the monitoring is reliant on two premises: A) that the model is accurate, and B) that the residual contains the necessary information. If either of these are not true at any point in the process then the results are unreliable.

The process model will always be imperfect, and modelling errors combine with unknown or unpredictable disturbances to cause the modelled output to deviate from the measured output. There are essentially two strategies to extract useful information,

either designing the residual generation to separate out the fault of interest, or post-processing the residual to focus on the fault of interest. Both of these may be employed.

3.3 Requirements for monitoring an IRF process

Chapter 2 laid out the generic challenges facing IRF. Looking now at the STR600 - the machine available for this research, there are constraints on the installation of a monitoring system. These can be considered as constraints on any monitoring system which might be developed for a similar process.

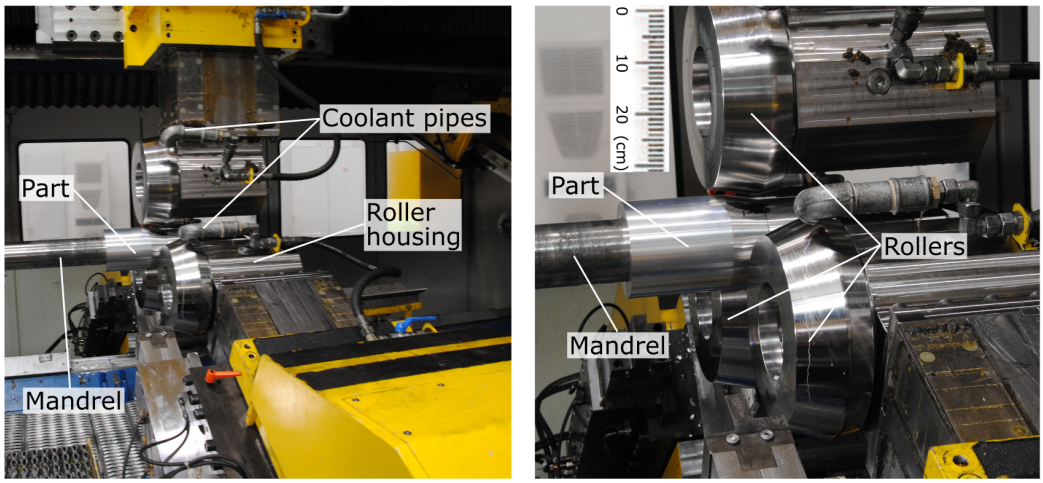

Figure 3.2: Overview of the STR-600 machine.

Figure 3.2 gives an overview of the WF Maschinenbau STR600 shear, spin and flow forming machine. This machine has a challenging environment for monitoring. The constraints for monitoring IRF processes on this machine are as follows:

- Operability in the extreme environment. The STR600 uses flood cooling and parts can reach elevated temperatures of over 300 degrees.
- Any mounted or installed sensors must cause minimal interference with the forming operation. This means both the quality of output from the process and the operation of the process (i.e. no stoppages).

- The mechanical integrity of the machine components themselves (rollers, housings, etc.) must be protected.

These considerations must be borne in mind when looking for relevant examples of process monitoring.

3.4 Review of relevant monitoring technologies and applications

Before considering existing uses of process monitoring, it is important to assess what information is being sought. In this case, it is insight into the best way to monitor IRF. The reported experience of operators using the machine in question (the WF-STR600) is relevant. The noise and vibration from the machine clearly changes during changes in the process. When a part fractures or is damaged, the operator can hear and feel a low-frequency rumbling. Given this known opportunity for insight, it is important to consider what approaches will best be able to capture this information.

This section will discuss a variety of approaches and draw out the common threads and how they apply to IRF and this project. There are many applications of monitoring and they feature a wide range of approaches, technologies and processing strategies. Many of these bear comparison to the IRF problem in their mechanics, geometries or other features. A wide set of examples will be considered for their potential to inform the monitoring of IRF.

3.4.1 Cutting tool condition monitoring

Cutting tools - whether on lathes, mills or other machines - represent a single point of contact between the process and the workpiece. The tools are susceptible to breaking or blunting, which can cause costly damage and downtime. The set of approaches called tool condition monitoring (TCM) aim to sense tool condition in real time. It is a deeply-researched field of monitoring.

Ambhore et al. (2015) identify a number of TCM technologies (shown in Table 3.1). There are two categories described, direct and indirect. For monitoring rotary forming,

there is a similar divide possible between actively examining the work-piece for issues and indirectly identifying them with signal features or variations in measurable variables that are correlated to wear.

Table 3.1: Tool condition monitoring technologies noted by Ambhore et al. (2015)

Direct Methods	**Indirect Methods**
Electric Resistance	Cutting force
Optical	Vibration
Radioactive	Temperature
Measurement of tool geometry	Acoustic emission
Vision system &c.	Surface roughness
	Torque/current &c.

The aim of the TCM is to examine the cutting tool itself rather than the part, so the direct measurement methods typically involve stopping the process to examine the tool. These methods are therefore only useful if they can be applied during the process, and would need to cope with the work-piece rotating. Direct monitoring approaches are further impractical because of the difficulty of accessing the forming process - the elevated temperatures and flood cooling would make their application very difficult.

The indirect approaches are more relevant. From as early as the 1960s, vibration amplitude was used as an indicator of tool wear (Weller et al., 1969). This was possible because of the simple mechanics of the system - low vibration is 'good', high vibration is 'bad'.

In the decades since, many researchers have monitored cutting tools with vibration (Dimla Snr. and Lister, 2000; Scheffer and Heyns, 2004), cutting forces (Rizal et al., 2013; Dimla Snr. and Lister, 2000), acoustic emission (Marinescu and Axinte, 2008; Ren et al., 2014; Jemielniak, 2001; Jemielniak et al., 2008) and other technologies. The field has seen a gradual increase in complexity as the understanding of the process has improved.

Dimla Snr. and Lister (2000) used a three-axis dynamometer on the tool-post to identify the three orthogonal components of force. The feedback was examined with

time-domain and frequency-domain (FFT) analysis and showed that the vertical cutting force and vibration signature could indicate failure. Rizal et al. (2013) also measured cutting forces, using strain gauges on the tool holder. They made use of the I-kaz method which decomposes the dynamic signal into three frequency channels.

Modern TCM work can make detailed predictions using complex models and multiple data sources in the process. The complexity and accuracy of the control, monitoring, prediction and modelling go hand-in-hand. This is perhaps an indicator of the long-term possibilities for IRF, if process monitoring receives sufficient attention and development.

3.4.2 Monitoring of rotating machinery

Monitoring of rotating machinery to identify faults is an area of research with a variety of work, mostly focussing on signal processing. Monitoring is carried out at low frequencies (near to the frequencies of the machine) and at high frequencies, although these are generally for different purposes.

Various types of machinery have been monitored. Bearings can be monitored to identify grease contamination (Saravanan et al., 2006). Fixed axis gearboxes are a larger research area but monitoring of planetary gearboxes is also carried out (Lei et al., 2014). Mark et al. (2010) present a method for detecting damage in gear teeth, which is presented here as an example of how these approaches can work. When one or more of the gear teeth suffers damage (a 'pit' or 'root' crack) there is a change in the geometry of the interacting surfaces and the elasticity of the gear. The authors describe how differing kinds of fault in the gears can be distinguished. Manufacturing errors common to all teeth on a gear (A); manufacturing errors which have strong correlations to multiple-tooth spans (B); and manufacturing errors which are weakly correlated to multiple-tooth spans (C). These last errors (C) produce regular vibration which contribute to the total harmonic of the gear. The size of the harmonic is dependent on the size of the tooth error; the phase is dependent on the location of the fault on the gear. The damage-detection is done as follows:

- The system is 'run-in' to remove manufacturing asperities

- Before any significant damage is likely to occur, the system is run to establish a baseline statistical distribution of harmonic activity.
- In later operation, the current harmonic is compared to this baseline - any significant deviation is an indication of a newly developed fault.

This approach can be fine-tuned by considering the various rotational frequencies of gears in a system. This allows the pinpointing of faults to a specific gear. Selection of harmonics to exclude the (B) type errors required careful consideration. The selected amplitudes showed marked increase when seeded gear faults were introduced.

Note that the understanding of the behaviour of wear in the gearbox, the vibration harmonics etc. is deep. This is a prerequisite for this kind of predictive monitoring.

3.4.3 Acoustic and vibration monitoring

Vibration monitoring is the process of analysing signals that arise incidentally out of a process. A process - drilling, for example - might produce a signature of vibrations at different frequencies. By analysing the changes in this signature and connecting it to changes in the process behaviour, it is possible to use changes in vibration to characterise process behaviour. This is particularly applicable to repetitive processes which show gradual degradation - for example with tool wear. Acoustics is a subset of vibration which deals with vibration signals transmitted in air. Another area, acoustic emission (AE), focuses on small amplitude, high frequency noises made by material deformation. Ultrasonic monitoring refers to sounds that are outside the range of human hearing because they are too high a frequency. It can refer either to listening to high frequency noises (passive ultrasonics) or generating the high-frequency sound wave and using it to interrogate a subject (active ultrasonics). For this work, passive ultrasonics is considered along with AE in the category of acoustic/vibration monitoring.

Vibration and acoustic monitoring principles

The principles of vibration-based technologies are common to acoustic, vibration and AE. The subject of observation produces vibrations and these vibrations are transmitted through solids, liquids or the atmosphere to the recording point - usually a contact transducer or microphone. Figure 3.3 shows how data collection works.

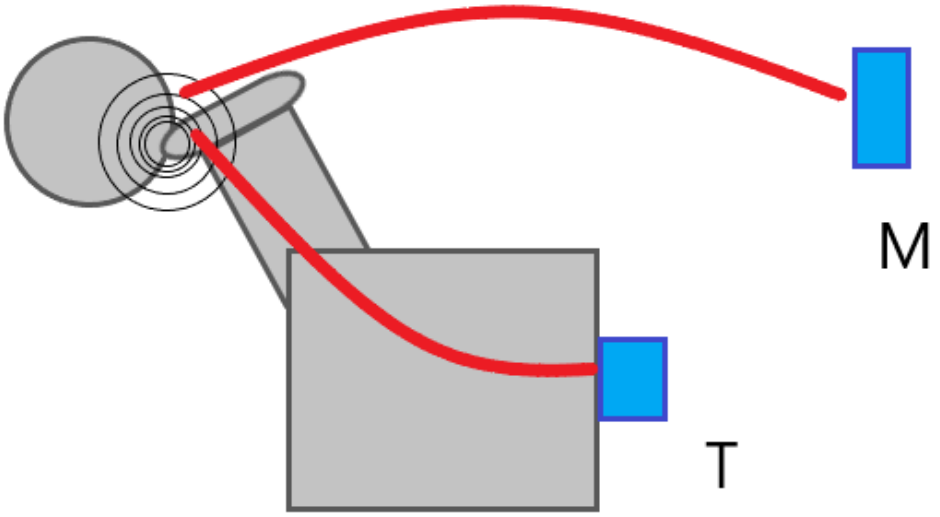

Figure 3.3: An example monitored process with a vibration source and the vibration pathways to a stand-off microphone (M) for collecting acoustic information and a contact transducer (T) for vibration and AE.

It can clearly be seen that the more complex the data pathway, the more opportunities exist for signal attenuation and transformation. This might occur by attenuation of the entire signal with a consequent reduction in signal-to-noise ratio (SNR), or in a more complex way. Some media or components dampen different frequencies at different rates. For example, a signal with strong 80 Hz and 800 Hz signals passing through a structural component that is resonant at 100 Hz will see greater attenuation in the 800 Hz component. Thus, a simpler pathway is preferable. This might suggest that acoustic monitoring is more effective. But there are similar concerns with vibrations in air. The solid-gas interface where the vibrations leave the

process may cause major and complex attenuation on the signal. In addition, the lower density in a gas medium means that signal amplitude is reduced with consequent SNR reduction. It can therefore be seen that the use of these processes requires careful planning and consideration to minimise these downsides as much as possible (Havelock et al., 2008).

Applications of acoustic and vibration monitoring

Machining has been monitored with sound, vibration and AE. Researchers have demonstrated the ability to characterise the process behaviour, tooling condition and the output quality (Teti et al., 2010). These technologies can often be installed on existing equipment with minimal cost or modification, and can be highly effective where it is possible to rigorously match the recorded data to an accurate process model. A number of commercial implementations exist which aim to detect incipient process failures. AE has been used for monitoring the condition of cutting tools (Ren et al., 2014; Pai and Rao, 2002) and for milling (Lee et al., 2006).

Sheet metal forming processes have been examined with AE sensing. In the right circumstances, the AE can characterise the plastic deformation occurring. Hao et al. (2000) identified dislocations from metal deformation which emerged in the vibration signal as high frequency sounds, which were captured under significant deformation and uniaxial yield. Only a small proportion of the emission from dislocations can be captured - smaller deformations were not detectable through AE. Some failures can also be found with AE monitoring, including galling, cracking, tool wear and stick-slip friction (Skåre and Krantz, 2003; Jayakumar et al., 2005).

There is much less work relating to bulk forming of metal. The emissions generated by material flow (from friction between crystals, plastic deformation and dynamic recrystallisation) can be captured, although it is hard to distinguish which sound comes from which source. (Hao et al., 2000). Behrens and Just (2002) used passive ultrasonic testing to identify fracture in cold forging by monitoring these acoustic emissions. They used statistical processing to help distinguish the AE from background noise - note that this was a cold process (no thermal noise) and in a laboratory environment, yet

still had major challenges with noise levels. Schneider et al. (2007) used AE in a similar way, to find the forming limits in open-die upsetting of high-alloy steel. Further laboratory experiments (El-galy and Behrens, 2008, 2010; Behrens et al., 2013) obtained similar results for hot and cold upsetting of steels and Mg-Al alloys. Although this work demonstrates the potential of AE ,monitoring in detecting fracture, it should be noted that the circumstances are somewhat artificial, i.e., the brittleness is induced intentionally and the experiment does not match a specific real world manufacturing process.

TCM has been done with stand-off microphones in conjunction with other signals (Salgado and Alonso, 2007; Kuljanic et al., 2009; Lu and Kannatey-Asibu, 2002; Tekıner and Yeşılyurt, 2004) as well as on its own (Seemuang et al., 2016; Weingaertner et al., 2006). Because the microphone is omnidirectional, it can collect a large amount of data from any nearby source. The sound signature can provide an overview of the entire process by recording the different frequency sounds from different parts of the process. However, this does raise the challenge that unwanted sound can be collected, adding noise to the signal. Post-processing can help to manage this (Salgado and Alonso, 2007), but if the SNR is too low then this is potentially a major issue.

In conclusion, there are many applications of these technologies which show two important lessons. For the best results, a simple acoustic pathway is preferable as the vibration can be altered, transformed and suffer damping in different frequencies if it travels through a complex pathway. The second point is that, in order to gain meaningful insight into the process, you must have an understanding of the vibration characteristics of the process. This can be as simple as *higher vibration amplitude from cutting tools is bad* (cf. Section 3.4.1) or can refer to a more nuanced model developed for specific process. There is no such model for IRF (see Chapter 2) so the application of vibration or related technologies would be speculative on the premise that the data might show correlations between vibration behaviour and forming behaviours.

3.4.4 Ultrasonic monitoring

As noted previously, US is related to acoustics and vibration in the sense that it measures high frequency vibrations which can be thought of as sounds. ultrasonic (US) monitoring refers to sounds that are at frequencies above the range of human hearing. For this work, US will refer to active ultrasonics - generating the high-frequency sound wave and using it to interrogate a subject.

Ultrasonic monitoring principles

US monitoring typically works as follows. An ultrasonic transducer (UT) transmits and receives the US signal by converting an electrical signal to high frequency vibration and vice versa. The vibrations travel from the UT, through the medium being examined at the speed of sound in that medium. Any interfaces in the medium send back a reflection to the UT. The magnitude of the reflection and the time-of-flight give information about the location and characteristics of the interface causing the reflection.

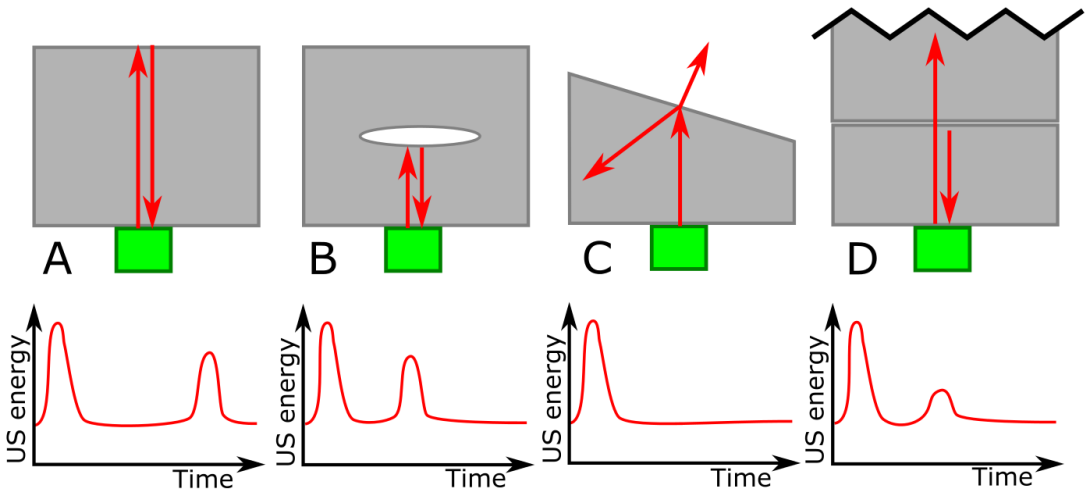

Figure 3.4: Different cases of US measurement: measurement of thickness (A), defect detection (B), angled reflection(C), and metal-to-metal contact (D).

Figure 3.4 shows four of the most important cases for US measurement. The first (A) is simple time of flight measurement. The time for the signal to travel to the reflection point and back (t) is given by the the speed of sound in the material (c) and

the distance from the UT to the reflection point (d). This is given by:

$$t = \frac{2d}{c} \tag{3.5}$$

The second case illustrated in Figure 3.4 B is the detection of defects. A porosity, gap or crack of sufficient size can cause significant reflection of the signal. Equation 3.5 can then be used to calculate the depth of the defect from the surface. The magnitude of the reflection will give some indication of the size and orientation of the defect: larger defects will give a larger reflections, as will those oriented at the normal to the UT (Rose, 2014).

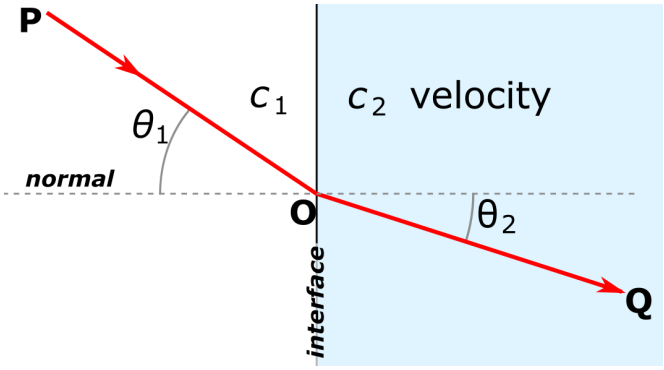

Figure 3.5: Snell's Law. Adaptated from Meijer (2006).

These principles are described in Snell's Law, illustrated in Figure 3.5. This law characterises how the transfer of waves though a boundary is affected by the angles of incidence, θ_1, and of refraction, θ_2, and the speed of sound in each medium, c_1 and c_2.

$$\frac{sin(\theta_1)}{c_1} = \frac{sin(\theta_2)}{c_2} \tag{3.6}$$

The cases illustrated in Figure 3.4C&D show how the the magnitude of the reflection can give information about the cause of the reflection. For example, an interface from metal to air would give a very large reflection (A), whereas a metal to metal contact would give a much smaller reflection (D). This is because the interface between media where sound has greatly different speeds is poorly conductive to sounds. Similarly, an angled face gives less reflection to a US system than a perpendicular one, as the

interface approaches total internal reflection at an angle that will not reach the UT (see Figure 3.4 C). The implications of these mechanics for IRF monitoring are discussed in greater detail below and in Chapter 7.

Applications of Ultrasonic monitoring

US monitoring is used for a range of applications. Measuring thickness of static objects and detecting porosities is very well established - it has its own ISO standard (ISO16831). The uses of this are largely for weld fault detection and cracking in mechanical structures. These applications are well researched; however they have minimal relevance or IRF monitoring because the conditions of measurement are static and repeatable (Schmerr and Song, 2007).

US monitoring has also been demonstrated in more complex configurations, involving tribological interfaces. In this format, the magnitude of the reflection is relevant because it can characterise the nature of the interface. Figure 3.6 (Havelock et al., 2008; Dwyer-Joyce, 2005), shows some of the models used for measuring interfaces.

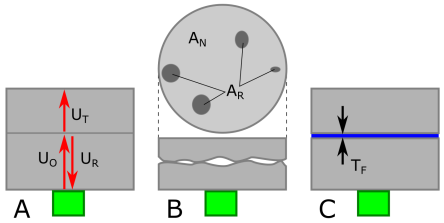

Figure 3.6: Types of US interface. (A) shows a perfectly bonded interface, (B) a rough tribological contact and (C) a thin-film interface.

The transfer of ultrasonic energy through a material interface can be described and modelled if the nature of the interface is known. In the perfectly bonded example, Figure 3.6 (A), the initial ultrasonic pulse with energy U_0 is partially reflected (U_R) and partially transmitted (U_T). Assuming that U_T accounts for all transmission losses,

$$U_0 = U_T + U_R \tag{3.7}$$

and the reflection coefficient is given by

$$|R| = U_R/U_0 \tag{3.8}$$

$|R|$ is determined by the geometry of the interface and the properties of the two materials, c_1 and c_2. When the roller is in air, $|R|$ is very high because the change in the speed of sound, δc is large. When the roller contacts the material, δc is reduced because the material properties are similar. There is therefore a reduction in $|R|$.

For dissimilar materials, it can be calculated as

$$R = \frac{z_1 - z_2}{z_1 + z + 2} \tag{3.9}$$

where z, the acoustic impedance, is given by $z = \rho c$ with ρ as density. Note that for a large area of perfect contact between identical materials, $|R|$ would approach zero.

In reality, the nature of the contact is imperfect and there is some reflection, the magnitude of which is determined by the contact properties (Figure 3.6 (B)). The contact has a nominal area, A_N and a true set of tribological contact points - A_R. Usually, $A_R << A_N$. The contact area can be inferred from the change in R.

Another case is a thin film interface (Figure 3.6 (C)). Kendall and Tabor (1971) developed a spring model for this type of contact.

This approach of interrogating interface characteristics with US has been used for a variety of purposes. A variety of work has attempted to characterise of metal-to-metal interfaces by the response of a US reflection at the interface. The simplest cases are static loading where the interface pressure can be inferred (Kendall and Tabor, 1971; Dwyer-Joyce et al., 2001). The tribological characteristics of contact can be related to the US response, principally the interface stiffness and contact area. There are numerous applications and calibration approaches for simplified, static systems with thin film interfaces Du et al. (2015); Hunter et al. (2012). As with static thickness measurement discussed above, this is of limited relevance as it requires precise calibration which is achieved with a tightly controlled experimental set-up. Such niceties are not available in the dynamic forming environment of a commercial

IRF process.

More promising is the work carried out on dynamic contact, such as Pau et al. (2002) who examined the dynamic contact between a rail and train wheel. Their approach used measurements of contact pressure to calibrate the measure of contact area. This area was much smaller than the nominal contact because it was a dry asperity contact - see Figure 3.6.

More relevant still are thin film interfaces between moving parts, like applications in lubricated shafts, seals and bearings (Anderson et al., 2000; Dwyer-Joyce et al., 2004; Hunter et al., 2012). These experiments can characterise the behaviour with the help of the cyclical nature of the signals which help to relate US data to process behaviour.

Another application with relevance is described by Holdich et al. (2017), who conducted thickness measurement in cold metal rolling. This system was effective for measuring thickness, but with several drawbacks - as the authors noted, it required interference that could not be justified on an industrial process. Additionally, the system had issues with noise levels and processing despite the relatively simple access to the process.

These examples indicate that it will be possible to use US monitoring on a rotating process, but that there are potential challenges. In the above cases which most closely resemble IRF, the material removal required was high. In a real IRF implementation this would be difficult because of the high point loading on the tool. Another area of concern for several of the examples was signal acquisition and the challenges around noise. In laboratory experiments this can be controlled by simplifying the system and removing interfering elements. In an industrial application, these constraints need to be faced head-on as they cannot be removed. Any use of this technology would therefore require a robust strategy to limit interference in the process and control noise levels.

3.4.5 Application to IRF

Sheet and bulk metal forming processes like forging, stamping and punching consist of a series of operations as each part is produced. These should, theoretically, be identical or nearly so for parts which are identical (within some tolerance). In these circumstances

it is a logical approach to capture a signal for each operation - the signals can then be compared to look for trends which appear slowly over time to spot sudden anomalous behaviour.

Note that for most machining and TCM applications, there are essentially two parts (tool and workpiece) of which one is rotating and one is fixed. For sheet and bulk metal forming, there are small numbers of moving parts, which generally have large areas of contact, giving a good acoustic pathway for monitoring sounds. These set-ups make it practical to attach a contact sensor (such as for AE or vibration sensing) to the fixed part - the sensor is near the site of activity with an uninterrupted acoustic pathway. For FF, it is impossible to access the site of deformation in this way due to the rotation of both tool and workpiece. Furthermore, the area of contact between the tool and workpiece is constantly moving and can change shape during the process.

When monitoring rotating equipment, there are often major challenges to be overcome. Moving parts can make the site of interest inaccessible for sensors. In addition, background noise levels can be very high. Wymore et al. (2015) consider vibration inferior to AE for data sensitivity, but it has the major advantage that it can be sited further from the source and remain effective. Vibration monitoring of this sort has been used for monitoring gearboxes and other rotating machinery, with contact accelerometers - mounted, for example, on the housing of a gearbox. Their effectiveness for fault detection can be limited by the poor SNR which results from this distance between source and sensor. (Nie and Wang, 2013)

The accelerometers used to record vibration and AE work on physical contact - they need to be attached to the vibrating part or as near to is as possible. If applied to IRF the vibration of interest would have to follow a complex path of propagation from the site of deformation, through the roller, roller bearings and roller housings to the accelerometer. All of these of these other vibrating components would likely introduce noise which would degrade the quality of the signal; in addition, the signal of interest would diminish as it crossed each of these boundaries. By comparison, a stand-off microphone, recording vibrations in air are simple to install. But they have a comparable, or even worse, issue with collecting noise as a microphone would capture

noise from the area of interest, other parts of the process, and other noise sources in the vicinity.

Ultrasonic monitoring technology has been examined for interrogating interface characteristics for a variety of purposes. A variety of work has attempted to characterise of metal-to-metal interfaces by the response of a US reflection at the interface. The tribological characteristics of contact can be related to the US response, principally the interface stiffness and contact area. This has been examined for static loading (Kendall and Tabor, 1971; Dwyer-Joyce et al., 2001) and dynamic contact (Pau et al., 2000, 2002). Thickness detection with US is a well established technique for non-moving materials with its own ISO standard (ISO16831) and has also been demonstrated in more complex configurations, such as for thin film interfaces between moving parts (Du et al., 2015; Hunter et al., 2012).

3.4.6 Key lessons from monitoring examples

How do the examples above apply to monitoring of IRF? They have been selected for their comparability, looking particularly at awkward, inaccessible and rotating processes. But there is a major difference. Most of the examples above are monitoring a process that is well understood and can be robustly modelled. For example, cutting mechanics in TCM are well understood and when they change the effect this has on the process and monitoring parameters can be predicted. In essence, a simple relationship to a simple mechanic is easy to understand.

In IRF, the underlying mechanics are poorly understood and modelled. Currently the most basic information is unknown during a process (the thickness, contact area, and whether fracture has occured). This information often cannot be found after stopping the process either. This means that the expectations of monitoring must be limited.

Practically speaking, any monitoring of IRF would be a step forward, even if it only provides very limited information. For that reason, the decision was initially taken to proceed with technologies that could allow the detection of major fracture events with minimal process interference.

3.5 Option appraisal and downselection

As set out in Section 1.3, the project plan is to investigate several avenues for monitoring. But how are these avenues to be selected? Two points must be considered. The achieveability of good experimental outcomes (see Section 4.0.2) and the practical realities of implementation.

The wide range of available technologies means that any choice involves discarding potentially suitable options. The project as undertaken is working in an unexplored area (live monitoring of IRF). Therefore choices were guided by what was likely to be achievable. The choice of technologies to pursue was guided by their experimental suitability:

- **Capacity to deliver insight.** The ability to scan the process and collect useful information about it.
- **Limited requirements for deep process understanding.** Some areas examined, especially TCM, need a robust predictive model of process behaviour in order to interpret the results. This does not exist for IRF, so it cannot be used as a basis for monitoring.
- **Capacity to deliver results in the scope of the project.** Some options discussed above required many iterations of design and implementation, over many years to produce meaningful results. This project aims to efficiently assess the options for monitoring IRF with the resources and time available.

With that in mind, the technologies selected below should be practically implementable. Similarly, the technologies which are discussed but not investigated have not been rejected out of hand, but are simply unsuitable in the context of the project.

In addition to the experimental principles underlying the selection of monitoring technologies, there are practical considerations:

- **Suitability for the process environment.** IRF processes are difficult to work with. The environment is harsh for sensors (flood cooling and heat). The

mechanics of engaging sensors to the process are complex: both the tool and workpiece rotate, and the point of contact between them moves in two dimensions.

- **Minimal interference in the processes.** Working in a semi-commercial setting, it is vital to limit machine downtime and minimise any risk of process interference.

If the practical difficulties are insurmountable then the potential is irrelevant. Where the potential for insight is significant, it is worth taking on the risk of some challenges.

Table 3.2: Review of the suitability of different monitoring technologies for application to IRF. Each has been rated from 1 (poor) to 5 (excellent).

Technology	**Experimental suitability**	**Practical applicability**	**Tot.**
Vibration	**4** This technology is widely applied to generate significant insight.	**5** Easy to implement by attaching an actuator to the roller housing.	**9**
Acoustic	**3** The ability of machine operators to hear breakages strongly suggests potential, but the opportunity for deep understanding may be limited.	**5** Stand-off microphone monitoring is very easily implemented.	**8**
Optical	**4** Scanning methods could potentially capture geometric information if access were achieved.	**1** The coolant issue makes this near-impossible.	**5**
Ultrasonic	**5** The ability to scan the roller-part contact could give unparalleled insight.	**2** Implementation would require substantial machine modification.	**7**
Temperature	**2** Temperature recordings would be useful for calibrating FEA models, but would not give immediate, practical process insight.	**3** Implementation of mandrel or roller temperature sensing would require substantial machine modification.	**5**

Of the many monitoring technologies in use to a greater or lesser extent across industry, many are obviously unsuitable. Table 3.2 shows the best options available for monitoring of IRF. The table scores the options by how suitable they are both experimentally and practically (as defined above).

Optical methods could be highly insightful, but the challenges of getting physical access for a laser scan or vision system are evidently severe. This option can be discarded. Ultrasonic methods have potential to give invaluable information about the DZ. This approach would require significant development to make changes to the machine and overcome practical difficulties. Forming - or cutting - force is a widely used monitoring method. In this case, the STR-600 already has a monitoring system which records the forming force. But this system is highly limited. The data it produces is a low sampling-rate signal of the current drawn by the slide actuators, which is not given a calibrated force value. Thus it lacks the granularity in time and magnitude to capture significant insight. The machine manufacturer would need to install an entirely new system for this to be useable. Temperature measurements would be interesting, as the "cold" processes do often rise in temperature due to friction in forming. This would be particularly useful for calibrating FE modelling. It would not directly produce useful insight into the process operation, which is after all the primary aim of this project.

Clearly the two winners by this method are vibration and acoustic monitoring. Vibration and acoustic based monitoring are widely used, cheap and do not interfere in the process. In this case, the technologies were selected because of the reported experience of operators using the machine in question (the WF-STR600). The noise and vibration from the machine clearly changes as the process changes. When a part breaks, the operator can hear and feel a low-frequency rumbling. This suggests that vibration or acoustic monitoring capacity could give useful insights into the process operation.

Simply put, major events (catastrophic fractures) cause loud noises. Gradual changes in operation cause varied sounds. Recording these noises and vibrations could allow them to be categorised and understood. This in turn could allow the better understanding of the process itself.

3.5.1 Conclusions

Three technologies were selected for investigation. Initially, vibration and acoustic monitoring were selected. These require very little financial outlay and no process

interference. The technologies are discussed below. Investigations into the application of these technologies was carried out, and is discussed in Chapter 5. The results of this work led to a third technology selection, US monitoring. The development of this monitoring system is discussed in Chapter 6 and its testing in Chapter 7.

3.6 Research questions

The research questions have been refined by the process of examining the literature. The broad research question remains: **Can monitoring of vibration or acoustic signals provide insight into an industrial IRF process?**

The questions put in Chapter 2 can be answered:

1. How can IRF processes be monitored? *By the application of monitoring technologies that are used on related process.*

2. What monitoring technologies would be appropriate? *Vibration and acoustic monitoring have been used in similar applications and meet the criterion of minimal interference.*

3. What lessons can be learned from the use of monitoring in other industries? *The complexity of insight is proportionate to the understanding of the system. For a poorly understood system, measurements will likely be coarse.*

The next question is: **What process changes in IRF can be detected with vibration and acoustic monitoring?**

3.7 Chapter conclusions

At present, IRF processes do not have rigorous models or good data collection. So it is impossible to effectively control them except by a trial-and-error approach. The aim is to make a small step towards better monitoring.

Vibration and acoustic sensing were selected for the potential to collect basic information about large changes in the process with minimal intervention. These technologies will be tested to see what they can show about the process.

The testing will be done in-situ on the WF-STR600 for any indication that they can capture useful information. The primary test will be if these technologies can identify the rumbling sounds and vibrations associated with material breakdown in FF. The next step will be to assess if there is capacity to gain insight into the subtler elements of the machine operation.

Chapter 4

Experimental approach

As described in the introduction, this chapter will address the general approach and specific methodology used to approach the problem of monitoring IRF. This consists of a discussion of the research approach and the experimental techniques which will be used to assess the monitoring technologies.

4.0.1 Research approach

In the broad world of engineering research, experimental approaches can be divided into the objective and subjective (Easterby-Smith et al., 1991; Muñoz et al., 2017). The objective approach takes the premise that the subject of research is a set of objective facts and relations. These can be identified and categorised by a researcher who is independent from the system. For some areas of study, the subjective approach is more suitable. This approach supposes that the experimenter is a part of the system and interacts with it.

The relevance of this dichotomy to experimentation on process monitoring can be summed up in a question: **how does the monitoring affect the process?** For higher order applications of monitoring, e.g. in a production setting, it is important that the monitoring is not affecting the process. This is a critical feature to establish, so that the monitoring data is independent of the system. Then it is possible to build large, complex, integrated monitoring systems (Talluri and Sarkis, 2002).

In this project, the independence of the monitoring and system is relevant, but it not the sole consideration. The motive is to explore the ways in which monitoring can improve understanding of the process, ultimately for use in a production environment. Therefore there are two competing priorities: to maximise the information collected and minimise the interference in the process.

The basis for selecting monitoring technologies was therefore established to be one of minimal intervention. Furthermore, there is a basis in operator experience. Operators using the machine can hear and feel parts failing. Therefore the initial point of investigation was to look at sound and vibration. For more on this, see Section 3.5.

Although a range of research approaches exist for more subjective areas, for concrete engineering problems a practical approach is often suitable. Blessing and Chakrabarti (2009) present a practical approach to research which goes through multiple phases of iterative experimentation. These initially give broad, shallow results and refine to give deeper understanding later in the process.

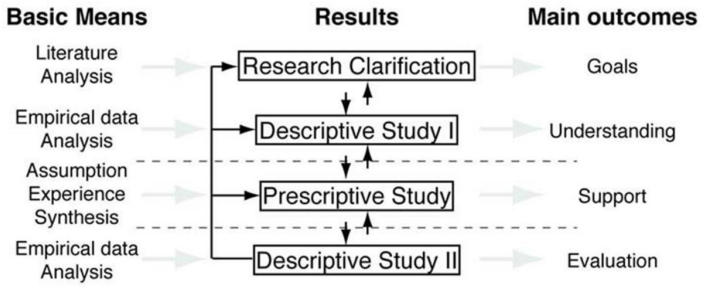

Figure 4.1: Research approach taken by Blessing and Chakrabarti (2009)

Figure 4.1 shows how this approach refines an engineering design. Analogously in this case the experiments will become more detailed as they proceed. The methodology for each experiment is improved by the feedback form the previous one, and this is how they are presented.

4.0.2 Experimental method

To gain the most information from a set of trials with a limited set of parts, it is important to structure the trials correctly. Decisions must be made in advance, but

this can be challenging when the experiments relate to a brand new subject. Monitoring of IRF is a new area, and it is therefore hard to ascertain what the best approach is for setting experimental parameters. For this reason, a two-stage approach will be taken. First some simple trials will explore the capacity of several monitoring technologies. Then a second, more formalised set of trials will examine in detail the potential of the most promising technology. For more on this structure, refer to 1.2.

The highest cost for the trials are preform manufacture and machine availability. Initial trials will look at several technologies, with a very limited number of parts. The IRF processes being examined must be tailored to create circumstances that are suitable for testing the monitoring technology. For example, a technology that might detect fracture should be tested by intentionally fracturing parts. It is difficult to plan these trials in detail, because detailed experimental design requires a detailed understanding of the monitoring behaviour. Consider, if a technology fails to capture information about fracture but shows indications of recording surface finish behaviour, it would be prudent to refocus the experiments in that direction.

The factors here, both in process behaviour and monitoring technology efficacy, are unclear. This is because there is no work extant on this specific are and a relatively small field of relevant literature. In addition, parts are very limited. Therefore experiments will be simple until behaviour is established, leading on to more complex experiments later.

This will constitute a phased experimental approach Pedaste et al. (2015). It will commence with an examination of several areas, and the insight gathered there will be used to refine the later work.

For this reason, the precise experimental procedures are not laid out in advance but rather within each process of iterative research. Figure 4.2 shows this process. The first set of trials for each technology examined takes the following simple approach:

- **Trial 1** A “good” part is formed according to known parameters. This will act as a baseline to compare later recorded parts.
- **Trial 2** A part is formed with defect or other difference from **Trial 1**. The

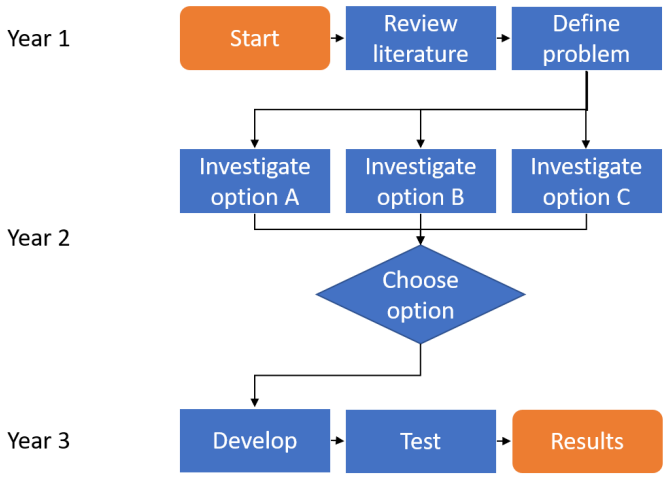

Figure 4.2: Approach to experiments

difference in the signals between these two parts is the residual (see Section 3.2.2).

- **Further trials** Further parts are formed based on what aspects of the process seemed most clearly evident in **Trial 2**.

Later trials use a more formal structured approach. Each area of potential insight will be clearly defined with a model explaining how the monitoring technology will capture information about the process. This will be formalised in a written hypothesis for each area to be examined. This approach is critical for proving rigorously that the changes in the signal are truly related to the changes in the process.

To conclude, it is hard to plan for process monitoring of IRF, when no work has ever been done in this area. Initial trials will attempt to understand what data is possible to capture. Further trials will use a more structured approach to attempt to quantify elements of the process behaviour.

4.1 Chapter conclusions

In general, the approach taken looks at several technologies. These are examined briefly. Where there is evidence of capacity to give process insight, the experiments are continued in a more detailed fashion.

Chapter 5

Vibration and acoustic monitoring

This chapter presents the early work carried out to assess the use of monitoring technologies for IRF. two avenues were explored: vibration and acousticF sensing. These were selected because of the minimal interference in the process operation and the wide use in process monitoring.

5.1 Aims

The aim of the experiments described below was to examine the capacity of these technologies for monitoring IRF at the most basic level possible. There was no aim of producing an industrial-ready system, or of devising an optimal signal processing strategy. Instead, the aims were to examine the capacity to detect catastrophic failure. This is an important capacity because of the risk of tool damage in a major failure which would cause significant downtime in an industrial setting.

5.2 Vibrometry

This section will discuss the first route of investigation - vibration monitoring. The choice of vibration as an approach, the planning of experiments, the execution of trials

and the examination of trial results are covered below.

5.2.1 Context and rationale

In the Master's element of the EngD, laser vibrometry was considered for monitoring rotating processes (Appleby, 2015). This was an attempt at low-interference monitoring, which worked to the extent that some information was extractable. It was very limited in application because it was near-impossible to meaningfully relate the data to the process (see Chapter 3). As discussed in Chapter 4, the vibrations from failing parts can be felt and heard. It is therefore clear that vibration measurement could be used to interrogate the process.

5.2.2 Planning experiments

Vibration monitoring is widely used in TCM, gearbox monitoring and structural health monitoring applications. It is low-cost and non-invasive, merely requiring the attachment of piezo-electric transducers. The method is very indirect, as the vibrations need to be measured from a fixed (not rotating) element of the process. In the case of IRF, this means that the vibrations from the process need to travel a convoluted path, from the site of interest at the deformation zone (DZ) to the accelerometer. The signal must then be processed to remove irrelevant information (for example, from bearings) and leave a useful residual (see above) to make some observation about the process.

At present, there is very little available information about the vibrations produced by IRF processes. For this reason, it is impossible to propose a signal processing strategy in advance. A simple strategy was therefore proposed to examine the usefulness of vibration monitoring. A short trial was proposed, using three parts of Al6061 tube with a 12 mm wall thickness. The intention was to make a simple test of vibration monitoring without becoming too committed down one path, so borrowed vibrometry equipment was used. The four trials were carried out with a standard test geometry at the limits of the FF process. The process selected was a single pass, three stage reduction of 25-50-75% deformation. Appendix B.3 and B.4 show the geometry of the preform and part. The X gaps were set as standard, at 1/3 of the reduction, and the Z

gaps at 2 mm each. See also Section 2.2. This set of parameters was selected because it was known to cause circumferential fracture in combination with this material and geometry.

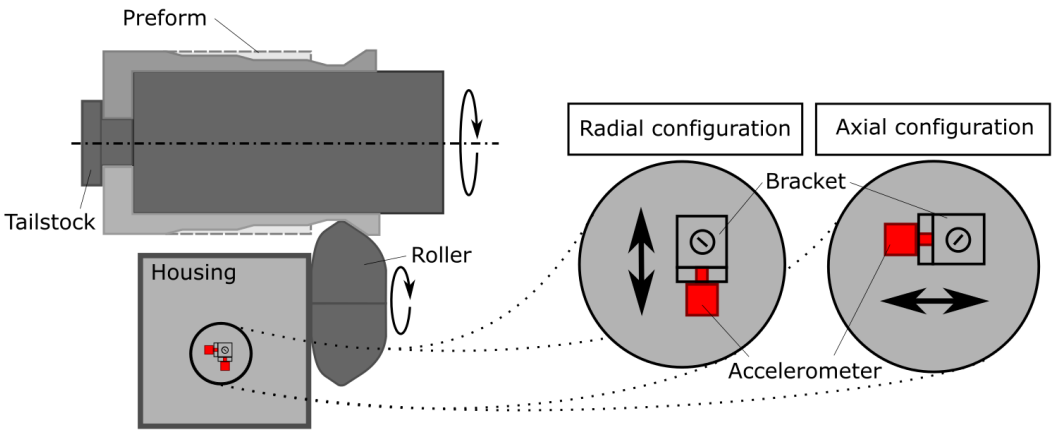

Figure 5.1: Vibration monitoring equipment set-up schematic.

Figure 5.1 shows how the equipment was arranged. The location of the sensor was highly constrained because no modification of the machine was permitted at this point. It was decided that the nearest possible location for the DZ would capture the highest magnitude of vibration from the process. In the absence of any literature on vibration monitoring of IRF, this was a 'best guess' decision. The nearest available mounting location was on the side of the roller housing where a threaded hole was located. This allowed the sensor to be attached in either the X (radial) or Z (axial) orientation. These two sensor positions were selected as the FF process deforms the part both axially (extension) and radially (thickness reduction). It is of interest to know how vibrations from the process behave for both of these aspects of deformation. For the exact sensor position, see Appendix D.1.

The sensor used was the Kistler 8705A50m1. This uniaxial accelerometer has a ± 50 g capacity with a sensitivity of 97.8 mV/g. Two positions were considered for the sensor - either aligned with the radius of the part or tangent to the part surface. A range of parameters were set at "best estimate" levels, including gain, sampling rate, buffer size etc. These parameters were adjusted during the experiments as necessary. For a

full list of settings used, including the sensor and software settings, see the published dataset of the experiments (Appendix C). The data acquisition system (DAQ) was a National Instruments NI 9201. The software used to record the data was National Instruments *LabView SignalExpress*.

5.2.3 Experimentation

The trials, as described above, were short and simple, aiming to gauge the feasibility of vibration monitoring. As intended, the trial plan was flexible during the experiments to obtain the best outcomes. This was to allow the improvement of the set-up.

Table 5.1 shows how the trials were run. An initial dry run of the full machine cycle with no part in place or coolant was run to establish a baseline. In the subsequent trials, the electrical operating parameters were left unchanged apart from the gain. These were set at full-scale output voltage: ±10 V, sampling rate: 400 kS/s, sample buffer: 100 kS. The gain needed to be set fairly high because of the weak signal strength. However this led to increased noise levels (and therefore poor SNR).

Table 5.1: Details of vibrometry experiments on tubular Al6061 components

Trial	Gain	Mounting	Notes
1	15	Axial	Dry run with no part and coolant
2	15	Axial	Part run as normal
3	15	Radial	Alternate accelerometer position
4	20	Axial	Repeat of trial 2 with higher amplification

All the parts fractured during the third land, as expected. These fractures were clearly audible to an observer standing outside the machine.

5.2.4 Results

The results from the trials were disappointing. They show broad-spectrum vibration during the forming process, but little connection to process behaviour. Each part fractured in the third land under severe deformation. There was no evidence of this in the vibration data. The positioning of the sensor made some difference - the results of

trials 2 and 4, with the same sensor positions, were identical. Trial 3, with the radial configuration, showed somewhat different broad spectrum vibration, but no indication that this was associated with roller movement or changes in force.

The recordings of vibration data can be presented spectrographically. Figure 5.2 shows these from Trials 3 and 4. The amplitude values have been represented comparably in a -60 to -20 dB range. It can be seen that the radial position gives larger vibrations across a broad range up to 500 Hz. The axial position lacks these broad-spectrum effects but does show activity from 500-650 Hz.

Figure 5.2 shows that there is information being collected. The wide band of noise is fairly uniform for the duration of the forming period and there is no clear association of fracture with the signal. It is likely that the data collected here is simply noise from the machine - vibrations from the roller bearings, spindle and roller actuators. Although it is reasonable to assume that there exists some experimental set-up which can extract useful information from the process, this is not an effective set-up. The SNR is simply too low.

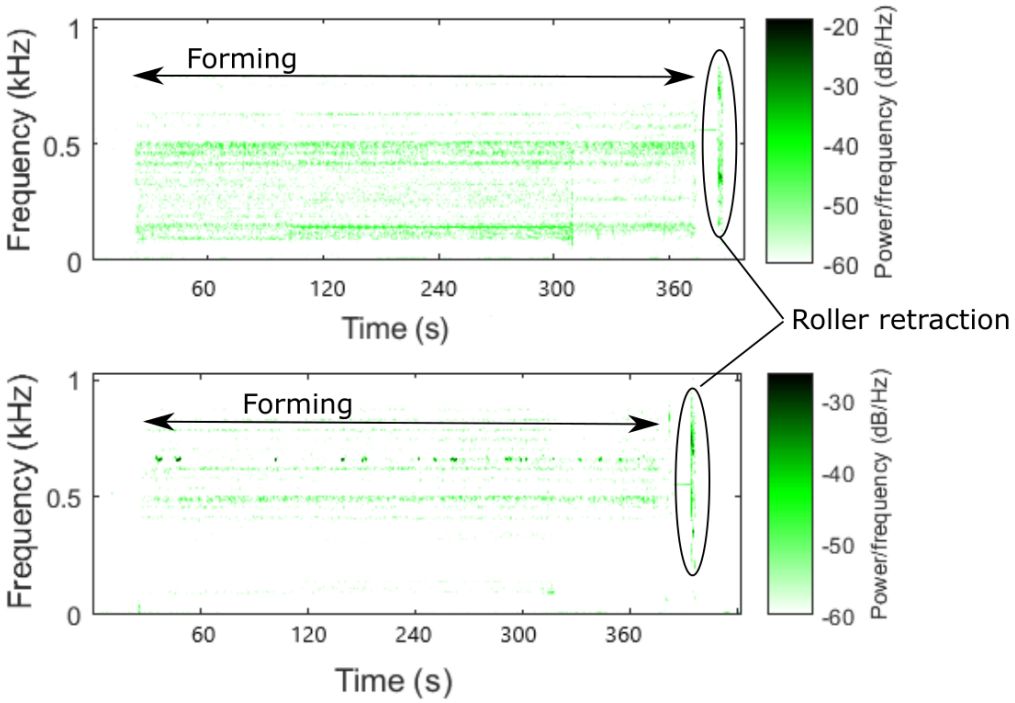

Figure 5.2: Spectrogram from trial 3 (above) and 4 (below).

The Goertzel algorithm was used to examine some of the frequencies with the highest magnitudes. Figure 5.3 shows one such examination - of the 650 Hz frequency observed in trial 4. These do not show any obvious relationship between the vibrations and the machine operation. Indeed, they show every indication of being pseudo-random noise.

In addition, there are many sources of vibration in the machine. These include the electrical motor components, coolant system, rollers, bearings, hydraulic slides, etc. As many of these components are rotating at the same RPM, it is reasonable to suggest that they will produce similar frequency vibrations which will be difficult to distinguish.

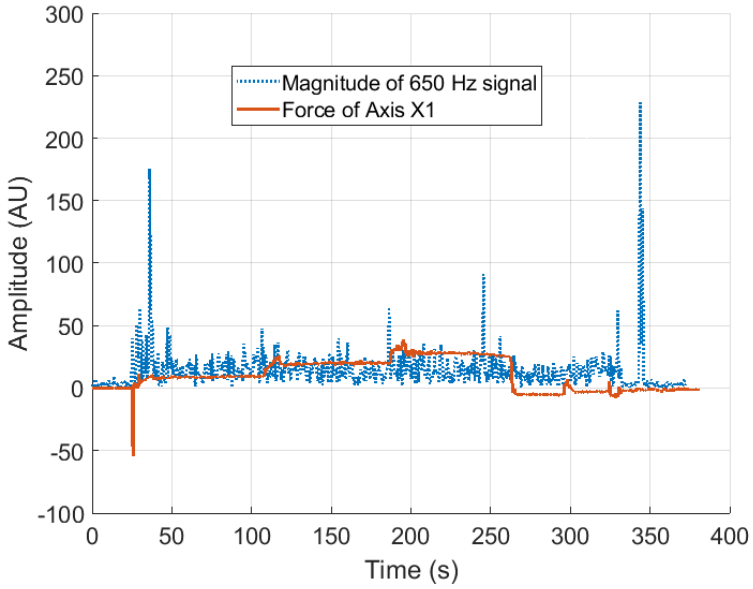

Figure 5.3: The relation between high-amplitude vibrations and deformation is unclear.

The challenge here is that the information is clearly available in the machine's sound and vibration signature, as it is detectable to operators. However the path for the vibrations, from fracture through the part, roller and bearings to the housing is complex. This path affects and transforms the signal, as well as introducing random noise. All this makes it very challenging to interpret. With the data collected, it is not feasible to connect the vibration behaviour to the process behaviours. Even when the fracture was clearly audible to the operators, there was no evidence of it on the

accelerometer as used. This is likely due to a sub-optimal experimental set-up.

5.2.5 Conclusions

The results indicate that contact measurement is impractical for this combination of process and experimental set-up. It is very challenging to detect microstructural deformations because of the complex and circuitous path taken by the vibrations. The detection of macrostructural material deformation and fracture is impeded by poor SNR for the same reasons.

In this situation, where the forming process is to some extent a 'black box' then adding a data source which is also highly complex and hard to understand will not readily develop process understanding (for more on this, see Figure 5.9). What is needed is a process monitoring technology that can be clearly linked to features of the process.

It is worth noting that the implementation of vibration monitoring in other process monitoring applications is usually based on a mechanical model of the system - often a damped-spring model. There is no such model for flow forming, which significantly hampers the ability to generate insight, because there is no prediction to compare the data to.

The acoustic method may offer a more direct path from DZ to data recording by acoustic propagation in the air.

5.3 Acoustics

Note: This section details work also described in the paper "A Novel Methodology For In-Process Monitoring Of Flow Forming" (Appleby et al., 2017).

5.3.1 Introduction

The literature discussed in earlier chapters indicates that IRF processes are poorly understood. They could have improved reliability with better instrumentation. Many existing process monitoring tools cannot be used on IRF, but acoustic monitoring is potentially effective. The challenges of using contact sensors (see Section 5.2) mean that micro-scale monitoring is impractical. But acoustic monitoring may be able to detect macro-scale deformation and fracture as it propagates through the air.

If a fracture occurs undetected, the tooling can friction weld onto the jammed part, causing serious damage. A monitoring system that can detect major fracture events would therefore be valuable.

Using the machine available, the WF-STR600, the FF process was selected for monitoring. This process suffers - in the AFRC - from unexpected fractures and failures of surface finish. These are often accompanied by noise or vibration audible to the human ear. This made a logical subject for monitoring, with obvious potential for capturing useful data.

5.3.2 Aims and scope

The principle aim of the acoustic work is to evaluate the use of acoustics for monitoring IRF. The machine operators can hear the change in noise when the process begins to go wrong, so the aims are to replicate this skill with a more repeatable monitoring system. The objectives are:

- To detect noises associated with fracture, if possible.
- To describe and categorise if possible those noises and their relation to fracture.
- To find, if they exist, indications in the acoustic data that precede failure.

The scope, as with the wider project, is limited to practical experimentation on industrial equipment.

5.3.3 Methodology

Similar to the vibration work carried out previously, acoustic monitoring is a very indirect approach. The sound comes from a variety of sources - the hydraulics, spindle motor, bearings and the three rollers.

The key input variables are the deformation rate and the presence of defects. Defects will be introduced by two methods - firstly using a range of radial deformation rates - this will alter the likelihood of failure and the failure type. Secondly, the use of artificial defects, which will allow a controlled investigation of the acoustic outputs of fracture. The time and location of the incidence of fracture is the key output.

Machine operators can hear the noise of major, catastrophic fractures from outside the machine housing. Smaller fractures can be heard under some circumstances, but this is more difficult. Ambient noises from the workshop environment and noises from the machine spindle and hydraulics can confuse the listener. An acoustic sensor (microphone) placed inside the machine housing should suffer less interference from ambient noise, and it should be able to detect the same failures as well as an operator, if not better. The frequency range for the sensor should be in the range of human hearing, i.e. 20 Hz to 20 kHz. For full details of the experiments, including the operating parameters for driving the equipment, see the published dataset in Appendix C.

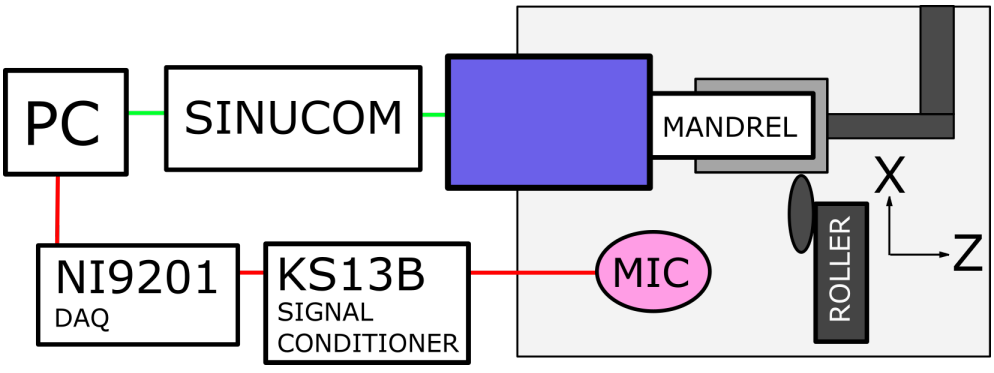

Figure 5.4: Acoustic monitoring equipment set-up schematic.

The equipment selected was a PCB Piezotronics 130E21 microphone. It was driven by a Kistler 5134B signal conditioner and connected to a National Instruments 9201 DAQ as shown in Figure 5.4. The DAQ interfaced to National Instruments *LabView SignalExpress*. The above system is cheap, portable and operable in real time. It is capable of recording the same acoustic information as a machine operator hears, and also of processing and replaying it.

The machine positions, speeds, feeds and forces are recorded by the Siemens *Sinumerik* software. The machine and acoustic data was collated and processed in Matlab 2016b. The data, initially recorded at 50 kHz, was examined and it was noted that above 380 Hz the signal was dominated by sound from the spindle. The data was therefore downsampled to 5 kHz to simplify processing, with a low-pass filter applied for anti-aliasing. Spectrograms were produced of the data using discrete Fourier transforms. These allow examination of the data in the time-frequency domain. The Sinucom machine data was time-matched to the acoustic recordings using the start of the noise band associated with spindle start-up.

Part selection and fault introduction

The nominal operating limits for FF are from 20% to 80% deformation. Forming less than the lower limit causes insufficient deformation for material flow, forming near or above the upper limit leads to failure because the material cannot deform so much without fracturing. For all the trials, a fairly standard FF testing program was used - three lands deformed to 25-50-75% respectively. The preform and part geometry are shown in Appendix B.3 and B.4. The X gaps were set as standard, at 1/3 of the reduction, and the Z gaps at 2 mm each. This geometry was selected for two reasons: it allowed the investigation of different deformation rates, and it is a typical test procedure for formability, meaning that the tests are industrially relevant.

Some of the parts were formed again with an additional 0.5 mm reduction, producing marginal deformations of 7, 10 and 21% - the total deformations in each land were 31-55-80%. The same X and Z gaps were retained. This geometry is shown in Appendix B.5 These high deformations allowed the examination of spontaneous fracture behaviour.

Al6061 was used in the annealed condition - its relative softness minimises the risk of tool damage in this sort of operational limit testing. In addition to the high deformation testing, defects were introduced into some of the parts. This was done to investigate the acoustic effects of failure.

Appendix D shows the planned list of experiments. If the acoustic monitoring shows a consistent response to fracture then this would mean that an emergency stopping system could be based on acoustic sensing. The risk of causing tooling damage in this kind of trial is not to be disregarded, therefore only a strictly limited number of parts were formed with defects.

5.3.4 Results

Characterising the audio signal

Each part that is flow formed showed similar characteristics in the sound signature. The acoustic signature of a forming operation is shown in Figure 5.5. At the start of the forming process, the motor spindle and coolant start up simultaneously, causing a large band of broad-frequency noise from 380 Hz upwards. The rollers move on hydraulic slides. Large movements of these slides in the radial direction cause noise at 190 Hz at the start and end of the process.

The signal has other notable features:

- Intermittent signal features at 50 Hz occur in all trials - this is probably electrical interference.
- Rumbling noises recorded as low frequency signals (sub 5 Hz). NB the spindle speed is 5 Hz.
- Where defects occurred, high-magnitude signals were recorded, notably at 10, 20, 35, 113, 118, 275 and 313 Hz

In this way, the spectrogram can be used to identify frequencies which are associated with fracture.

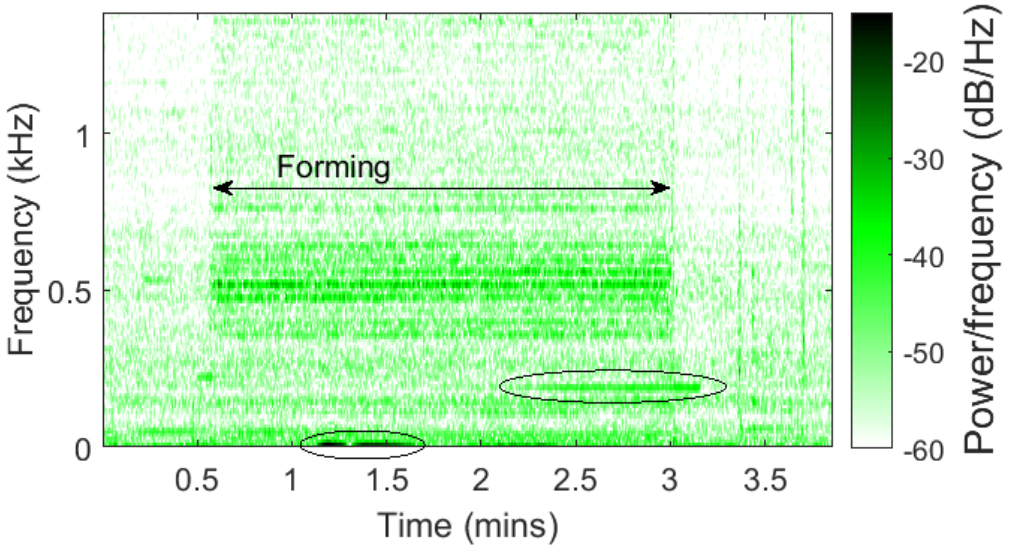

Figure 5.5: Acoustic data from a single pass FF part shown as a spectrogram. The spindle motor and coolant system make the band of high intensity frequencies shown across the middle of the graph. Hydraulic machine slide noise and rumbles at low frequency are circled.

Signal of process failures - single pass

Defects were added to a part before forming. Holes were drilled 200 mm and 400 mm from the flanged end of the preform with diameters of 2 mm and 4 mm respectively. In this case the holes did not instigate failure: the part formed with material flowing over the drilled defects. This resulted in the defects unchanged on the inside face but masked by moved material on the outside. The defects did not expand or propagate into circumferential fractures as expected - this is likely due to their small size and the high formability of the annealed Al6061.

The acoustic recording of the forming process is shown in Figure 5.6(a). Disturbances in the low frequency signal occur at 50 s and 1 m 44 s into the process. The recording of the roller positions shows that the noise at 1 m 44 s occurs when the roller is deforming the material with the second, larger defect. The elevated noise level which occurs at 50 s does not occur when the roller is in contact with the first, smaller defect. It is likely that the change from 25% deformation to 50% deformation causes this signal.

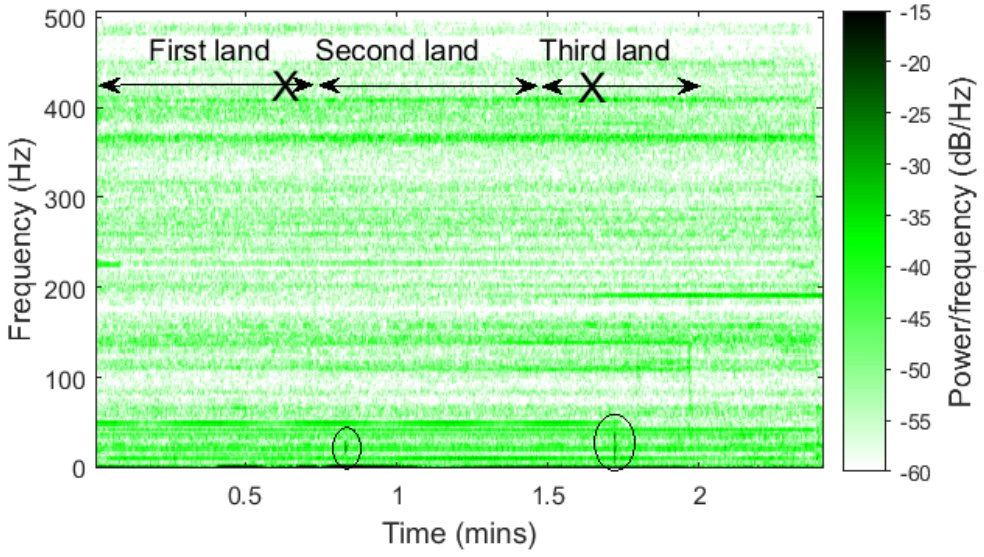

(a)

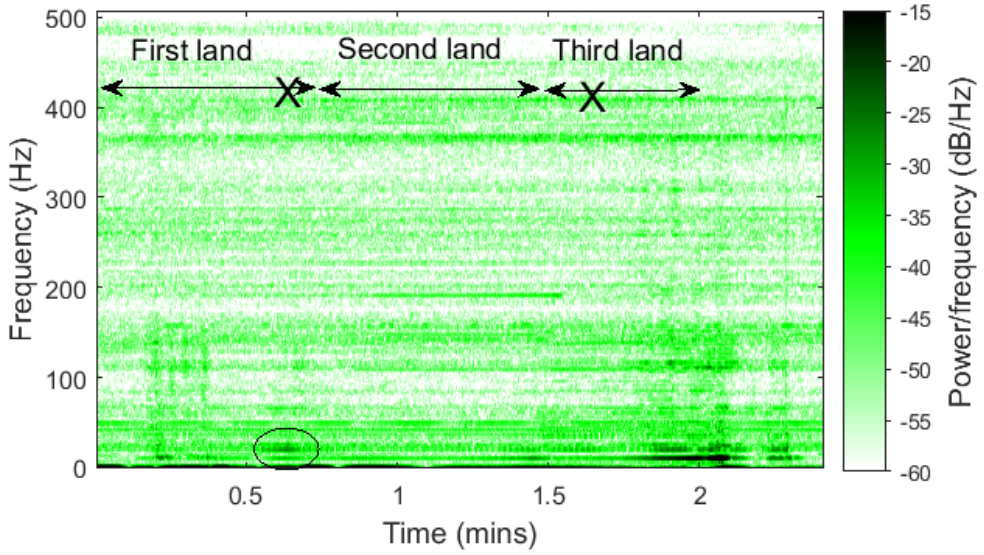

(b)

Figure 5.6: (a) Acoustic signal from a single pass flow forming with holes drilled in preform. The rollers pass the holes at 38 s and 1 m 44 s. Note acoustic signals at 50 s and 1 m 44 s. (b) Acoustic signal from a single pass flow forming with slots cut in preform. Note acoustic signal at 38 s.

Another part was modified with a bench saw before forming. Cuts were made: the first 7 cm long and a maximum of 8 mm deep; the second 9 cm long and entirely though the preform wall. They were located 200 mm and 400 mm from the flanged end.

Figure 5.7(a) shows how the process formed over the first slot. The material almost

sealed over the defect. The wall thickness after forming was 7.1 mm at the first defect. At the second defect the crack propagated circumferentially, causing total failure - see Figure 5.7(b). The trial was halted in an emergency stop - wall thickness was 2.4 mm at this second defect.

It can be seen in Figure 5.6(b) that there are large disturbances in the acoustic record. These are particularly notable below 40 Hz in frequency. Early in the first land, there is broad frequency noise. Then, just before the roller crosses the first defect, there is a rumbling at 30 Hz. As the part is undergoing deformation, the response in the part is altered by the presence of a defect, which is ahead of the rollers (in the z direction). This defect is likely causing unusual deformation in the part which shows up in the acoustic signal. Similarly, the second, larger, defect has accompanying sound. This time the sound is at various frequencies. These sounds accompany the beginning of the breakdown of the material and then the catastrophic failure of the process.

Clearly, the presence of major defects makes these trials somewhat unrepresentative of real-world IRF. But they demonstrate that it is possible to detect major process events through acoustics.

(a) 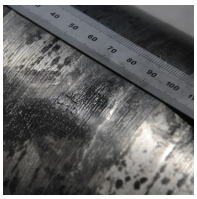 (b) 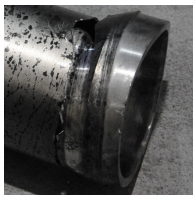 (c) 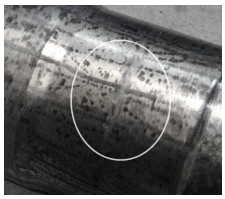 (d) 

Figure 5.7: Results from forming parts with defects: (a) Saw cut with material which flowed over it during forming, (b) Circumferential crack instigated by a saw cut, (c) Surface roughness, a prelude to spontaneous fracture, (d) A part formed in two passes showing drilled defects (circled) and circumferential fracture which occurred spontaneously under high deformation.

Signal of Process Failures - Second Pass

Figure 5.8(a) is the sound from a part being flow formed with a second pass . Despite undergoing high levels of deformation, the part formed without fracture. It can be seen in Figure 5.7(c) that under the highest deformation (80% in total) there is a roughened area on the part surface. This is the material beginning to break down.

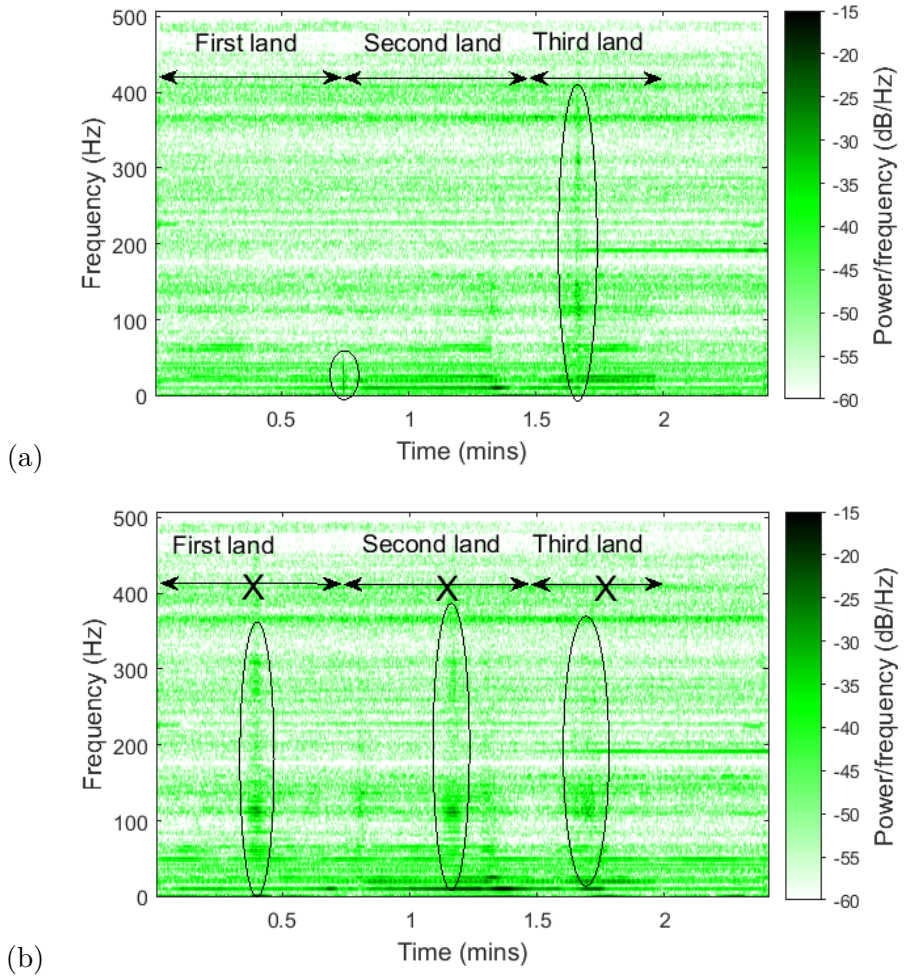

Figure 5.8: (a) Acoustic signal from a second pass flow forming with no added defects.(b) Acoustic signal from a second pass flow forming with holes drilled in each land (marked).

The sound which occurs at 45 s (Figure 5.8(a)) matches the time of the deformation at the transition between the first and second land. At 1 m 40 s, there is another band of noise which happens at the moment the roller is at the area of surface breakdown. It can be inferred that the noise is connected to the surface breakdown; an indicator of oncoming failure.

Another, otherwise identical, part had a hole drilled in the middle of each land after the first pass, of 4 mm diameter. The rollers formed the material over the first two defects. When this happened, there was significant noise in the frequency range 100-

500 Hz. There was also a strong 113 Hz noise at each of the defects - see Figure 5.8(b). In the middle of the third land (80% deformation) the part broke - this happened at 1 m 45 s. The fracture was spontaneous and happened at the same point in the process as the surface breakdown described above.

5.3.5 Conclusions

The results show that the approach and equipment used can capture data about the FF process. The most important region for acoustic monitoring identified by this work is below 400 Hz. Catastrophic failures and small defects both have an impact in the signal. It was even possible in one case to record a change in signal associated with surface damage that did not lead to a fracture.

There is no other existing method for gathering this sort of information. The demonstration that acoustic monitoring has the potential to detect fracture and near failure means that this approach deserves further attention. An acoustic system could potentially be developed that identified these behaviours in real time. This system could be used to improve process understanding and to iterate process design, as well as automatic emergency stop at failure.

There are limitations to this approach. Clearly, the data captured here is noisy and does not give granular detail about the process. It is a very indirect form of monitoring, which makes it hard to associate elements of the signal to elements of the process. Similarly, it cannot be said from this evidence that the acoustic signal has the potential to predict failure.

The main conclusion to draw is that acoustic monitoring can detect catastrophic process breakdown. To detect any more detailed process behaviour would require a better model of the acoustic behaviour and improved signal processing.

5.4 Research direction and research questions

This chapter has described work undertaken to examine some simple, non-invasive approaches to monitoring IRF. This work led to some interesting results, however

there may be more beneficial avenues to pursue for IRF monitoring.

5.4.1 Research direction

The results of these exploratory trials show that it is possible to extract information about IRF processes with minimal intervention. However, these results are largely limited to detecting very large changes in process behaviour. Minor defects are hard to detect, and the results are hard to interpret. It is possible that, with improved process understanding and signal processing, these techniques could be reapplied to give greater insight. But extended development in signal processing is outside the scope of this project, so this work is left for others to take up.

The results shown above give insight into the difficulty of matching a vague and noisy residual to a poorly understood process. For example, the inputs to the vibration and acoustic monitoring systems are unclear. They collect very general data - noise or vibration from the entire machine and its surroundings. The information of value must traverse a long and complex chain connecting the point of interest to the point of data collection. This makes it hard to identify the results of the process in the data.

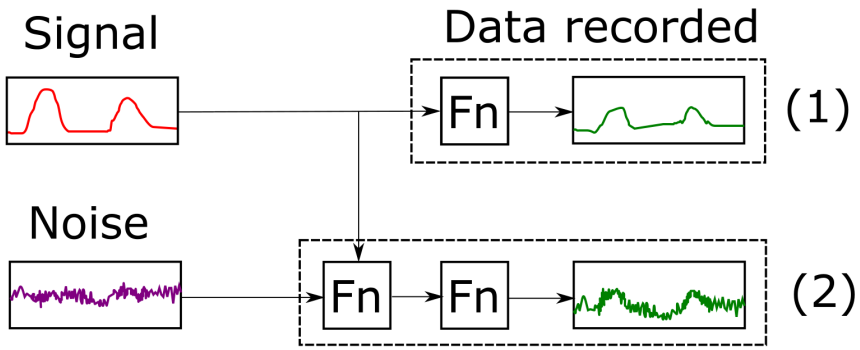

Figure 5.9: Indirectness introduces more noise and uncertainty to a signal. The data collected in method (1) has a simple path, where method (2) has a more complex path and more noise.

Figure 5.9 shows that a system with a complex path from signal in to data out results in a poorer representation of the process in the data. The simple path with fewer transformative functions (Fn) shown in (1) gives an output closely related to the input. The more complex the path from data to sensor shown in (2) has more opportunities

to introduce noise to the signal. This complex path confuses the relationship between the process and the data output.

A monitoring approach which was more direct (1) would suffer less from this problem. A more direct design would place the sensor closer to the DZ and remove some of the external sources of noise. A set-up like this should improve the ability to link the data outputs to changes in the process. It may be possible to gain much better process insight with this approach.

5.4.2 Selection of US monitoring

Investigations into the application of these technologies was carried out, and is discussed in Chapter 5. The results of this work led to a third technology selection, US monitoring. The development of this monitoring system is discussed in Chapter 6 and its testing in Chapter 7.

5.4.3 Research questions

The broad research question **Can monitoring provide insight into an industrial IRF process?** can begin to be answered. The question posed in Section 3.6 was: can vibration and acoustic monitoring detect major process changes in IRF? This can be answered simply: Major and some minor happenings in the process can be detected. But to do so consistently would require much more work.

The next research question is **What insight can US monitoring provide into an industrial IRF process?** Chapters 6 and 7 will attempt to answer this question.

5.5 Chapter conclusions

In this chapter, the methods examined were remote and non-invasive methods were examined. Although they can detect large changes, they do not capture granular detail. This is because it is hard to relate small changes in the process to small changes in the signal. It might be possible to fix this this with signal processing, or with process modelling. The lack of a robust model of the vibrations from the process certainly

limits the ability to interpret the data. The aim of this body of work as a whole is to improve the monitoring of IRF as it exists in an industrial setting. Therefore the development of simplified models is a sideline. Instead, it would be better to look at monitoring options that address the process more directly.

A more direct method could have the ability to capture more detailed process information. It would also increase the potential to link the signal behaviour to the process behaviour. For that reason, the decision was taken to return to the options examined in Chapter 3. As noted in that chapter, the most promising technology for a more direct look at the process was US monitoring. Using the results shown in this chapter, it was possible to secure funding for an US system to monitor IRF.

Chapter 6

Ultrasonic monitoring system development

6.1 Chapter introduction

Better monitoring for IRF would allow improved understanding, modelling and operation (Chapter 2). It is described in Chapter 3 how effective monitoring and control requires a reliable model which can be linked to measureable data to produce process insight. Chapter 5 shows how the vibration and acoustic monitoring techniques were found to be limited in their capacity for gathering information about the operation of the process. This is largely due to their indirect nature which, when paired with the non-deterministic process render it difficult to make insights.

Given these challenges, US monitoring presents certain advantages. Work discussed in Chapter 3 shows how a US solution could focus on the exact area of contact - the DZ. Data obtained from the DZ can then be combined with a model of ultrasonic behaviour to help understand the forming behaviour through the process. There is potential capacity to measure a suite of variables including material thickness, contact pressure and area, and crack presence and location.

The US approach also offers the potential to make much less indirect measurements of the forming conditions than acoustic or accelerometry measurements. If the UT can

interrogate the roller-part interface then it can be more easily understood what physical effects are being measured.

Funding was secured from the *HVM Catapult: Digital Manufacturing Fund* with the aim of creating a more direct monitoring approach to the DZ with the capability to measure several variables. The system design was carried out to capture these advantages while preserving the integrity of machine function.

The system was designed with the principal aim in mind: to test the viability of US technology as a monitoring solution for IRF processes. The created system will not be optimal. But it will attempt to lay the groundwork for future work in this area by identifying the possibilities and pitfalls of this new combination of technologies.

In developing a new system, many decisions are made that influence the type and quality of data which can be collected. Each choice necessarily removes other options. This chapter will lay out the rationale for the design of the US system.

A note on design authorship

The design of the system was carried out by the author with the assistance of Tribosonics Ltd., a company which specialises in producing US monitoring systems. The options available in the configuration and components were researched and considered by the author, and the design decisions were made by the author. The work of fabricating the system was done by Tribosonics with input from the author. Tribosonics staff carried out some work which fell outside of the project scope: specialist US modelling, and manufacture of the DAQ. The DAQ constructed was an simply industrial PC with a high speed board to control the sensor, running LabView to collect the data. They also advised briefly on the commissioning of the system. The entirety of the experimental planning and execution, as well as the data processing and analysis, were carried out solely by the author.

6.2 Initial design

The design of the UT system was carried out with specific aims in mind. A set of priorities and constraints was devised based on the capabilities of US monitoring and the lessons learned in Chapter 5. These were then applied to the main choices in the design - the type of sensor and coupling, and its positioning in the machine.

The design followed the process shown in Figure 6.1. In essence the process had three stages. First, the priorities were set and the information gathered to determine which decisions were critical in affecting other elements of the design. A sensible sequence was found for taking the decisions. The options selected were considered as a whole and then reviewed against the initial criteria.

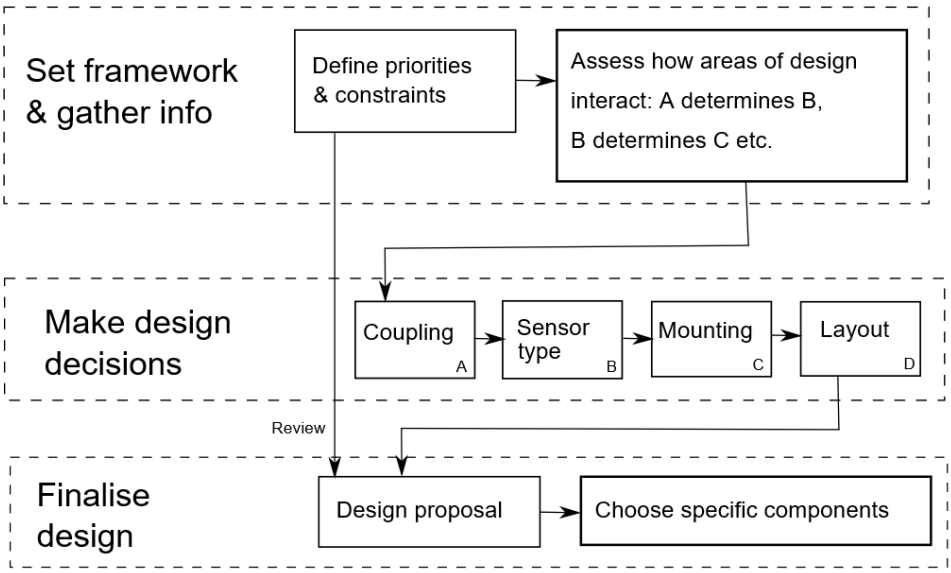

Figure 6.1: Overview of the system design process.

There are a number of requirements for the development of the system (see the system properties as discussed in Sections 2.2 and 3.3). These requirements are discussed in detail in Section 6.2.1.

6.2.1 Priorities and constraints

The design of the US system was guided with specific aims in mind: firstly, to optimise the signal quality and information gathering capacity, and, secondly, to minimise interference in the normal operation of the machine. These objectives were pursued throughout the process of system design. They can be given in more detail as three priorities and four constraints. These are derived from the research developed in earlier chapters.

Priorities

The priorities are drivers to produce the best output possible from the system. They are as given as follows:

P1 The UT should interrogate the DZ as directly as possible.

P2 The configuration should be suitable for capturing data that relate to contact properties, material thickness and the presence of defects in the forming process.

P3 The data quality and SNR should be prioritised even if this results in some challenges for implementation.

The first priority for the design is one of proximity to the deformation zone. One of the challenges of earlier investigations is the difficulty of connecting the data to the behaviour of the process (see Chapter 5). This challenge exists because of limitations with the technologies used - their output has an indirect and convoluted connection to the process. To access the benefits of US monitoring, it is desirable to have the UT point to the DZ as directly as possible - this means a position near the DZ with line of sight to the DZ. This will assist in the analysis and interpretation of the results.

The next priority is related to the continuity of data collection. Since the aim of the system is to gain insight throughout the process, it is necessary to have a continuous process of data collection. A sensor fixed to one point on the roller would only gather data when that part of the roller was contacting the workpiece. This causes two issues: low sampling rate and poor coverage. For a typical FF spindle speed of 240 rev/min,

the effective sampling rate of a single fixed sensor is once per revolution, or 4 Hz - a poor sampling rate, especially for a system where catastrophic failures can unfold quickly. Additionally, the roller and mandrel turn at a similar speed (with only a small slip), meaning that a single, fixed sensor would survey the same part of the workpiece on every rotation. Even with multiple fixed sensors, there would be blind spots on the workpiece that would never be scanned. A degree of intermittency may be acceptable if that is the only way to implement US sensing, however, any delay in detecting changes in the process would be a disadvantage.

An important broad aim is that the quality of the data should be as good as possible - i.e. to maximise the SNR. This is most obviously the priority which will conflict with the system constraints listed below. Maximising the SNR with disregard to constraints could result in the machine being inoperable.

Note that these priorities depart somewhat from the earlier aspiration of minimal intervention. Chapter 5 concluded that these low-interference methods were unsuitable for collecting detailed information. Instead, this new approach aims to strike a balance: limiting process interference as much as possible while collecting richer data than the previous methods.

Constraints

The constraints relate to practical limits on the potential to maximise the priorities. There are four principal constraints to the positioning:

C1 The mechanical integrity of the roller and housing must be maintained.

C2 The position must provide the necessary clearance for the UT and its connectors.

C3 The mounting must be stable and resilient during the operation of the machine.

C4 The UT must be suitable for exposure to the liquids and temperatures in the forming environment.

The primary constraint is the preservation of the machine functionality. While modifications are possible and may be necessary, it is vital to protect the capacity of

the machine to function normally, for commercial, research and safety reasons. The commercial reasons for protecting an expensive and complex machine are obvious. For the benefit of the research, the machine should stay as near as possible to its original operating characteristics - the experimental set-up should reflect the machine's industrial operation. The aim of this research is to observe the machines normal function without interference. Finally, the safety of the process is vital. The machine components undergo very high stress during forming. Failures could occur if they are modified in an unsuitable way. To protect the machine and operators, any modifications will need to be carefully considered and analysed with respect to the effect on the machine.

Space for the UT and its connectors is the second constraint. Figure 6.2 shows the limited space around the roller and housing. The UT will need to fit in the available space. However this will restrict the available locations due to limitations on material removal (**C1**).

The cabling for the sensor could in theory be wireless, but in this case, the requirements of a wireless sensor (power supply, data recorder and transmitter) would be too bulky to fit in the available space. Therefore the UT must be cabled, and the design and position must allow the cabling. If the UT is in a rotating position (fixed on the roller), a slip-ring system will be needed. If it is fixed, then a path for the cable should be planned. Any access for coupling fluid, if necessary, should also be planned in at the design stage. These points, which might easily be overlooked, are vital to simplify the commissioning and operation of the final system, as well as the fulfilment of **C3**.

The mounting system should be stable. This is important for meeting **C1** and **P3**. During operation, the flow former undergoes high forces and high rotation speeds. If the UT were to catch on a rotating element during forming it could cause damage to the machine or the sensor. The mounting of the UT must therefore be resilient to any forces or shocks that may occur in the process cycle. For example, when the machine's hydraulic slides can move and stop abruptly, which would cause a sharp deceleration to an attached sensor. In addition, any vibration in the mounting system of the UT

would be problematic for the data quality (**P3**). This is because the nature of US measurement is dependent on the linear distance of the UT from the point of interest. If the mounting system allows vibration of the UT, it may affect the data in a way that cannot be distinguished from the effects of the forming process. This is essentially the problem encountered in Chapter 5 which this new system aims to alleviate. Therefore the mounting system must be stable.

The final design constraint, **C4**, is related to the resilience of the sensor. The environment in the flow former is hostile to electronics. Although the process is nominally cold forming, it does experience elevated temperatures. There are oil- and water-based coolants in the DZ which contain powerful chemicals, known to degrade some plastics.

The process of design is therefore one of balancing these seven competing interests. Each was considered in the choices made in the design process. The main choices for designing the system were the type of sensor; the sensor interface; the position and type of mounting; and the selection of the DAQ. These are discussed in the following sections.

6.2.2 Layout

The basic layout of the system is limited by the requirements of the application of US sensing to the FF process, as discussed in Section 3.4.6. This means that the sensor must point directly at the area where the roller contacts the material. This could happen from the roller side or the mandrel side. However, the axial movement of the rollers along the mandrel and the practical challenges of accessing the mandrel for this purpose make the mandrel side an undesirable option. If the sensor moves with the roller, these issues are avoided or simplified. Figure 6.2 shows the roller housing layout, with the available space and limitations. for more detailed machine information, see Sectionsec:srt.

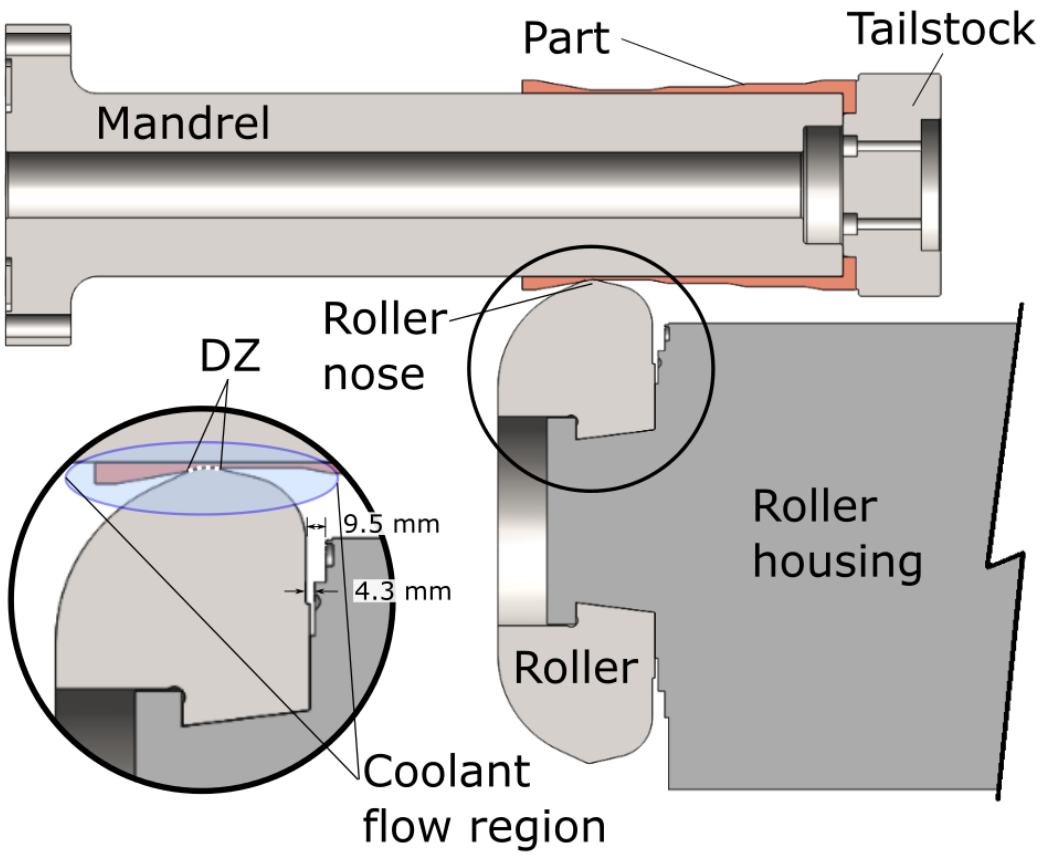

Figure 6.2: The housing and roller, showing the available space and other constraints. The space around the roller is very limited, and the nose of the roller is obscured by coolant flow during operation.

6.2.3 Sensor type

The most crucial component of the whole system is the sensor itself. The chosen sensor needs to meet the priorities and constraints - the most relevant are **P3**, **C2**, and **C4**. That is, the chosen UT needs to be able to capture high quality data with minimum clearance in a harsh environment.

UTs are available in a variety of sizes and types. For general applications, however, size is not a priority, so there is a poor selection in the smaller size ranges. The design and fabrication of bespoke UTs falling outside the scope of the project, it was necessary to work with the commercially available options. Many UTs are designed longitudinally (Figure 6.3), with the cable extending from the end. This configuration

naturally takes up more room than a design with the connector attaching to the side - another limitation. Another consideration is that the UT must be available in the appropriate 5 MHz frequency range (see Chapter 3).

Figure 6.3: Longitudinal sensor (left), perpendicular sensor (middle) and bubbler probe (right).

There are two main types of UT: shear and non-shear (longitudinal). Shear transducers can send both shear and longitudinal waves, whereas longitudinal transducers send only the latter. In general, longitudinal waves are effective at examining geometries that are perpendicular to the wave, whereas shear waves have advantages for examining oblique features. The longitudinal waves allow the detection of contact pressure behaviour. The shear wave response can be used to measure the stick-slip condition (Mulvihill et al., 2011). In this case, as the US signal is produced by the transducer and the information is gathered by how it is reflected by the system, the question is what sensor type can be: a) practically installed, b) gather continuous data, and c) gather the most useful data.

For the fast-changing properties of IRF, continuous data collection is important to understand how changes in the system develop. For more on this issue, see Section 6.2.4 below.

Some UTs are available with a connected fluid cable for the transporting coupling fluid. The pipe typically surrounds the head of the sensor to provide a constant flow of coupling fluid (Figure 6.3). This set-up is called a *bubbler* and is designed to make

it easier to maintain a good, consistent fluid couple (see Section 6.2.4). Bubblers are only available for a limited number of probes and take up additional room.

Conclusion

The different UT varieties offer different advantages as shown in Table 6.1. Because of the interplay with the coupling type, the decision on the sensor type must be taken in conjunction with the coupling decision - see Section 6.2.4.

Table 6.1: Sensor type

	Advantages	Disadvantages
Shear	Allows shear wave monitoring	Must be fixed couple
Non-shear	Allows continuous monitoring	No shear wave monitoring
Bubbler	Helpful for fluid coupling	Bulky, limited selection

6.2.4 Sensor coupling

The type of coupling between the sensor and roller is an important decision that will have a major effect on the project. The choice of transducer type and coupling are interlinked because shear transducers would require physical bonding to the roller, whereas longitudinal sensors can be fluid coupled. A fluid-coupled or fixed sensor would give the system different operational properties, strengths and weaknesses.

The sensor type constrains the type of coupling between the sensor and the roller. A non-shear sensor can be coupled to the roller through a fluid medium - a *fluid couple*. Shear waves cannot pass through this medium, so a shear transducer would need to be in physical contact with the roller. In other applications, this is normally achieved by bonding the UT to the surface with adhesive or clamping it with bolts.

The bonded connection would need to be fixed to a single point on the roller and wired out through a slip ring. This would limit the system to one measurement per revolution (see Figure 6.4).

The requirements of shear-wave transducers in the coupling realm are relevant because of the capacity to capture shear information. In the IRF context this would

mean the difference in speed between roller and part, which is termed slip. Although slip is understood to exist in the industrial setting, it is little commented on in the academic literature (Wong et al., 2003; Marini et al., 2015). Slip is not regarded as a key forming parameter.

A fluid couple uses a fluid intermediary (in this case coolant) between the transducer and the measured part. This allows a continuous connection between a fixed transducer and a moving roller.

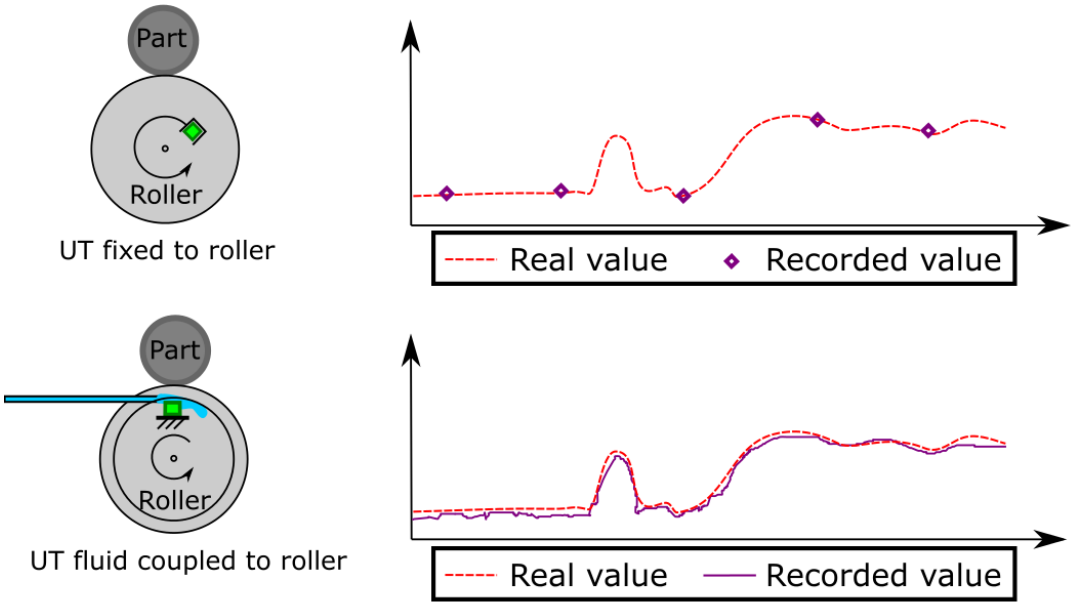

Figure 6.4: Fixed coupling (above) and fluid coupling (below). Note how the the fixed sensor gives correct intermittent values but can miss sudden changes, where the fluid coupling continuously scans the contact area.

The essential benefit of fluid coupling is that it would allow a set-up which could continuously monitor the DZ (**P2**). The interface of the turning roller and part are fixed relative to the roller housing. This means that a UT which was fluid-coupled to the roller could continuously survey the DZ (**P2**).

It is clear that the choice of coupling is not a simple choice. There are advantages and disadvantages of fixed and fluid couples, which are discussed below. Creating an interface area on the roller for the sensor to couple would be necessary, which would mean significant material removal across the full 360 degrees of the roller. The large

nature of this material removal, which is problematic for **C1**, would mean that the cross-sectional area of material removed would need to be limited. The nature of fluid coupling would make it more challenging to commission and operate the system. If the coupling faces are not parallel then the signal quality will quickly drop off; turbulence or air bubbles on the couplant flow could also disrupt the signal. These issues are potentially a problem for **C3**. There is also a potential for poorer SNR as discussed in Chapter 3.The STR600 has a continuous flow of coolant which could be used for coupling.

Conversely, the benefit of a fixed couple is that the signal quality would be improved (**P3**). Once the sensor is bonded to the substrate, there is typically an excellent signal. An application discussed in Section 3.4.4 featured a rolling wheel on a surface with the sensor is inserted under a plug in the wheel. This approach is unsuitable here because of the high point load on the roller face and the complex shape of the roller nose. Instead, space for the UT would need to be cut into the roller. If this approach was pursued, it would be possible to remove a large amount of material. This is because the material removal would only occur at one point in the roller, rather than the full channel removal needed for a fluid coupling. This fixed sensor would scan the part once per revolution.

As noted above, the effective sampling rate of a fixed sensor would be low (in the 4-12 Hz range for flow forming). In addition, this sample would be taken at the same rotation angle of the part and mandrel each time. Consider when the fixed sensor in the roller is aligned to the part. After one full rotation, it is again aligned. But the mandrel and part have also made one full rotation. This means that the fixed sensor can effectively only make a line-scan of a narrow strip along the length of the part. By comparison, a fluid-coupled sensor which scans continuously would be able to scan the path of the roller over the tool - scanning a helical motion on the part surface. This means that the entire part and the entire toolpath can be scanned with a functionally unlimited sampling frequency.

Conclusion

The fixed and fluid coupling approaches offer different advantages as shown in Table 6.2. The fluid couple would allow continuous interrogation of the DZ throughout the entire forming process but needs a lot of material removed. This material would have to be removed in a channel around the full circumference of the roller. There are also some challenges in coupling, although there is a ready supply of coolant.. The fixed couple would potentially give a better SNR with less material removal, at the penalty of an intermittent signal. Because of the benefit of continuous surveying, fluid coupling was chosen as the better option.

Fluid coupling forces the decision on sensors - it can only be a non-shear sensor. There is a relatively small available range of compact immersion-proof sensors in the correct frequency range of 5 MHz. The transducer from Olympus Scientific Solutions (IR-0508-R-RU) was selected as the most compact UT that met the requirements.

Table 6.2: Coupling type

	Advantages	Disadvantages
Fixed	Better SNR	Intermittent signal
Fluid	Continuous monitoring	Coupling difficulties and losses

The fluid-coupled approach was selected for its continuous sensing ability. This meant a non-shear sensor.

6.2.5 Sensor mounting

The positioning of the sensor in the machine is an important area for the design. A wide variety of configurations are possible and will deeply affect the capacity to collect good data. The UT transducer should be mounted so as to meet **P1** and **C1**-**C3**.

Maximising the capacity for data acquisition is necessarily a speculative process, aided by modelling and process understanding. The starting point for the design was a internally mounted position just behind the nose (Figure 6.3). This position is the optimal one from the perspective of US sensing (**P1**,**P3**). This is because of its proximity to the DZ. It would require significant material removal in the area of the roller that undergoes significant stresses. It would also need to be a permanent

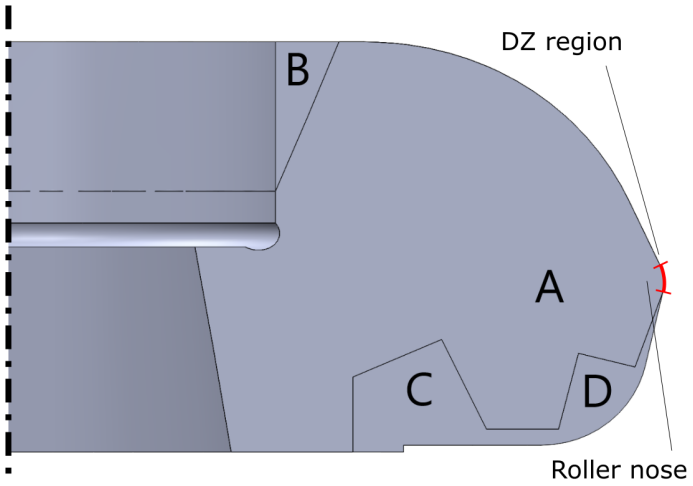

Figure 6.5: Proposed mounting locations shown against the unmodified roller: A) Fixed internal, B) Outer, C) Inner, D) Nose.

fixture (see Section 6.2.4). Limiting the material removal from the roller (**C1**) is a prime consideration. Therefore this design would have to be a fixed sensor at a single point.

Alternatives were considered suitable for a fluid-coupled continuously sensing set-up. These are more limited in where they can be placed due to the requirement to remove a large amount of material. Three possible locations were proposed on the roller: the outer face ("outer"), the inner face near the axis ("inner") and the inner face near the nose ("nose") - see Figure 6.5. There were differing advantages and disadvantages for each position, given in Table 6.3.

Each configuration was considered for its ultrasonic response, ease of mounting and effect on the integrity of the roller.

The primary consideration for the quality of response is the US reflection behaviour of the face of the roller. The US propagation dynamics for the outer and inner positions were modelled by Tribosonics using SimSonic software. Figure 6.6 shows the results. Simplistic assumptions were used, taking D2 steel properties (see Appendix B.7) and modelling the roller in free air. The aim was to compare the positions on the complexity of propagation dynamics, i.e. the directness of reflection from the area of interest (the DZ). The inner position (C) was highly affected by the curved back face, resulting

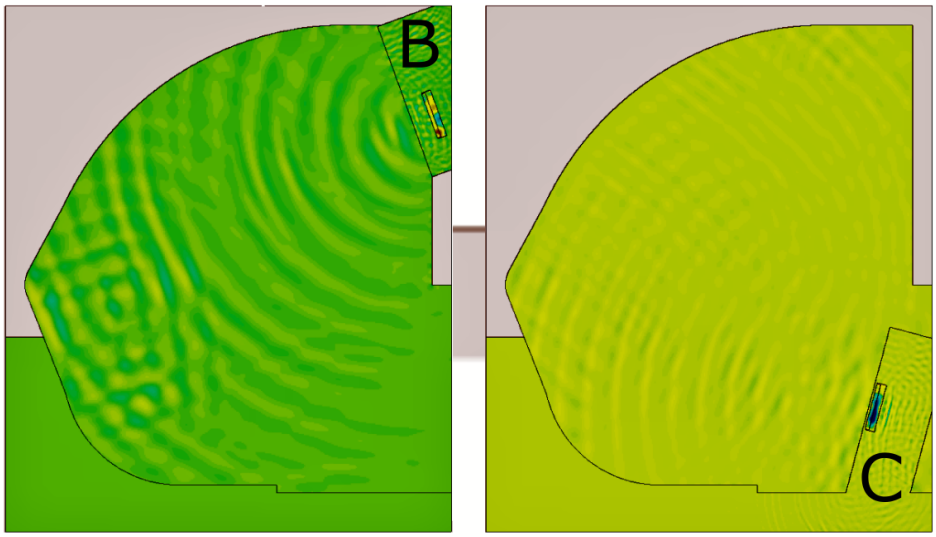

Figure 6.6: US simulations: Outer (B) and Inner (C).

in complex reflections which spread out. This means that the US response could be somewhat distributed in time and confused by complex reflections. The outer position (B) has simpler propagation dynamics.

The most obviously preferable after the modelling of the ultrasonic response was the inner position. This was due to the lack of complex reflections from the face - the relatively simple acoustic path limited the complex reflections. However the majority of reflections were from the rear face of the roller - not the front where the main contact area is. The front face is at a steep angle to the sensor direction, meaning little data will be gathered from this face. On the plus side again, the outer position requires very little material removal. However, this position requires some sort of frame around the roller to hold the sensor. This would be at risk of vibrations interfering with the signal (**C3**).

The inner position results in strong reflections from the front face of the roller. Although there are some complex reflections, this should ensure a good collection of data from the DZ (**P1**). In order to get the necessary clearance, a significant amount of material needs to be removed. It is important to be sure that this removal will not interfere with the machine operation (**C1**). The opportunities for mounting the sensor in this position are good, as it can be bolted to the housing of the machine (**C3**). it

will be possible to run the cables out along the housing (**C2**).

The nose position is the best for constraints **C1**-**C3**. It needs very minimal material removal. It would be an easy position to mount and connect the sensor. However it has a major problem. The UT points to the front face (**P1**), but at a very steep angle which is problematic for the data quality (**P3**). Much of the information from the DZ is lost in this configuration.

Conclusion

Table 6.3 shows the relative strengths and weaknesses of the four positions which were considered. The internal position was used only as a reference point as the material removal required is too significant **C1**. The outer position has some points to recommend it - little material removal and simple US response - but the practical problem of a frame mounting is deemed too major. In addition the modelling shows that this position focuses too much on the back face and not enough on the front. The nose position has too poor a US response to be acceptable, because of the high interface angle. The inner position is a compromise. It has some weaknesses (complexity of mounting, large material removal) and some strengths (good signal strength, perpendicularity to front face).

Ultimately, the quality of the signal from the front face is not met sufficiently by the other designs. Therefore the inner position is the most suitable, and the challenges in positioning and material removal need to be overcome.

6.3 Detailed design

The decision was made to move forward with the design of a system with a non-shear UT, fluid coupled, mounted on the inner side of the roller, near the axle unit, pointing towards the front face. A detailed design was developed.

Figure 6.7 shows the proposed material removal (see also Appendix B.1). The modification is sized to the IR-0508-R-RU, and designed to point it at the DZ on the front side of the nose. The inner edges of the channel are broken by radii to reduce

Table 6.3: Mounting position

	Advantages	**Disadvantages**
Internal	Ideal position for US response	Most significant material removal in high stress area, permanent fixture only
Outer	Least material removal, strong US response	Issues with external mounting, angled to back face
Inner	Good US response, sensor angled to front face	Significant material removal and complex mounting
Nose	Easiest mounting/access	Poor US response

stress concentration. The design also specifies the removal of additional material off the back face to allow access for cabling (**C2**). The material of the roller was left otherwise unaltered and the alterations were machined with a total runout tolerance of 0.1 mm and 0.8 Ra finish.

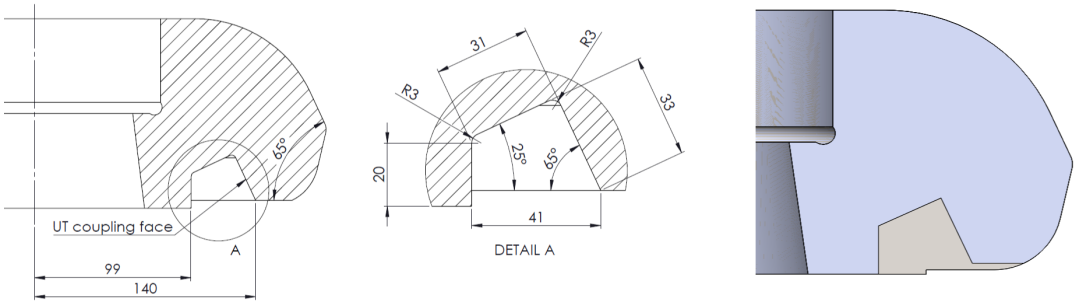

Figure 6.7: Detailed proposal for modification of the roller showing dimensions (left and centre) and comparison with unaltered roller (right)

Roller modelling

Any indication of serious risk to the roller integrity at this stage would require a major redesign of the modification, so modelling was carried out to assess the impact on the roller integrity from the modification (**C1**).This was done in Abaqus: the roller was constrained by its axle with 350 kN point load on the roller nose the maximum cut-out force of the machine. The outputs were the deflection and stress through the roller.

Figure 6.8 shows the results of the modelling. The modelling shows that there is no significant risk of failure. The stresses are highly concentrated at the nose and do not cause significant deflection or stress at the modified channel in the roller.

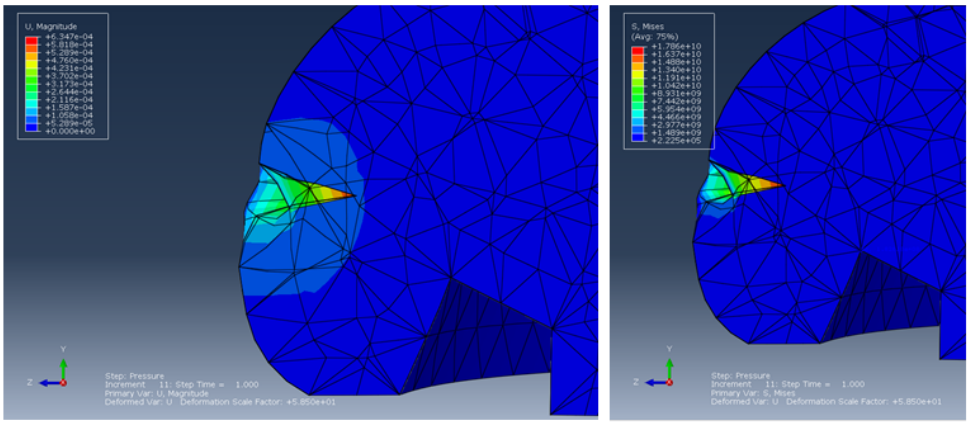

Figure 6.8: Abaqus simulations of deflection (left) and Von Mises stress (right)

6.3.1 Bracket design

The mounting system is designed to be simple, stable and adaptable. It consists of a simple bracket, which can be mounted onto the roller housing using existing bolt holes. The positions were determined using hand measurements, and the bracket was given long bolt holes to allow lateral movement - see Figure 6.9.

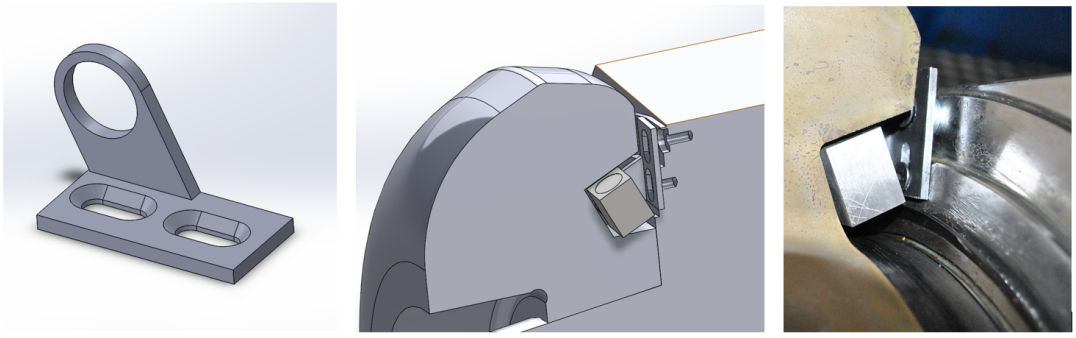

Figure 6.9: UT mounting bracket: CAD models of bracket (left) and assembly (centre). Manufactured bracket in place (right) with UT and sectioned roller (see Section 6.4).

The bracket was designed to mount the UT in the roller channel by clamping it as a

washer where the connector screws onto the sensor. This allows for angular adjustment. It was designed as a flat component with bending allowances (see Appendix B.2). It was fabricated in mild steel in the AFRC workshop where the flange was bent on the press brake.

6.3.2 Coolant control

The coolant system for coupling is designed to make use of the existing coolant. The HOCUT 795 B-EU coolant is pumped by the machine to three pipe heads, mounted on each of the three rollers. These heads then have nozzles which can direct the flow of coolant over the rollers - see Figure 6.10.

The coolant in the machine serves a function of cooling the parts and lubricating them. The coolant is pumped cyclically from a 4000 litre tank, and cannot be altered in part, only replaced in its entirety. It is not possible to run the machine without coolant (although this would make experimentation much simpler) because of the risk of damaging the tooling. Because this is an industrial machine and the tooling is used regularly for commercial work (experimentation was carried out in gaps in the commercial schedule), it was not practicable to change the coolant within the scope of the project.

It is clear, however, that the major consequences of this are practical rather than affecting the experiments. The coolant, being water-based, will have US properties close to that of water. Because the other materials in the system (metals) have radically different US properties, any small deviation from the characteristics of water will be irrelevant.

A new nozzle was fabricated with a section of curved pipe. The pipe will deliver a flow of coolant onto the interior coupling face of the roller which fills the gap between the UT and the roller. The exact behaviour of this system is hard to describe as it required minute adjustments. However the general principle of improving the noise is described in Section 7.4.1.

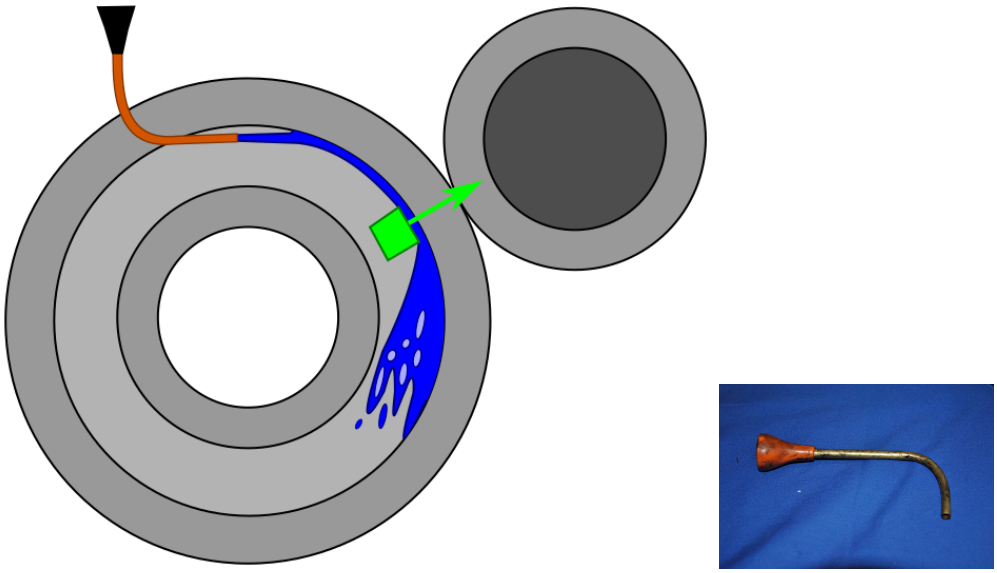

Figure 6.10: Coolant flow schematic with detail photo of the pipe which directs the flow.

6.4 Commissioning

An important part of the development work was the commissioning of the system. There were a series of challenges in the installation and operation of the system. The most notable related to the mounting system, the control of the coolant, and the selection of operating parameters. The aim of this commissioning process was to carry out very simple tests and assess whether the system could produce a signal.

The initial commissioning of the system took place over two months. A Tribosonics engineer was on site for two days to advise on the operation of the software and use of the equipment. The testing of the system proceeded systematically through increasing levels of complexity. Initially, fully static tests were conducted with the roller off the machine. Then the same tests were attempted on the machine, statically, and finally the rolling condition was attempted.

Static tests were carried out using ultrasonic couplant gel and then liquid coolant to check for the presence of a reflection from the roller nose. A test was then carried out to examine the response to contact on the nose. With the sensor operating and the nose coated with couplant, a hand pressed against the nose shows a reduction in the

reflection magnitude. This indicates that the system is working as expected.

The system for data acquisition is an industrial PC using a Labview virtual instrument. This simple software controls the operating parameters of the transducer and records the data. The minimum sampling rate is 160 Hz. Figure 6.11 shows the data captured.

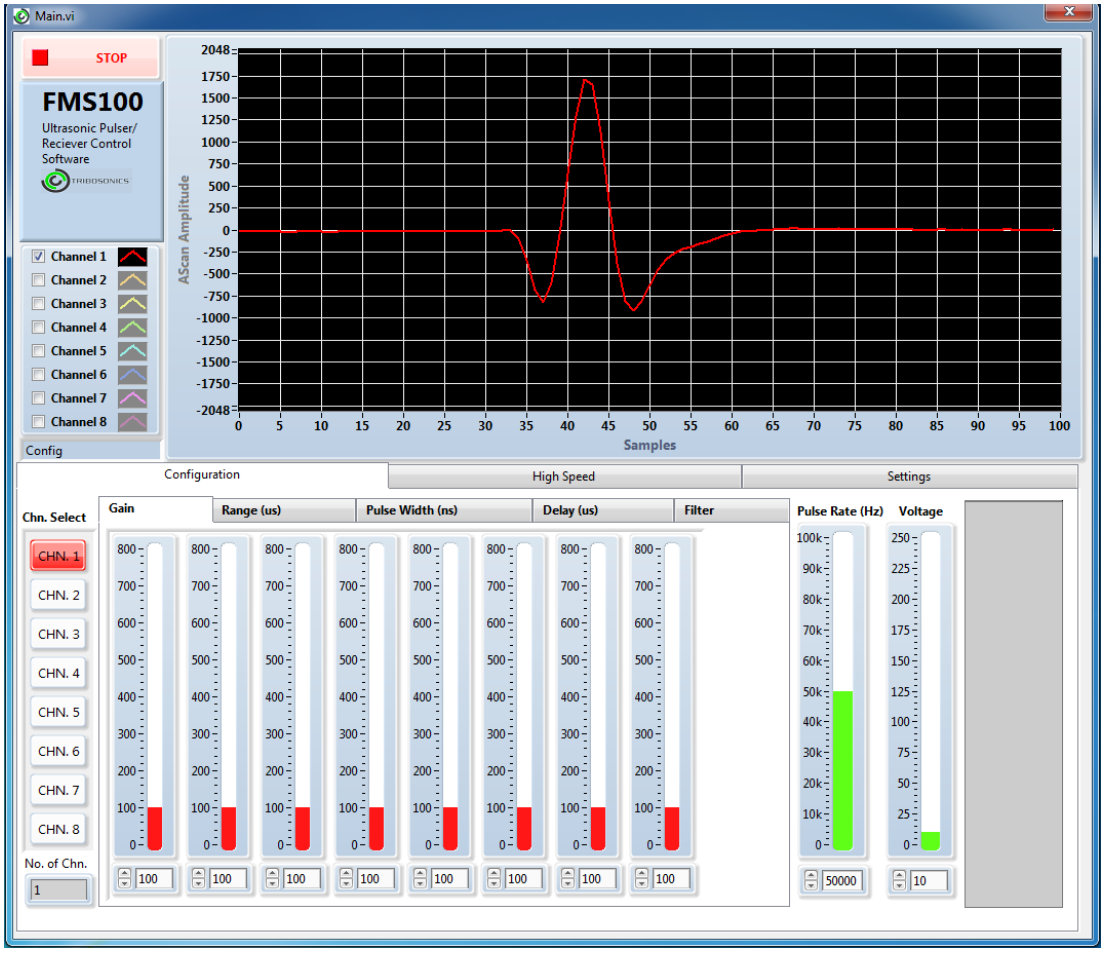

Figure 6.11: The LabView virtual instrument that controls the UT

Once it was shown that the system worked off the machine, it was attempted in-situ. The task of coupling the UT to the roller is much more challenging on the machine. The coolant needs to fully fill the space between sensor and roller without any interruptions or bubbles (see Figure 6.10). When the coolant flow is too low, the coolant flows out of the gap faster than it moves in. When the coolant flow is too high, the flow is turbulent,

which disrupts the signal. For aligning the sensor statically, a spare roller made of mild steel of the correct dimensions was modified to have the sensor channel cut out and a one quarter section removed (Figure 6.12). This roller can be used to position the bracket and roller for the best obtainable signal, and find the best approach for coolant flow.

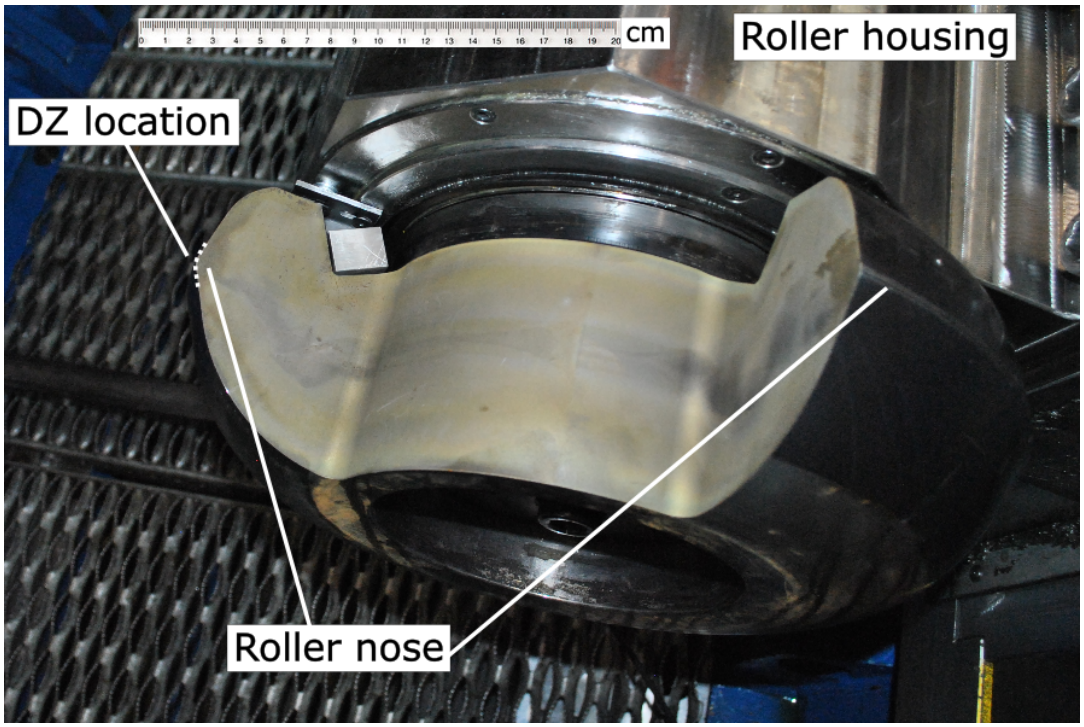

Figure 6.12: Sectioned roller being used in sensor alignment.

The challenges are greater still when the machine is rolling. There is significant noise associated with the rotation of the roller.

After trial-and-error in both static and rolling conditions, it was found that the best result possible with this equipment relies on two factors: decreasing the gap between sensor and roller, and controlling the coolant flow precisely.

Decreasing the gap allows the coolant to fill the gap more easily. This is both because volume of the gap is lower relative to the volume of liquid flow and because the small gap allows the surface tension of the coolant to hold it in place. The best signal is achieved with a gap of 0.5-1 mm.

The coolant flow rate must be controlled carefully. It must be high enough to constantly refill the gap, but low enough to avoid splashing. The flow must also be directed carefully. The best effect was achieved by directing the flow onto the coupling face above the sensor. From there it flows down the face into the gap (see Figure 6.10).

6.4.1 Conclusions

The commissioning of the system showed two things. Firstly, the system is operable and produces signals. Secondly, the quality of the signal is strongly affected by the environment and process parameters. The fragility of the signal means that more work is needed to understand how to get the best out of it. This work is carried out in Chapter 7.

6.5 Final design

The system consists of several parts. Figure 6.13 shows the system. The roller has material removed axisymmetrically from the rear face to allow the positioning of the UT, directing the US pulses at the front face of the nose. The bracket is mounted on the roller housing using existing tapped holes. The coolant pipe enters the space behind the roller "uphill" of the UT and directs the coolant flow onto the internal coupling face. This means that the turning of the roller draws the coolant on and down into the gap.

This design represents the result of a carefully considered process. Initial commissioning indicates that the design is effective. Further testing in Chapter 7 will uncover the successes and shortcomings of the design.

6.6 Chapter conclusions

The design of the US system was a complex process, carried out over several months. The design was guided by a set of priorities and constraints, with the broad aim of producing a prototype that could answer the research questions.

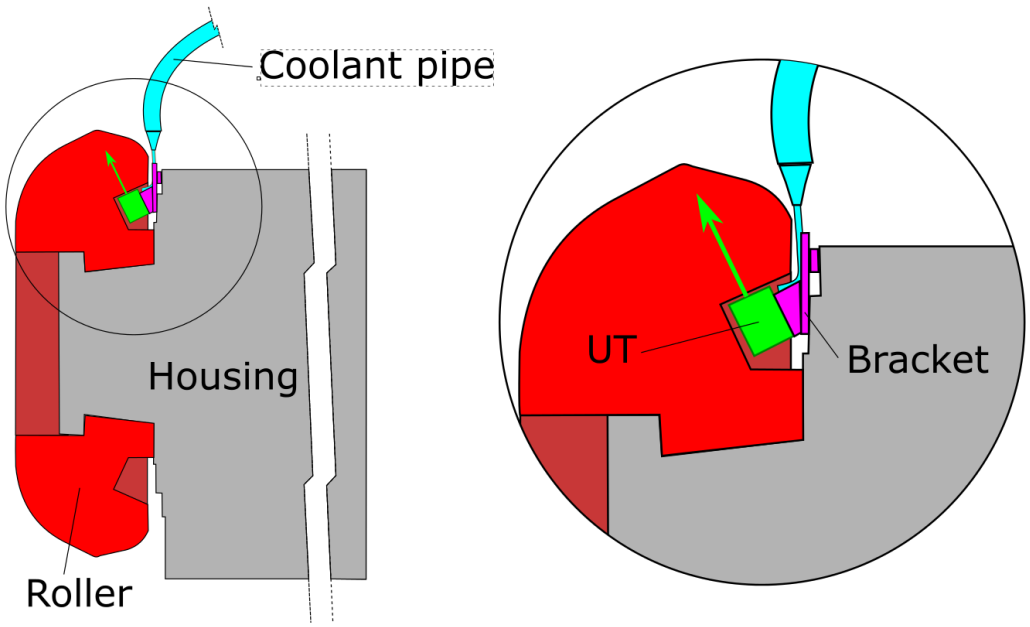

Figure 6.13: An overview of the final US monitoring system design with labelled components.

The priorities were met by choosing a fluid-coupled UT that directly pointed at the deformation zone, allowing continuous data collection. The constraints were met by minimising material removal from the roller and choosing a compromise position for the sensor that balanced the needs of data collection and quality with functionality and stability. A hardy sensor was chosen to suit the forming environment.

The output of the design process is a prototype ultrasonic monitoring system that will function in a real-world IRF environment. It is not claimed to be optimised or perfected, but it will provide insight for subsequent process monitoring by answering the research questions. To reiterate these:

1. Can the operation of IRF processes be improved by process monitoring?
2. What are the most appropriate technologies for monitoring IRF?
3. What process information can monitoring capture during IRF?

Questions 1 and 2 were examined earlier, and the evidence of Chapters 3 and 5 directed the path of this research towards ultrasonic monitoring. Chapter 7 will show

how the system was tested in pursuit of answers to the third research question.

In addition to making specific measurements, the development of a system is itself a contribution. There is value to industrial research and development in the knowledge that such a system has been created and tested (as it is in Chapter 7).

Chapter 7

Ultrasonic experimentation

7.1 Chapter introduction

IRF has untapped potential for near net-shape manufacturing, but the processes need improved understanding and control. In the long term, monitoring, feedback and control could render these processes fully autonomous. The motivation for this work is to demonstrate the initial stages of that ultimate project.

The aims of the ultrasonic (US) work are:

- To design an ultrasonic system system suitable for monitoring IRF processes.
- To test the system's response to changes in material thickness and forming behaviour in-process.
- To evaluate the potential of such a system to affect the operation and design of IRF processes.

The motivation of this work is a fully optimised system with integrated feedback for machine autonomy. While this goal should be borne in mind, the principal aim here is to test the validity of the approach: it is not the aim to produce a fully optimised or calibrated system. This chapter will address the second and third aims above by trialling the system (designed in Chapter 6). There are many ways in which this system could be tested. For example, finite element simulations or scale testing rigs

could be used to help interpret the results. However the aim of the project is to look at capability in the real forming environment. For that reason, the focus is on small empirical trials which assess the potential for system performance in realistic forming conditions. Detailed modelling or laboratory studies of roller-material contact and deformation behaviour is therefore out-of-scope.

The specific aim of this chapter is to explore some of the crossover between ultrasonic monitoring and incremental rotary forming. This will be done in an empirical fashion, looking firstly at how best to use the system within the limits of its inherent flexibility. Then systematic trials will aim to explore the potential in this new area of research. Although this may not produce definitive answers, it will form a test of viability and lay the groundwork for any future work in this area.

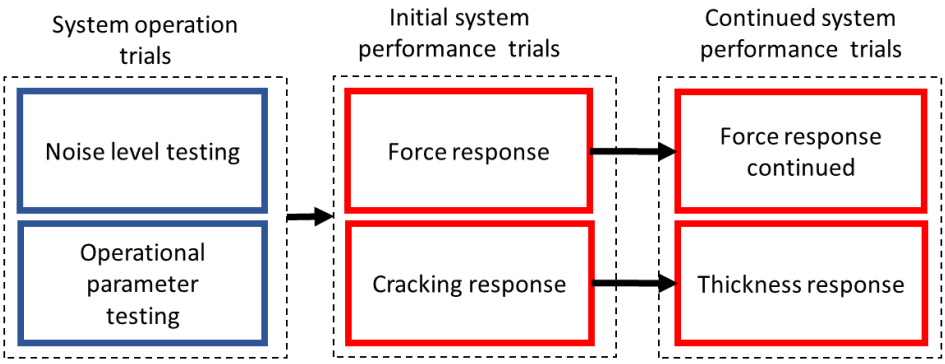

Figure 7.1: Overall diagram of chapter contents.

Figure 7.1 shows a visualisation of the work discussed in this chapter. Firstly, the operation of the system is examined with respect to noise levels and operating parameters. Then trials are carried out to assess the system's response to changing forces (US magnitude response) and cracking parts (US time-domain response). Both of these pieces of work give rise to results of interest which are extended in further trials. The research question is therefore: **Can the US system detect changes in forming force and part geometry?**

7.2 Model to interpret US data

7.2.1 Introduction

This section will introduce and develop a model of how US waves behave in the context of the system as installed. It explores the contact properties and the possibility for thickness measurement, and assesses how likely these are to prove fruitful.

The US transducer is focused on the nose of the roller and records the reflection from the nose. Each ultrasonic pulse from the transducer will traverse the roller, roller-part interface, part material and mandrel. Reflections are created when the pulse crosses a sudden change in material properties - most importantly the speed of sound, c, in the medium - see Chapters 6 and 3.

The general model of US behaviour in the installed system is given below. It is constructed from two sources of information: the available understanding of roller-part interface properties and the material properties of the system's elements. There are two areas which can be modelled: the response magnitude and the time delay of the response. These models are the basis for the interpretation of any data collected.

7.2.2 Roller-part interface properties

There are three possible elements of the roller contact, which are all unknown. The nature of the interface, the size of the contact patch and the position of the contact patch.

There are various conditions of contact discussed in the literature, but for this purpose the contact can be assumed to be either elastic-plastic or fully plastic, with, potentially a thin film of lubricant interposed. These conditions all behave differently - see Chapter 3. The optimal way to examine this property would be with a full-scale test rig. Such a set-up would allow testing of contact conditions while controlling other elements of the roller-part interaction. This could help describe the interface. To build a separate laboratory test rig and demonstrate the system in an industrial environment is not realistic in the available timescale. Therefore the detailed examination of roller-part interface properties lies outwith the scope of this project.

The contact is under very high pressure, meaning that the surfaces will conform. Indeed, it is known that they largely conform because of the significant deformation. Any changes in interface property (such as the effects of films) are likely to be small because of this overwhelming deforming pressure. For the purpose of this examination of the technology application, it is sufficient to assume that the contact is fully plastic during forming. The development of a model for dry asperity contact or thin-film contact would not be appropriate.

The size and position of the contact patch are hard to control and understand. They could be examined through FE modelling, but, as discussed in Chapter 2, this is itself a lengthy and imprecise activity. The location of the contact patch is hard to predict during complex changes in roller position, however it should be stable during the forming lands. By controlling the forming paths as much as possible, it should be possible to assess the size of the contact patch. The size of the contact area could potentially unlock other process information, like the force and forming characteristics (e.g. if a lip of material is growing in front of the roller). The area of contact in forming is a principal unknown in the process, and, controlling the forming path and contact type, it should be possible to assess this.

7.2.3 Material properties

The speed of sound in the system elements is important for making time-domain models of the behaviour. Knowledge of the speed is used to categorise what surface the returning signals have been reflected off.

The speed in the coolant, HOCUT 795 B-EU, will be close to the speed in water (1450-1500 m/s) because it is water-based; the speed in the steels will be in the range 5800-6000 m/s (Lynch, 2019). The harder steels in the tooling will have a slightly higher speed than the soft part material, but this will not have a major impact, because the speed difference between steel and water are so significant. It is unlikely that the system will have the resolution to distinguish between the time delays in different steels. Indeed, the given values for the speed of sound are taken at standardised temperatures with no deformation ongoing. In the real case of IRF, the temperatures and pressures

will be both varied and unknown, so the time-domain figures can only be approximate. Instead, the time-domain model will be based on the geometry of the system.

7.2.4 General model

Accepting the unknowns given above, a general model can be postulated which characterises the behaviour of the system in the ways which are of interest to this project. It is not necessary to have a full model of every aspect of the system to extract useful information. Instead, it is important that the model relates the measurable change (the residual) to some changing aspect of the process behaviour.

Figure 7.2 shows the model. There is uncertainty inherent in the model relating to the shape of the DZ and the distribution of coolant around the contact area. As there are no published approaches which specifically aim to measure the DZ in-process it is therefore the case that the model is simplified. The UT gives out a pulse P which travels through the coolant and into the roller. Part of this pulse is returned as a reflection, R_1. The pulse traverses the roller and is partly reflected from the roller nose (R_2), and continues through the part to the part-mandrel interface where it creates reflection R_3. The remaining US energy is dispersed into the mandrel (L_4). There are also losses at each previous interface, from US energy that is absorbed or reflected away from the UT. These occur at the interior roller face (L_1), the roller-part interface (L_2) and the part-mandrel interface (L_3).

The total starting energy of the pulse (P) is divided between all these reflections and losses.

$$P = L_1 + R_1 + L_2 + R_2 + L_3 + R_3 + L_4 \tag{7.1}$$

Note that if the losses or reflections at a given interface change for any reason, they will change the amount of available US energy passing through that interface. This will reduce the available energy for later reflections. That is, if the L_1 losses are increased by gaps in the coolant flow, it will also affect the magnitude of reflections R_2 and R_3.

The reflection R_2 and the losses L_2 are particularly notable because this is the area

of greatest interest - the DZ. These losses will come from three sources:

- Reflection from the outer face of the roller
- Conduction of energy into the coolant
- Conduction of energy into the part

This last loss is the one of most interest, as it relates to the roller-part contact behaviour. Experimental conditions will attempt to keep the coolant losses constant so that the reflection R_2 describes the DZ behaviour.

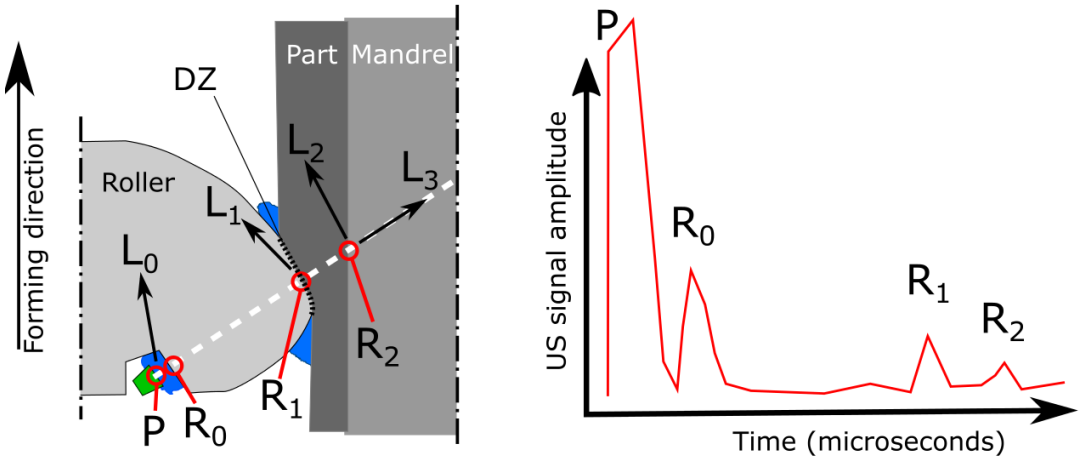

Figure 7.2: The model of US system behaviour shown schematically (left) and in collected US data (right). The labelled components are: P - the initial pulse, R_1 - the reflection from the gap, R_2 - the reflection from the roller nose, R_3 - the reflection from the mandrel, and $L1-4$ the losses from each region.

The collected data should look like the graph shown in Figure 7.2. By looking at the time delay and magnitude of the peaks, it should be possible to gain insight into the system.

7.2.5 Time-domain measurements

Before drawing any conclusions about the process, it is important to be sure that the data represent what they are thought to represent. Time-domain measurement, i.e. time-of flight, will be used to identify the reflections referred to above.

For a time-of-flight measurement, the distance of the echo site is given by

$$D = \frac{1}{2}ct \tag{7.2}$$

where c is the speed of sound in the material and t is the time to travel to the echo site and return. For traversing through multiple materials the distance is the sum of the component sections, so for the last reflection, R3:

$$D_{UTtomandrel} = D_C + D_R + D_P = \frac{1}{2}c_C * t_C + \frac{1}{2}c_R * t_R + \frac{1}{2}c_P * t_P \tag{7.3}$$

Where the subscripts C, R, P refer to the coolant gap, the roller and the part. By filling in the variables it is possible to measure the distance. In fact, it is not strictly necessary to know the all of the variables precisely, as long as they are accurate enough to distinguish the major peaks from each other.

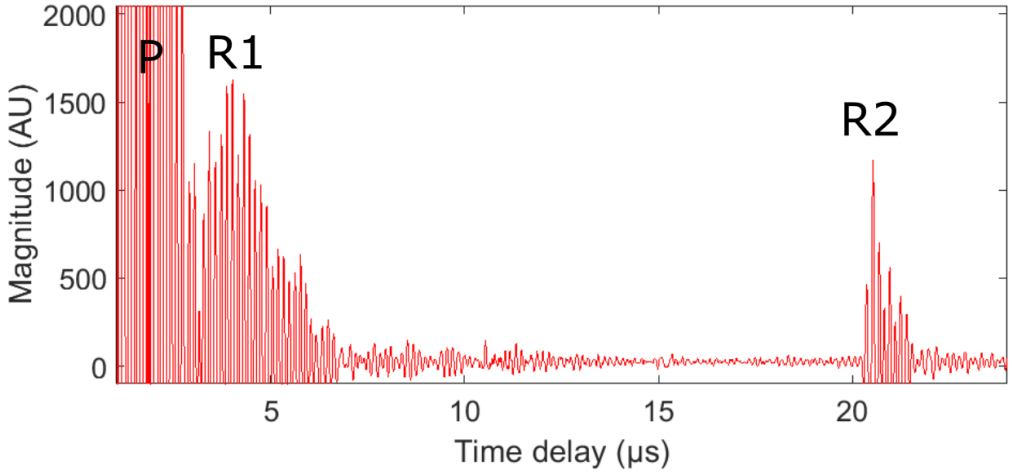

Figure 7.3: Data from an early set-up trial - the so-called 'spit test'.

Consider Figure 7.3. This result, as with all the US results, is a 'snapshot' taken out of a continuous stream of data. It is repeatable both in a single trial (i.e. R1 does not vary in time delay during a 100 s run of the system) and between experiments. Reflection 2, as termed above, can be identified by the timing. The peak is at 20.5 µs and the distance, in the steel body of the roller, is 60.5±1 mm, depending on the speed of sound value taken. This matches the known dimension of the roller (from sensor

channel to nose) of 60.3 mm. Further confirmation comes from the simple 'spit test' where pressure is applied with a wetted hand to the nose of the roller. It can be seen that the second reflection diminishes in magnitude during this test, confirming that the second reflection is certainly from the nose.

The nose reflection is the key for identifying process behaviour in the signal. Once identified, signals nearer to the sensor relate to behaviour in the couple or roller, and any signals further away relate to behaviour in the part or mandrel.

7.2.6 Magnitude measurements

Predicting the behaviour of reflections in contacts is difficult, and requires tightly controlled conditions - see Chapter 3. It must be accepted that the practical demonstration which this works aims to carry out does not take place in tightly controlled, laboratory conditions. The understanding of the basic mechanics that control the magnitude of the reflection are well described in the literature in a general sense. Rather than aspire to a predictive model, the aim in this work is to test the behaviour in real-world conditions.

To that end, consider Figure 7.4. When the roller compresses the part, first elastically and then plastically, the surface area of contact between the two increases. This increases the signal absorption and hence decreases the reflection. Note that the shape of the DZ will change and move during forming. However, the principle that reflection will be negatively proportional to contact area will still operate.

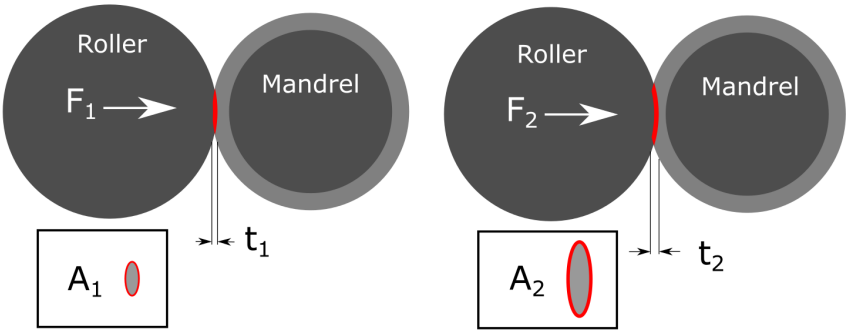

Figure 7.4: A schematic depiction of the mechanics which relate forming force to contact area size: where $F_2 > F_1$, $A_2 > A_1$.

There are various properties of the roller-part interaction that may affect how the contact area changes. These are: the roller and part geometry, the film thickness of lubricant between the roller and part, the mechanics of contact and deformation (elastic/plastic contact), and roller-part slip. The behaviour of coolant around the interface will also affect the signal magnitude. In scenarios where the interaction conditions are constant or tightly controlled, the contact area can give a proxy measure of contact force. It is unknown what the dominant factors are in a real-world IRF process. The contact forces involved are enough to plastically deform the workpiece. Therefore it is plausible to suggest that the effects of force may dominate the roller-part interface. If so, the change in contact area, as inferred by the change in reflection magnitude, will give a measure of contact force.

7.3 Data

US data for all trials was collected in the Tribosonics software. Machine movements, speeds and forces were recorded in Siemens' *Sinucom* software. The force recordings in *Sinucom* are a measure of the current draw on the roller slides which is given a nominal kN value by the machine - this is then recorded by *Sinucom*. Because the kN value cannot be calibrated they are effectively repeatable measurements in arbitrary units (AU).

The US data for all trials was collected in the .tdms format at a 160 Hz sampling rate and then processed in MATLAB. The files were converted to the .mat binary file format and mined for the operating parameters. For handling purposes, the data was downsampled for some elements of analysis. Where this was done it was filtered to prevent aliasing.

Extraction of the peak US values was carried out algorithmically. These values could then be plotted against time to observe the nose reflection behaviour through the process.

Time-matching between the US and *Sinucom* data was achieved by matching the characteristic spike in US response during initial roller movement. The *Sinucom* data

was then interpolated to match the higher US sampling rate so that the two datasets could be freely compared.

The relevant code is supplied in Appendix E.

7.4 Operational trials

Figure 7.5 shows a visualisation of the work discussed in this chapter. The highlighted region shows the operational trial work which was carried out to test that the system was being operated at its full potential. A series of tests were planned and carried out to test for the causes of noise in the system, and to find the best operating parameters to use. These are described below.

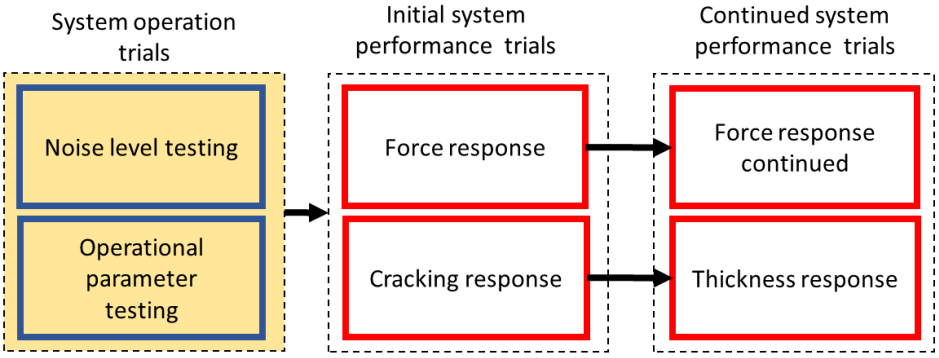

Figure 7.5: Diagram of chapter contents with the operational trials highlighted.

7.4.1 Noise testing

The commissioning process showed that there were issues with noise levels in the US recordings. An experiment was planned to identify the sources of the noise.

Plan

Starting with the machine totally shut down, each stage of the process was carried out. Recordings of the signal were made at each stage. Table 7.1 shows the procedure for testing for the source of noise.

Table 7.1: Noise testing procedure

Trial	Machine	Coolant	Hand Turning	Noise expected
1	Off	Off	Off	Background electrical interference
2	On	Off	Off	Electrical interference from machine
3	On	On	Off	Splashing noise
4	On	On	Hand turning	Rotating noise from roller only
5	On	On	Rolling	Contact rotating noise

Firstly, the machine and its power supply were totally switched off (1), then turned on (2). The coolant was turned on (3) and then the roller was turned by hand (4). Then the spindle was started, and the rollers brought up to touch the surface of the part, so that they turned freely (5). Finally the part was formed under load (6). This approach isolated each potential source of noise as much as possible. Trials 1 and 2 tested for electrical interference from other machines in the workshop or the flow former itself. Trial 3 assessed the impact of coolant in affecting noise levels. Trials 4-6 attempted to distinguish the different noise impacts of the roller turning under controlled and real circumstances.

Results

In Trials 1-2, the sensor was not coupled into the roller as there was no coolant flowing. The experiment immediately revealed the presence of background electrical interference. This takes the form of small spikes of noise which move across the data. They are present even when the FF machine is switched off and do not change when it is switched on, indicating that they originate from the other equipment in the workshop.

This noise could cause inaccuracies - when the spike of noise coincides with a region of interest it will cause the result to be high. However, they are relatively small and rare. Figure 7.6 shows representative electrical interference from Trial 1.

Trial 2 showed identical behaviour to Trial 1. This means that the electrical and hydraulic systems of the machine do not cause problematic interference in the process.

Trial 3 showed a significant change in the data when the coolant was turned on.

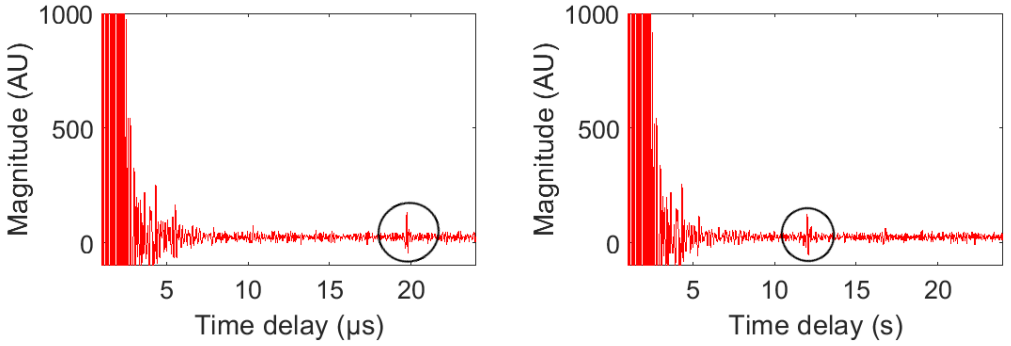

Figure 7.6: Data captured from Trial 1. The spike at left is the initial ultrasonic pulse. Random electrical interference is circled.

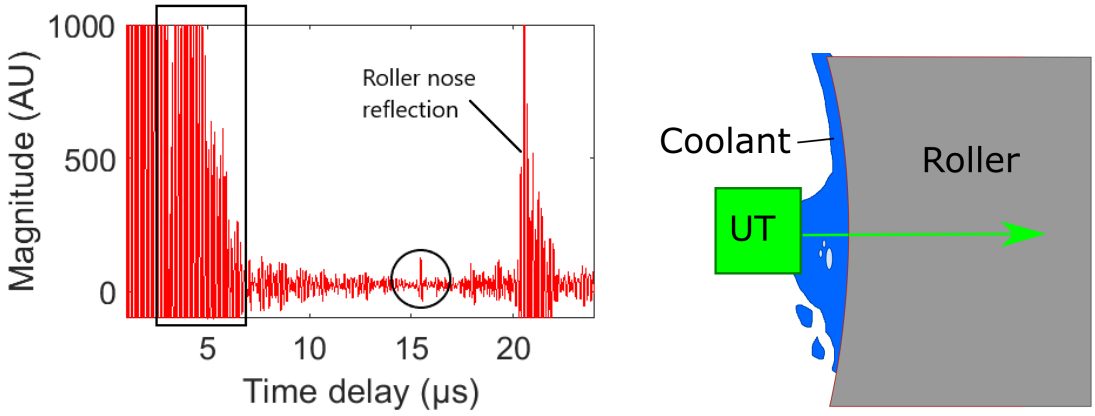

Figure 7.7: Results from Trial 3 (left) showing coupling noise from 3-7 microseconds (boxed) and electrical interference (circled). The diagram (right) shows how this coupling noise occurs, from air bubbles or incomplete filling of the UT-roller gap.

The major reflection from the nose of the roller can be seen at 21 µs. There is also an immediate additional source of noise noticeable. Just after the initial US pulse, there is a large reflection. Figure 7.7 shows how the coupling fluid between the UT and the roller can cause reflections. These are caused by incomplete filling of the sensor-roller gap, or from air bubbles in the coolant. Misalignment between the sensor and roller faces (i.e. away from parallel) will exacerbate this. This noise should not cause significant problems as it is far from the region of interest.

In Trial 4, the roller was rotated by hand to examine the effect of this movement. The results showed a similar result to Trial 3. This means that the rotation of the roller in and of itself was not an important factor in the noise levels.

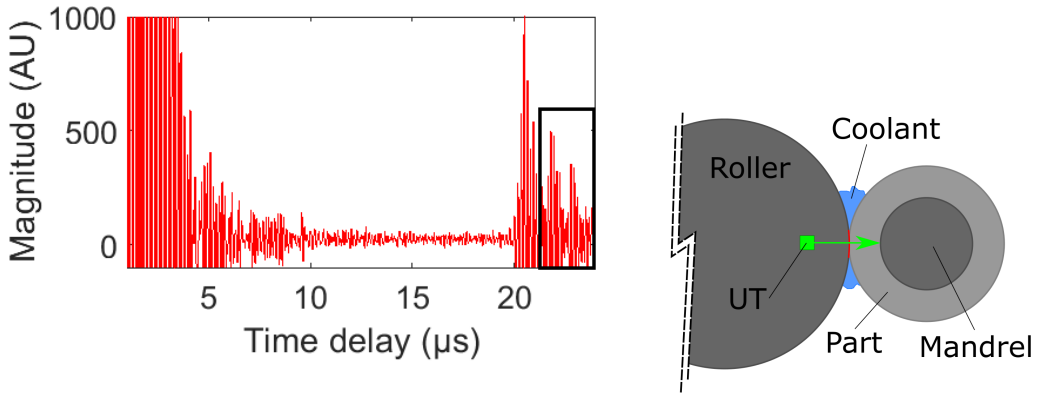

Figure 7.8: Results from Trial 5 (left) showing splashing noise from 22-25 microseconds (boxed). The diagram (right) shows where the coolant splashing occurs at the roller-part interface.

Trial 5 had the machine spindle running and the roller just touching it so it rotated sympathetically (i.e. the spindle rotates clockwise and the roller anticlockwise, driven by the spindle). This test showed a new source of noise. The coolant used for the process (not for coupling) runs down the face of the roller. During Trials 3 and 4, this flow was undisturbed and laminar. But when the roller touches the part on the mandrel, there is a splashing effect around the rotating contact between roller and part. This manifests in the US data as noise just after the roller nose reflection and a variability in the magnitude of the nose reflection. Figure 7.8 shows the impact.

The variability in the nose reflection magnitude is caused by the varied amount of coolant around the DZ. This coolant forms a smooth interface with the roller which allows the transfer of US energy into the coolant. This lost energy results in a reduction of the nose reflection's magnitude. This is potentially a problem because this magnitude will be used to infer some process characteristics.

Note that coupling noise is actually greater in Trial 3 and 4 than in 5. This is because the smooth turning of the rollers under rolling/forming conditions produces a less disturbed flow on the roller's inner face than when the roller is still or turned by hand.

Conclusions

The results show that there are three important sources of noise. Table 7.2 shows them in order of significance. Mitigation has been considered, however there are limited possible changes to the set-up. Some observations are included here as an aid for potential future designs.

Table 7.2: Noise sources

Importance	Description	Causes
1	Splashing	Turbulent coolant flow on roller outer face
2	Electrical	Other machines in the workshop
3	Coupling	Sensor alignment, gap and coolant turbulence

The splashing is the most significant noise and the most difficult to alter. The coolant is required during the process to maintain the cold-worked nature of the parts. Iterative experimentation with the coolant dispersal system on the machine failed to find a solution that significantly reduced this noise without impairing the process function. It is to be hoped that the random variation in splashing noise will have a small net effect once averaged over time.

It is not possible to turn off all electrical sources in the building, so this noise can only be mitigated by defensive strategies. Shielding the electrical components of the system and shortening the cables would reduce the magnitude of interference. A geometric redesign of the system that gave a stronger overall SNR would proportionately reduce the impact of this noise.

The coupling noise is relatively insignificant during actual operation (Trial 5) as opposed to the more artificial test procedures. Iterations of the sensor position show that it can be further reduced by reducing the sensor-roller gap and ensuring the sensor-roller faces are as near parallel as possible.

7.4.2 Parameter testing

The Tribosonics software allows the adjustment of some parameters for operating the sensor and recording information from it. These were examined systematically with

the aim of improving the data.

Plan

A design of experiments (DOE) procedure was used for testing the operating parameters. This was done in order to establish good operational parameters. A full factorial approach was used, with no repeats) to examine the effect of each variable and account for any interactions. The primary parameters that can be altered are the voltage, bandpass filter and pulsewidth. The voltage affects the magnitude of UT vibration while delivering the initial pulse, which should affect the output. The bandpass filter level selects a bandwidth of frequencies, discarding any signal at higher or lower frequencies. The pulsewidth affects how long the initial vibration pulse from the UT is. Different systems respond differently to US stimulation, so the best pulsewidth must be found by experimentation. The parameter values are shown in Table 7.3

Table 7.3: DOE for parameter testing

Level	**Voltage (V)**	**Filter range (MHz)**	**Pulsewidth (ns)**
L	50	4±0.5	25
M	-	5±0.5	90
H	150	6±0.5	150

Three values - a low, medium and high - were selected for the filter and pulsewidth (two levels were chosen for voltage to limit the number of trials). The filters were set using the Butterworth Filter virtual instrument, within LabView. The range of frequencies was selected to be centred on 5 MHz because the response of the transducer is maximal at this frequency. The levels were set after examining the available limits of the software and discarding settings which produced extremely poor results (e.g. bandwidth filters above or below those selected which completely blocked any response).

The machine was set up with the coolant running and the rollers moved up to touch the workpiece so that they rotated (see Section 7.4.1). The factors were altered, and a recording of the US response was made of each combination for a full factorial experiment. The full plan of experiments is given in Appendix D.3. The key output

was the magnitude of the reflection from the nose of the roller.

Results

The principal results are shown in Figure 7.9. The responses give clear indications of how to set the operational parameters for the system. The interactions between the factors were not significant (see Appendix D.4).

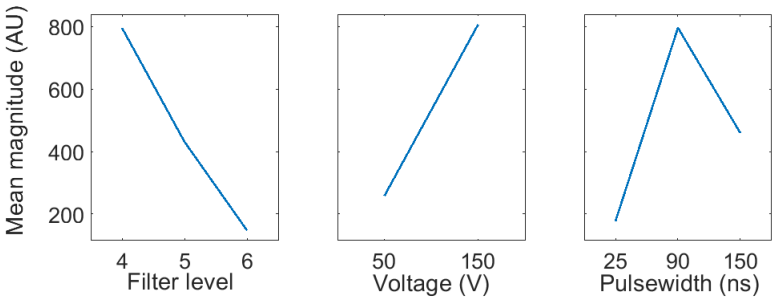

Figure 7.9: Main effects plot of the parameter factors

It can be seen immediately that the highest voltage produces the largest response, as expected. There is an arguable downside in that a very high voltage produces significant noise near the sensor (see Figure 7.10). However this is far from the region of interest, and much less important than the obvious benefit of improving the signal magnitude (and hence improving the SNR).

The filter levels shows a similarly clear result - centering the bandpass filter on 4 MHz gave the the strongest response. At lower frequencies, effect of electrical noise becomes overwhelming, while at high frequencies the SNR diminishes rapidly. These filter levels make small changes in the magnitude of electrical interference, but these are of little relevance in comparison with the changes in signal magnitude. In a future iteration of the monitoring system, a purpose designed filtering system could possibly maximise the signal strength while minimising interference.

The pulsewidth result is the most interesting. The highest and lowest pulsewidths show markedly poorer responses than the middle value. The specific geometries of the system are best suited to a pulsewidth in this region. Further iteration indicated that the best magnitude was achieved in the region 85-100 ns.

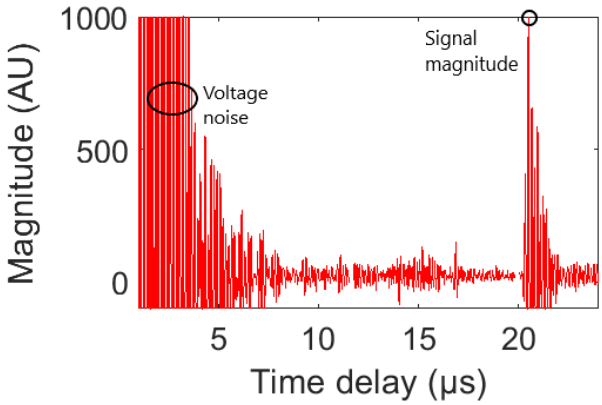

Figure 7.10: Results of the parameter test showing the region of increased noise from high voltage and the measure of signal strength - the nose reflection magnitude.

Conclusions

The parameter trials show that the selection of operational parameters are important to the SNR. This is an important result because the system, once installed, is lacking in flexibility. The system parameters are one of the only options available to improve the signal. Better operating parameters can now be used at no cost to the operation.

7.4.3 Conclusions from operational trials

The operational trials showed that the operating parameters and procedures are important to the signal quality. There is limited capability in the system to change the operational procedures and parameter, but where possible these have been adjusted to improve the SNR in the following trials. The information gathered here could also feed back into an improved later version of the system.

7.5 Performance trials

7.5.1 Introduction

It has been established that the system can record a reflection from the nose of the roller (referred to as the nose reflection). The experiments below aim to proceed from there, to inform the research question:

3. What process information can monitoring capture during IRF?

The questions that naturally arise are: What response will this reflection have to forming? Can further reflections be recorded from other features of the process? Can the system's responses be clearly linked to process behaviours of interest?

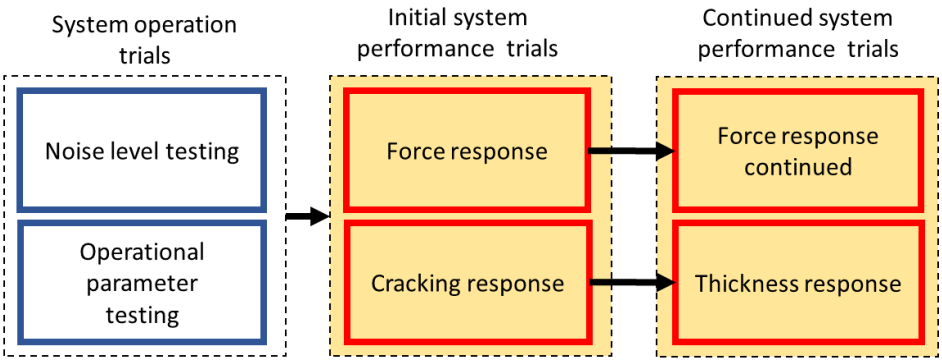

Figure 7.11: Diagram of chapter contents with the performance trials highlighted.

These have been divided into two streams of trials, shown in Figure 7.11. The upper stream looks at the response to force in terms of signal magnitude. The lower stream looks at signals in the time domain. As described below, the initial trials raised questions that led naturally to the continued trials. These trials aim to answer 4 questions:

1. What insight into forming forces in IRF can be gained with US monitoring?
2. What insight into contact area in IRF can be gained with US monitoring?
3. What insight into fracture in IRF can be gained with US monitoring?
4. What insight into part thickness in IRF can be gained with US monitoring?

With this intention - to look at the US system's capability to detect various behaviours of interest - the trials of the system were organised in the following way:

a) A testable hypothesis was written, based on the relevant simplified model of the system behaviour.

b) A plan was developed for testing the hypothesis.

c) Data was gathered to verify the hypothesis or falsify it.

d) Conclusions were drawn.

This approach allowed the systematic examination of the system's capabilities.

7.5.2 Force response in flow forming

Aim

The aim of this trial was to examine the response of the magnitude of the nose reflection. This reflection occurs at the primary point of interaction between the roller and part, the DZ. Little is known about the size and behaviour of the DZ during forming.

It is not clear whether or how the US signal will respond during the process. The model suggests that increased contact force and contact area will decrease the US response at the nose. As well as the behaviours of interest (force and area) the response could also be affected by the presence of coolant, the contact angle, changing material properties and, perhaps, other unknown factors. This should create a measure of force by measuring the contact area. The force recording on the machine should help with the interpretation.

Trial plan

The trial plan is simple. Three cylindrical preforms were manufactured in stainless steel with a 15 mm wall thickness and 300 mm length. The test procedure was selected to be a standard 25-50-75 % deformation (see Figure 7.12 and Appendix B.4). These deformation values were chosen to put a range of forces on the part during forming. It is known that increased feed rate causes increased forming forces. For that reason the three parts were formed at three different feed rates to cause a range of force values (see Table 7.4). It should be noted that the machine is CNC position controlled. Thus the roller positions can be expected to be accurate to the plan. The feed rates may vary slightly at any given moment but are generally found to be within a few mm/min

of the nominal value. In any case the key input which is being assessed is force, which cannot be directly controlled on the machine (only position), but the data for which can be extracted afterwards.

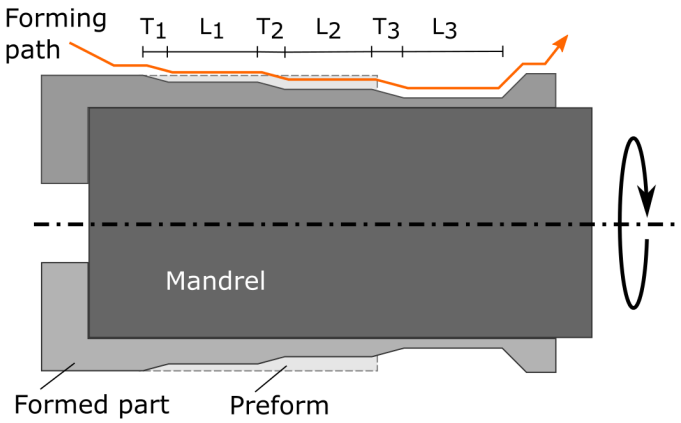

Figure 7.12: Preform and part showing forming path, transitions (T 1,2,3) and lands (L 1,2,3).

The key variable is the forming force and the key output is the magnitude of the nose reflection. It is expected that these will be negatively related, because of the established principles of US tribological contact measurement (Dwyer-Joyce, 2005), but unclear how strong that relationship will be.

Table 7.4: Trial plan for force response

Trial	**Geometry**	**Feed rate(mm/min)**	**Speed (rpm)**
1	50-60-70%	200	150
2	50-60-70%	80	150
3	50-60-70%	100	150

Hypothesis

Ultrasonic reflection at DZ will be negatively proportional to forming force.

Results

The three trials show a strong relationship between the radial forming force and the ultrasonic response. Figure 7.13 shows the trials results with the obvious relationship between the forming force and the US response.

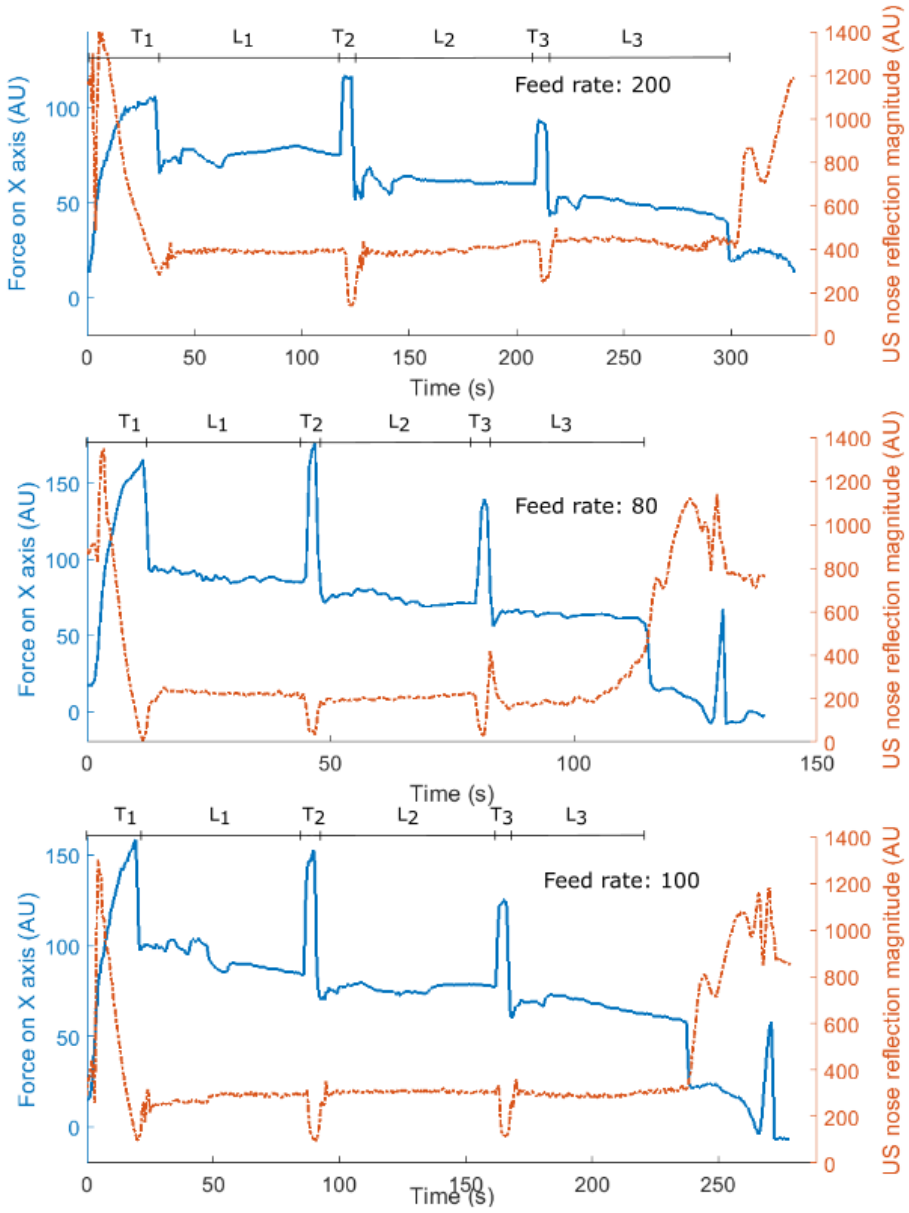

Figure 7.13: The force response recorded by the machine (solid) and the US response (dashed) for the three parts. Note the initial spike in force which settles down to steady state. Note also the different feed rates.

The results show three points of interest. A) The force and US response are strongly inversely correlated where the force values peak. B) The overall magnitude of the US signals is roughly correlated with the overall force. C) During the lands the correlation is not as expected.

The first observation supports the hypothesis. The force peaks sharply at the transitions, where the roller is driving into the material. The US response has a matching inverted peak which shows the reduced reflection (i.e. greater energy transmission) at these points.

The second observation also agrees with the hypothesized behaviour. The overall magnitude of the US response can also be seen to correlate with the overall magnitude of the force. Across the three trials, the feed rate increases. This increases the peak forces at the transition and the semi-static forces during the forming of the lands. The magnitude of the US response lowest with the highest forces and highest with the lowest forces - exactly the inverse relationship predicted.

The third observation is not in line with the hypothesis. It can be seen that the levels do not always respond inversely to the changes in force. Across the three lands in each trial there is a steady decrease in force. But this is not well matched in the US response across the lands, which stays more level. Additionally, the settling in the force levels after the transitions is not present in the US data.

While forming in the lands, the forces are semi-static. The behaviour of the coolant, the contact area and other factors should also be fairly constant. So if the force was the primary driver of the US response, the force variance in the lands should be replicated in the US signal. The fact that it is not suggests the presence of another important factor which the US is responding to.

Discussion

The hypothesis was that the US response would be inversely correlated to the forming force. On initial inspection, this appears to be the case, and it is tempting to assume that the US response is effectively a measurement of force. However it is also possible that another factor, which may be related to force, is also affecting the US response.

This is suggested by the fact that the US signal does not always correspond to the force behaviour. Therefore it may be that the US response is a combined measure of several process elements, one of which is forming force.

The most likely candidate for another influencing factor is contact area, for two reasons. Firstly, contact area is known to have a major impact on US transmission. Secondly, the contact area should be related to the force. If the force increases, there will likely be an increase in contact area - the two effects should mostly work together. Their effects would both be to reduce US reflections. It is hard to tell which effect is more significant at any stage of the process. It is possible that under fully plastic contact there is little or no force response and the driving factor is contact area. It may be that sometimes the force has more significant impact, and sometime the contact area is more significant.

In conclusion, a relationship clearly exists between force and US response. The US response is likely to be a combined measure of force and contact area. More work is needed to disentangle these elements.

7.5.3 Force response in shear-spin-flow forming

The first set of trials showed that there is a definite relationship between the forming force and the US response. There are still questions about what that relationship is, and what the impact is of contact area (and perhaps other factors) on the response.

Aims

The aim of this series of trials is to look at varied forces during forming and assess what the the ultrasonic response is reacting to. The trials will attempt to disentangle the effects of force and contact area on the US response. The trials will be designed to cause a wide range of forming forces and conditions by varying the size and order of the deformations as well as the feed rate. These changes in known conditions should show which aspect of the process the US response is recording. If the US response is independent of the force, this would suggest that the contact area is the dominant factor being recorded.

It can be postulated that: *If changes in force do not cause predictable changes in US response, then the US response cannot usefully be said to be measuring force.* A set of trials with significant changes in force across the process will test if the force is contributing to the US response.

Hypothesis

US reflection at DZ is controlled by contact area independent of forming force.

Trials

Cylindrical FF preforms are expensive to produce, which limits the number of trials that can be done. Starting with flat preforms means that it is possible to carry out many more trials because of the significantly reduced material and machining costs. For the remainder of the experiments, the SSF process was used with disc preforms. The FF stage of SSF has very similar forming mechanics to FF on a smaller mandrel, meaning the principles are transferable.

The trials were planned with advice from the machine operators, to give a large range of forces while successfully forming the parts. The shear-spin part of the process was not monitored due to stability issues with the *Sinucom* and *Labview* software for recording very long processes.

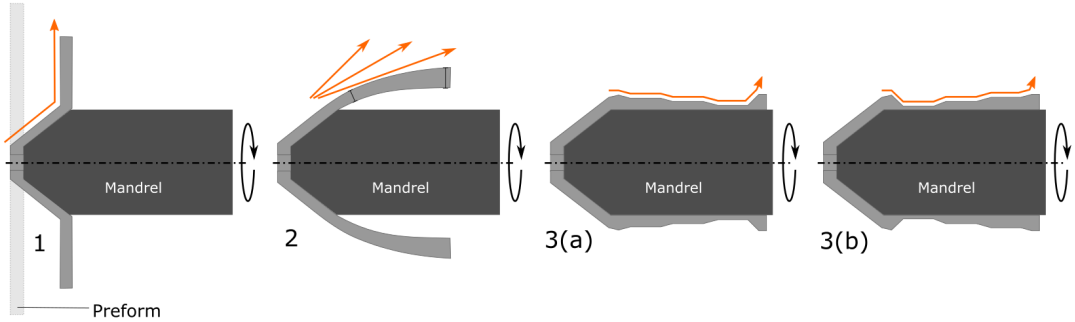

Figure 7.14: The forming process for the SSF trials. (1) The shear forming of the cone section from the flat preform is first. (2) The spun condition is done with three passes. Note the variance in wall thickness along the length. The two flow-forming path alternatives are shown in 3(a) and 3(b).

Figure 7.14 shows the part geometries being formed. Once the shear-spin process has formed the part into a cone-cylinder, the FF process thins and lengthens the cylindrical section. This is done in three lands of three different thicknesses.

Three variables were altered through the trials: the thickness of the lands, the ordering of the lands, and the feed rate.

The spun section is thinner at the conical end than the other as noted in Figure 7.14. This is due to a thinning at the change of angle and a slight build up of material at the flange end. Therefore the largest thickness values for the reversed order formings are decreased to 5 mm to ensure they directly contact the material. Table 7.5 shows the parameter values used.

Table 7.5: Parameters for force response testing

Level	**Lands (mm)**	**Lands (reversed) (mm)**	**Feed rate (mm/s)**
L	2-3-6	5-3-2	150
H	3-4-7	5-4-3	300

The full DOE plan is given in Appendix D.5. This plan should elicit a wide range of force responses

Key variables and outputs

The key independent variables are the forming path and the feed rate. The outputs are forming force and US response. The relationship of these outputs should clarify what the US response is measuring.

Results

The results show a variety of responses. There are three obvious types of response to note. These are shown as examples in Figure 7.15 and 7.16.

The first four trials showed the expected response - a high force in the initial land with the highest deformation and spikes of high reflection where the force dips at the transitions. The lands in these four trials were formed in the order of most-to-least deformation. The overall trend of the US response through the lands also seems to

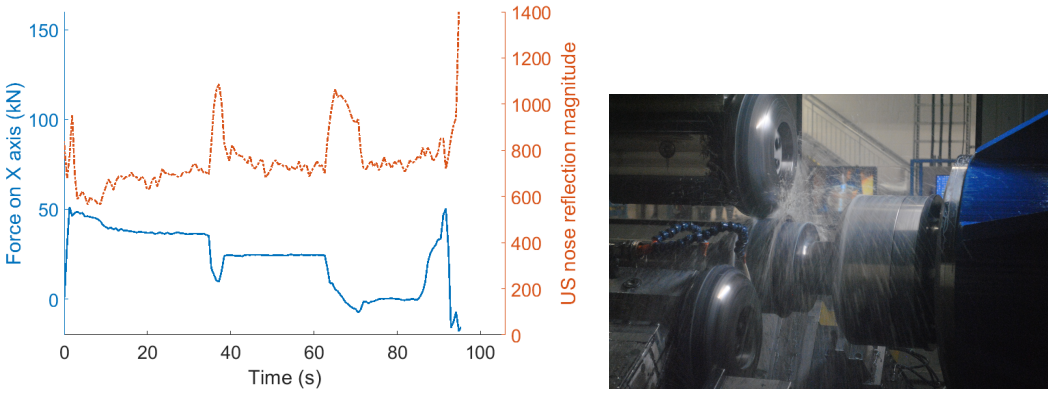

Figure 7.15: The graph shows the results of Trial 1. The force response is solid and the US response dashed. The photograph shows flow forming in the SSF process.

inversely follow the force response. Figure 7.15 is one such example. The next question is therefore whether that trend in rising US response is reversed when the order of lands is changed.

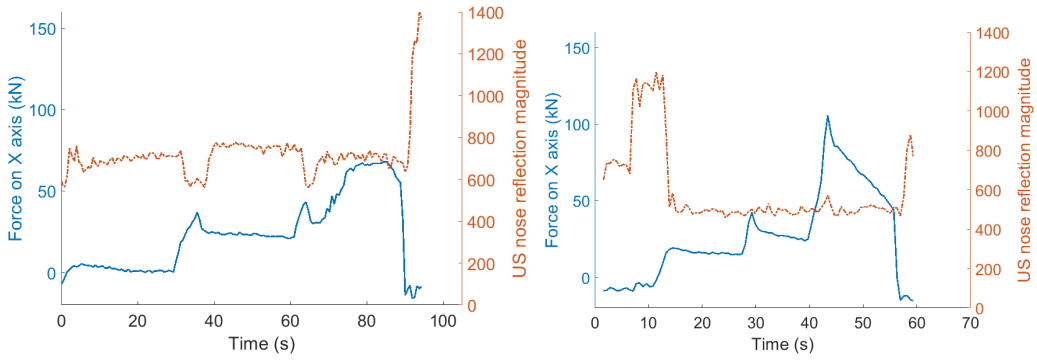

Figure 7.16: The results of Trial 11 (left) and 16 (right). The force response is solid and the US response dashed.

Trial 11 in Figure 7.16 is an example where the lands were formed in the order of least-to-most deformation. It is clear that the force is behaving as predicted. The smallest deformation again produces the smallest force and vice versa. There is also the repeated phenomenon of the peaks in force corresponding inversely to the peaks in US response. However the overall trend of the US response in the lands is fairly flat and similar to the result in Figure 7.15.

Trial 16 in Figure 7.16 is an example with the higher (300 mm/s) forming rate.

As expected, the higher forming rate causes higher force levels in the lands and higher peak forces at the transitions. There is at the same time a damped overall US response which does not show any obvious relation to changes in force.

The results for all the trials were collated and examined. Figure 7.17 shows the stable force values collected across the first two forming lands. Some results in the third land were discarded where the force response was highly unstable. This was mostly in the parts with a very small deformation in the third land. The force was variable for reasons relating to the geometry of the roller-part contact. The end of the cylinder, as spun, curves out away from the mandrel. This results in an initially low force in the third land where the material is not fully clamped against the mandrel, then a high force as the roller strikes the bulge of material. The recordings from this area were set aside as atypical results, not representative of normal forming conditions.

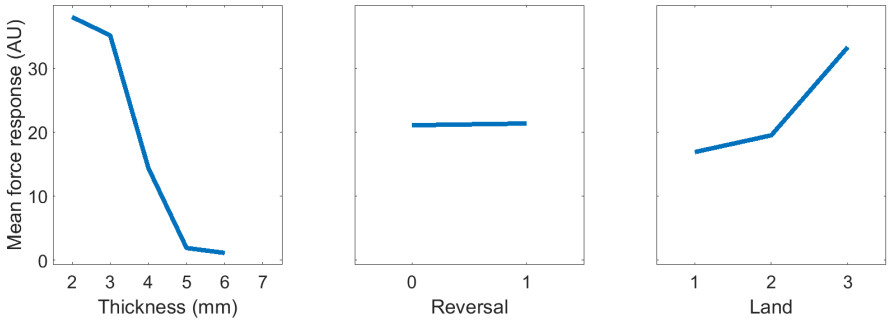

Figure 7.17: Main effects plot of the forming force.

The result for the force response in Figure 7.17 is clear and as predicted. Reducing the wall thickness by a greater amount increases the forming force. Meanwhile, reversing the direction of forming has little effect on the force.

It can be seen that there is an increase of force in the third forming land . The force in the third land is unstable and varied in many of the trials. This is likely due to the geometry of the third land, where the roller strikes the flange of spun material shown in Figure 7.14.

These results mean that the experimental plan was successful in creating a wide variety of forming forces. The next step is to assess how the US response relates to the

forming force.

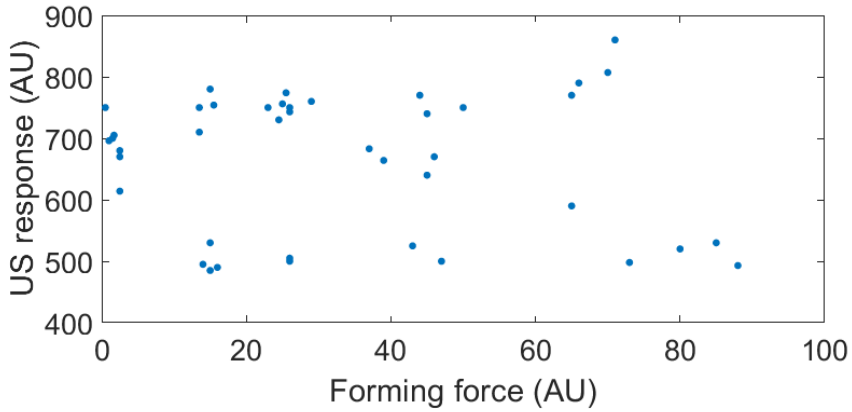

Figure 7.18: Scatter plot of forming force and US reflection at the roller nose.

Figure 7.18 shows that there is not a linear relationship between force and US reflection. The postulate was taken that *if changes in force do not cause predictable changes in US response, then the US response cannot usefully be said to be measuring force.* This result suggests that that is indeed the case as large changes (50 times) in force do not elicit the expected US response.

The result taken earlier, that force and US reflection response are somehow related should not be discarded. Clearly under some forming conditions they are related. But these trials demonstrate that, for this range of forming conditions, force is not a dominant factor controlling the US reflection. The US response should therefore be examined with respect to its response to the input variables.

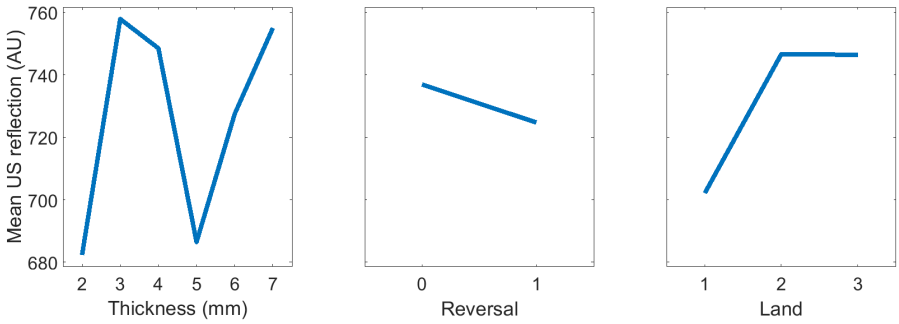

Figure 7.19: Main effects plot of the US nose reflection.

Figure 7.19 shows the response of the US reflection at the roller nose to the varied forming conditions. The response to changing thickness is confused. This is likely because the thicknesses 2, 3, 4, 5, 6 and 7 mm are not being measured in isolation. Rather, they are part of a complex forming path and associated roller-workpiece interface. They cause a different response depending on where they come in the process. Consider Figure 7.20. The same thickness is being formed, but the contact on the roller is entirely different. To form a given thickness (e.g. 2 mm) in the first land, the front face of the roller strikes the bulk of material. Forming the same thickness in the second or third land, more of the deformation will be carried out on the nose and less on the front face. Because the UT is directed at the front face, it is naturally sensitive to this difference.

The US measurements for the 5 mm and 2 mm points in Figure 7.19 are distorted because they are being measured at the point of initial contact between roller and part. It can be seen that the data supports this. The contact in the first land shows significantly less reflection than the other two. This is due to the effect described above and shown in Figure 7.20. Effectively, the US measure of contact is biased towards contact on the front face.

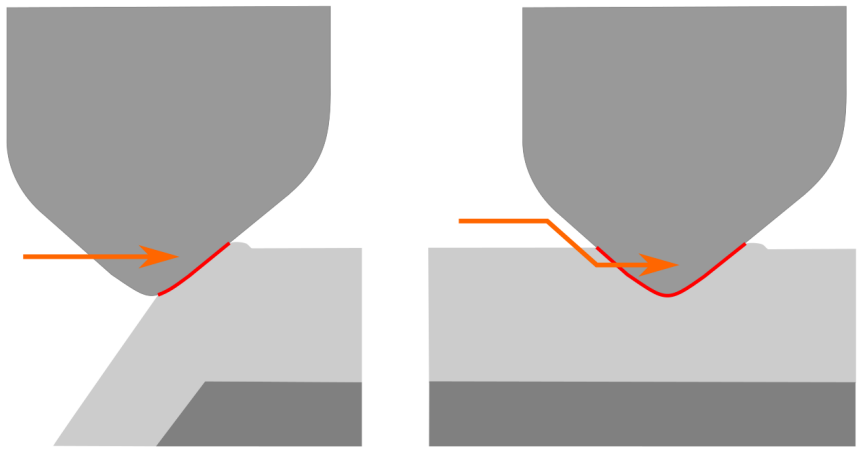

Figure 7.20: A comparison of the contact geometry for different parts of the flow forming stage of the SSF process. The interface where the conical section meets the cylindrical section (left) is much smaller than the interface when reducing in the cylindrical region (right).

It can also be noted that reversing the direction decreases the reflection slightly. There are two likely contributing factors to this result. Firstly, the largest land thickness was greater in these trials (i.e. there was less deformation occuring). Secondly, the low-deformation forming was taking place at the end of the formed part, where the material after spinning stood off the mandrel further. It is therefore likely that the material was not always pressing against the mandrel in these lands - forming partly in free air would also decrease the force.

Examining the high feed rate data (Figure 7.21) shows two things. Increasing the feed rate increases the forming force (as expected) and decreases the US reflection.

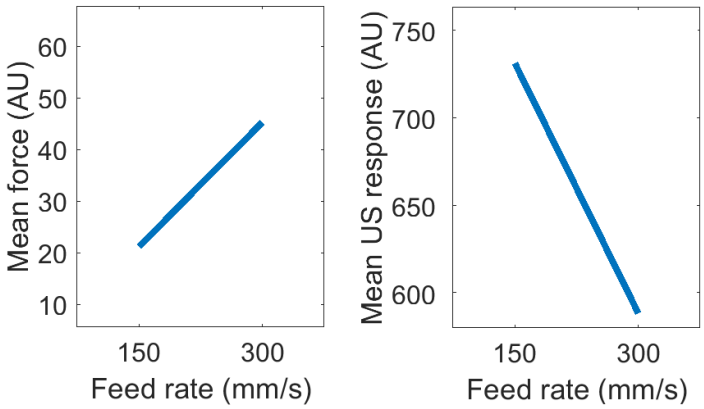

Figure 7.21: Main effects plot from the higher feed rate trials.

This association of increased feed rate with increased US conduction (i.e. reduced reflection) can be explained by two contributory factors - forming contact and coolant flow. Clearly, the coupling from the roller to the part is significantly better than in the low feed rate condition. This could be caused by a larger contact area because the roller is "biting" more deeply. This is likely because with this higher feed the same amount of deformation is being achieved in a shorter time period. It may also be that there is a larger lip of material forming in front of the roller, causing more coupling on the front face. The flow of coolant could also be changing. It is known from the work in Section 7.4.1 that the coolant can significantly change the amount of reflection. The higher feed rate parts are cooler during forming because the process is shorter and they have less time to build up heat. This may lead to less evaporation of coolant, and this

coolant may be conducting away the US energy.

It is therefore clear that there are (at least) three causes of variance in the US signal: the position, size, and nature of the roller-part contact. The variance of the reflection across the lands suggests that the position of the contact has an impact. The size is clearly a factor, for example where it is associated with greater force as in Section 7.5.2. The nature of the contact (e.g. asperity/thin film/fully plastic) and the impact of coolant is demonstrated by the high feed rate results. These entangled factors make this a complex area, resistant to simple interpretation.

Conclusions

There are two important conclusions to draw. Firstly, that this approach is measuring aspects of the forming condition that are independent of the forming forces. Secondly, that the details of contact area measurement could be better described with further work.

In a very simple US model, contact force and contact area are cognate. Where all other factors are held equal, an increase in force will result in increased contact area which will result in increased conduction (i.e. decreased reflection) of US energy. In the complex contact mechanics of IRF, however, force and US conduction do not correspond. This is because of the complex and changeable characteristics of the geometry of the DZ and the dynamics of coolant flow. This is a useful result because of the simple fact: *forming force is already measureable.* Contact area and dynamics were not previously measurable in-process. This is a demonstration of US tribology in a new environment.

Unfortunately it has not been possible to calibrate an area value of the contact area, for several reasons. Firstly, the force recorded by the machine is uncalibrated. Secondly, the influence of DZ position on reflection cannot be separated from the effect of size with the data captured. It may be that calibration is impossible without a simplified experiment without coolant, which is difficult to achieve in an industrial setting.

However, more work is needed to understand how the measurement of US reflections relates to contact area. There are several different aspects of contact area that are not

distinguishable in these results - the position of the contact, the size of the contact and the nature of the contact. It is a challenge for this technology that a millimetre of change in position could cause entirely different results in the US reflection. With the above indications that these measurements are possible, future work could clarify the information contained in the US response.

Process modelling, in combination with carefully controlled forming conditions could create a more robust measurement. These results could therefore be used to understand how to design a new system or set-up.

7.5.4 Crack detection in flow forming

Some parts were SSF formed from a material with inclusions that exhibited unusual forming characteristics. The parts were separating from the mandrel and some were undergoing laminar cracking failures. It was seen that this would be a good opportunity to test the system's capacity for crack detection. This section documents a natural experiment which presented itself in the failure of these parts. As such, there is no formal hypothesis, but an examination of the results will illustrate how crack detection could function in an online monitoring system.

Model

As described in Section 7.2, every interface could potentially produce a measurable reflection. Where an internal crack occurs, the air gap presents a significant change of sonic properties to the US wave. Part of the wave is expected to reflect off the surface of the crack. Figure 7.22 shows how the system is expected to respond to the presence of a laminar crack.

Results

Nine parts were formed, all of which exhibited separation from the mandrel, and 5 of which showed laminar failure. The results of the US recordings are discussed below.

During the forming, the parts were springing off the mandrel. As the rollers approached the ends of the mandrel the internal circumference of the part was greater

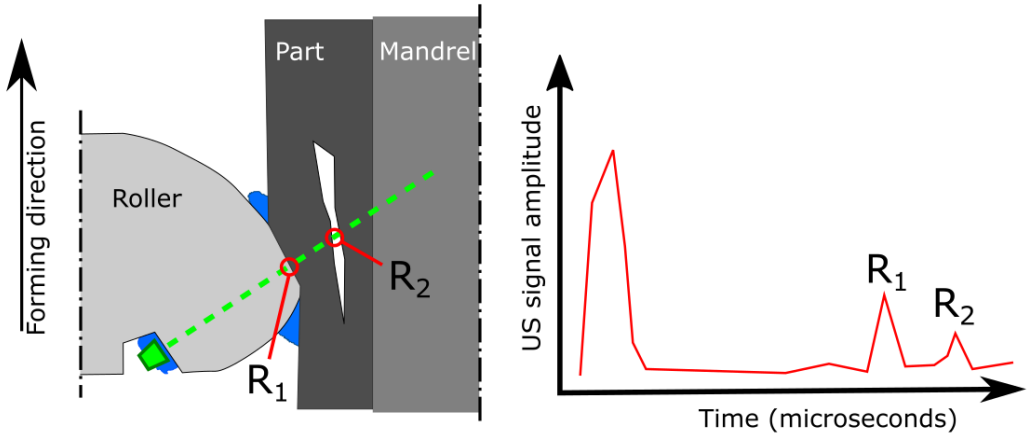

Figure 7.22: Model showing the behaviour schematically. Note the roller-mandrel reflection (R1) and the reflection from the metal-air interface at the crack (R2).

than the external circumference of the mandrel. When the parts were removed it could be clearly seen that there was a slight air gap between the part and mandrel. This is a recognised failure phenomenon, although the causes are not clear (see the notes on diametral growth in Chapter 2). In this case, the geometry was not new, and previous parts with this geometry had not faced this issue, but the material was from a different supplier.

The US results were consistent across all of the parts. During the last forming land, as the part was separating from the mandrel, a second reflection appeared between 23 and 24 µs. Figure 7.23 shows an example output.

The thickness of the final part land was 10 mm. Bearing in mind the taxonomic difficulty of identifying the start of the reflection, the separation between the two signals is approximately 3.25 µs. This, by Equation 7.2, is a gap of 9.75 mm. Therefore the reflection is in the region described by the model, and it is possible to say with some confidence that it is the reflection from the back face of the part.

In some of the parts, a failure occurred where the outer surface of the part separated from the inner with a laminar crack forming through the full circumference. This phenomenon can be seen in Figure 7.24, where the material is divided roughly evenly, in the middle of the thickness. This created two layers of material, each approximately

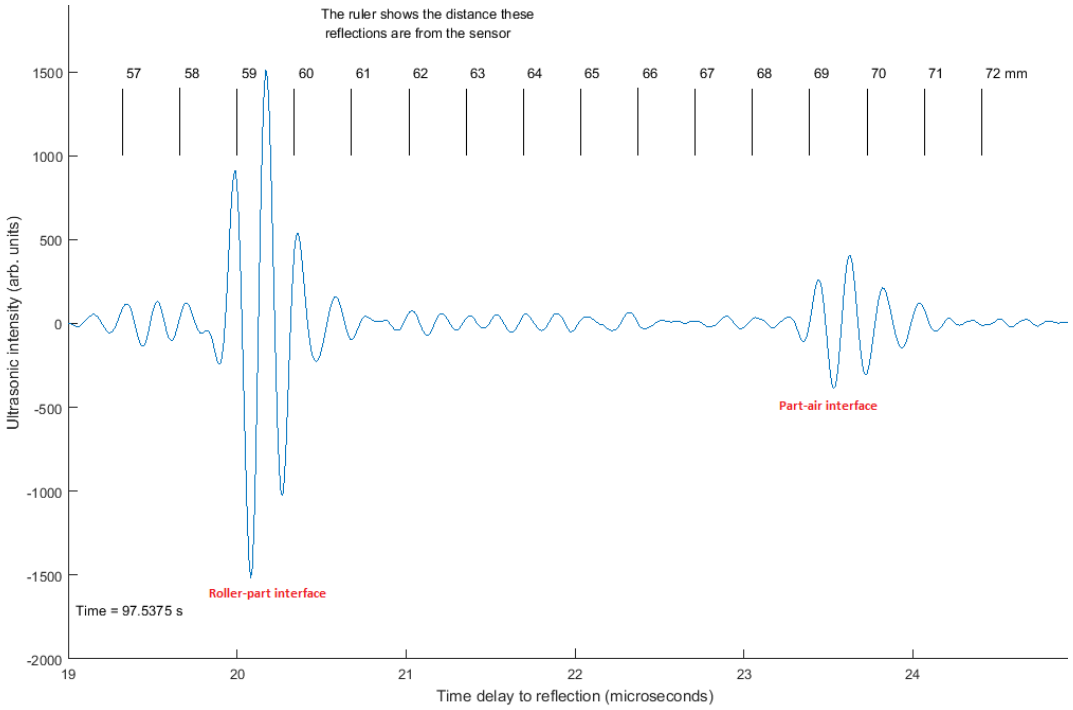

Figure 7.23: Reflections

5 mm thick (although this dimension varied slightly around the circumference). This behaviour is likely caused by the low cost rolled mild steel having inclusions which caused the laminar separation.

The resulting US signal, shown in Figure 7.24, shows three distinct reflections. The reflections are each separated by 1.5 µs. This equates to a distance of 4.9 mm. This suggests that they are from the internal crack and the back face of the component. The onset of the reflections was sudden. It is hard to say if this coincided with the onset of cracking in the part itself as the timing of the onset of cracking is unknown. There was no audible or sensible vibration from the part and the presence of the cracks was only detected after the parts were removed from the machine.

The properties of the roller-material-part interaction for this set of trials are hard to know. Unfortunately, there was no availability of *Sinucom* recording. The dimensions of the parts are clearly different in post-process measurement - the crack stands open for the whole circumference on many parts, yet when they were on the machine the crack

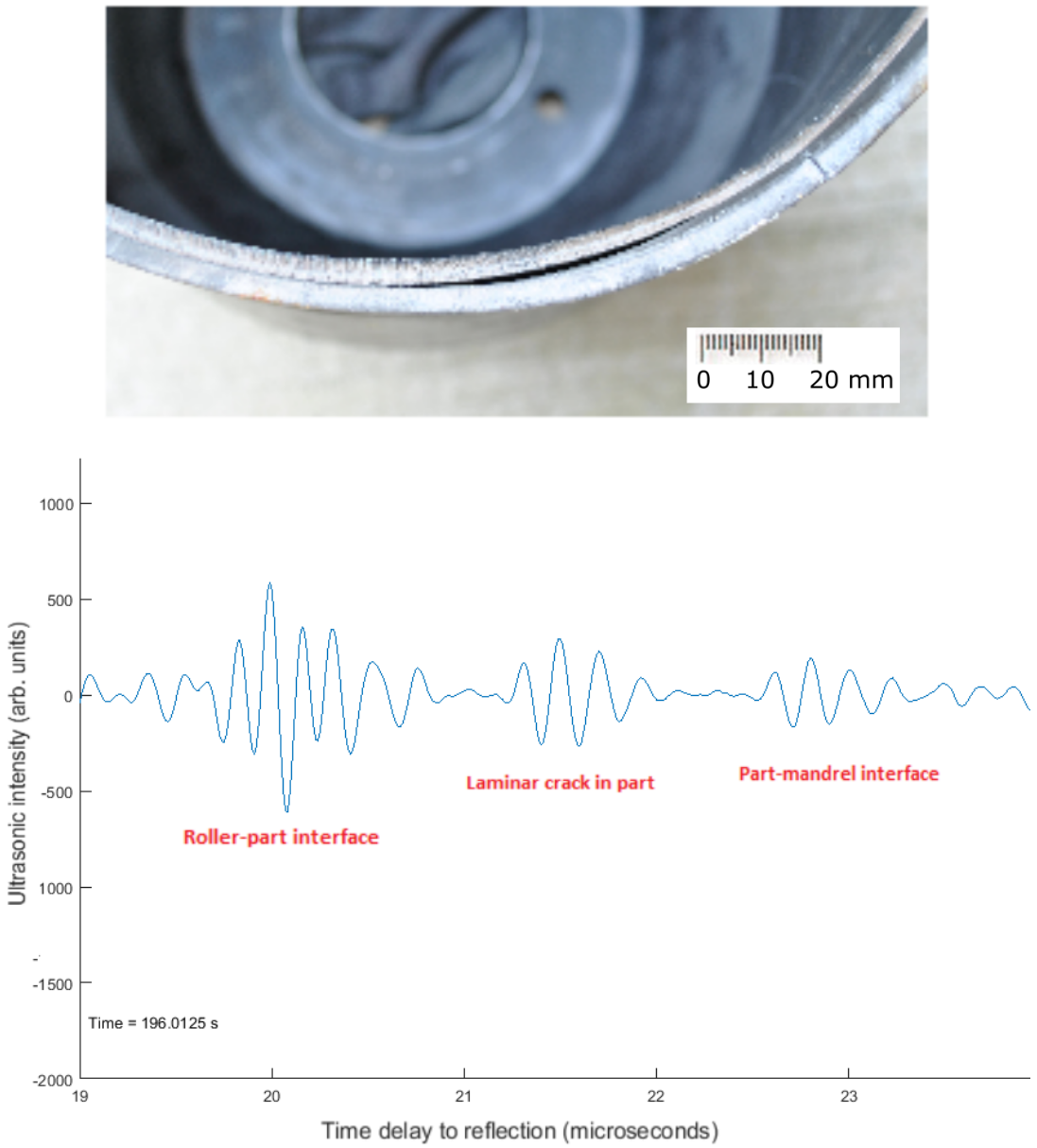

Figure 7.24: Laminar cracking in a SSF part (above) and the corresponding US reflections (below)

must have been at least partially compressed where the rollers engaged. In addition, as with all of these trials, the material properties of the part while it is formed undoubtedly change and the effect of this on US behaviour cannot be accounted for.

These challenges, combined with the difficulty of repeating this natural experiment,

mean that this result is only an indication of what is possible. But these very challenges underline why in-process measurement is important. Because of the dynamic nature of the process, measurements made after the fact do not record the same information as measurements made during the process. This makes in-process measurement techniques hard to verify, but it gives the ability to provide powerful insight.

Conclusions

The principle conclusion from these trials is that this system is capable of collecting reflections from beyond the roller-part interface. That is to say, the system can gather information on the internal mechanics of the process in real time. This is information that has never before been collected to the best of the author's knowledge.

Specifically, the system is capable, under some circumstances, of detecting two important properties: part thickness and the presence of interior cracking. It should be noted that the size of the cracks in this trial was large and the aspect (parallel to the surface) was the most conducive possible for the US system. Cracks in IRF processes are likely to be smaller and in a circumferential direction, which will be harder to detect as the reflections will be smaller.

Although this trial does not by any means give a comprehensive solution to detecting these elements of the process, it proves that it is possible. The ability to carry out real-time flaw detection has potential for process design and improvement, so an improved application of this result could benefit IRF processes.

7.5.5 Thickness detection in spinning

So far, the work has mostly examined the reflection from the roller nose. But Section 7.5.4 showed that measurements of thickness are possible. Another set of trials was planned and carried out to investigate the behaviour of reflections from the back of the part. The reflection from the back face of the part is hard to detect under most circumstances during FF. This is for two reasons. Firstly, the continuous steel-steel interface of part to mandrel will cause only a small reflection because the materials are in contact and are very similar. Secondly, the interface which causes the reflection is

angled away from the sensor, meaning that much of the US energy that reflects from the interface will not return to the sensor.

For this reason, the spinning part of the SSF process was selected for examining the response to changing thickness. In spinning, the part is being formed in free air, meaning that there should be a large reflection from the back face of the part (in comparison with FF. This means that the thickness is not feedback controlled, as the forming side workpiece is against the roller (i.e. the position is known) but the back side is in free air and the thickness is not known in process. In practice, these processes are refined iteratively because predictive models are not sufficient to give good geometric accuracy. Indications from earlier trials on the SSF process suggested that this was the case. A plan was therefore devised to test the ability to detect changes in thickness.

Aim

The aim for this set of trials is to detect the reflection from the back of the part at different thicknesses, and consequently demonstrate the capacity to detect thickness.

Plan

Parts will be spun with material with differing reductions of thickness. The timings of the reflection from the back face of the part will be examined through the process to look at the change through the process.

Twelve parts will be formed using a two-pass spinning process. The forming path will be changed to spin the material more, which will result in greater thickness change. The part thickness will be measured and the thickness compared with the reflection timings.

Hypothesis

The time delay from the nose reflection to the reflection from the back face of the part will be correlated with the part thickness.

Model

The trials were planned using CAD models of the roller and part. This allowed prediction of how the part and roller come into contact. Unfortunately, the complex shape of the roller and part flange mean that there is only a limited amount of contact suitable for gathering US information.

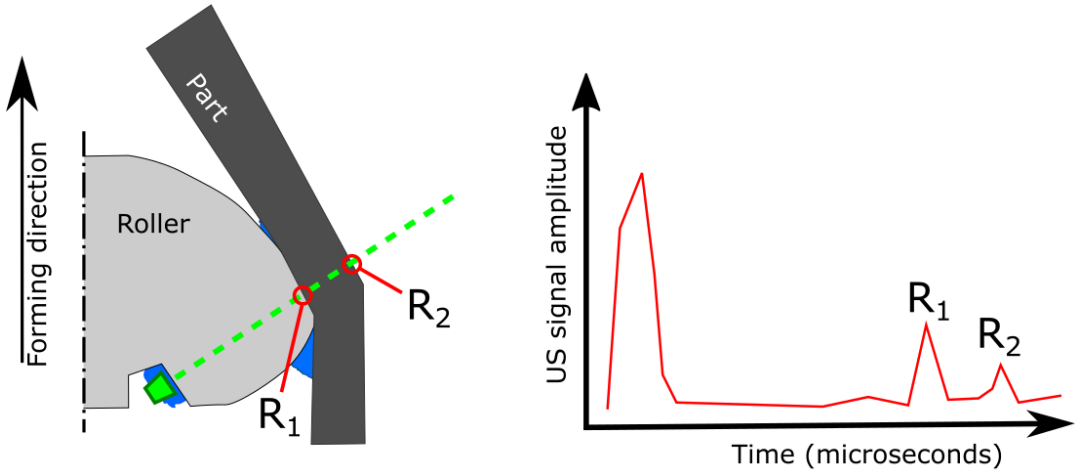

Figure 7.25: The model of spinning shown schematically. Note the reflection from the roller-part interface (R1) and the reflection from the metal-air interface at the back face of the part (R2).

Figure 7.25 shows the spinning process. Consider the small region of the roller which is effectively instrumented - an area of the front face above the nose. When the roller first strikes the part the contact is high on the front face of the roller. The contact region gradually moves down the roller face to the nose. Even in subsequent passes, the contact is not continuously in the same place, but moves towards the nose through the pass. Therefore it will be necessary to look at the periods where the contact is in the instrumented region.

Key variables and outputs

The key variable is the forming path. The key outputs are the part wall thickness and the time-delay on the US reflection from the back of the part.

Results

The inconsistent and complex patterns of reflections make it difficult to interpret the results. Signals in the region beyond the roller nose (i.e. inside the part or mandrel - see Figure 7.22) are detectable at various stages of the process. However it is immediately clear that the signal magnitude is only appreciably large at certain points in the process. This is because of the specific circumstances that allow this reflection to be captured. There are two important factors in this magnitude - the location of contact on the roller (as mentioned above) and the aspect of the part.

Initial tests with a three pass spinning procedure show two periods of good signal - during the first and second passes. Figure 7.26 shows the signal captured in the first pass. This signal is very strong but only for a short period of 1.5 seconds. It is likely that this period is a short duration where the geometry is particularly suited to US reflections. This would be where the roller-material contact is in the area scanned by the UT, and the back face of the material is close to perpendicular to the direction of US propagation (cf. Figure 7.20).

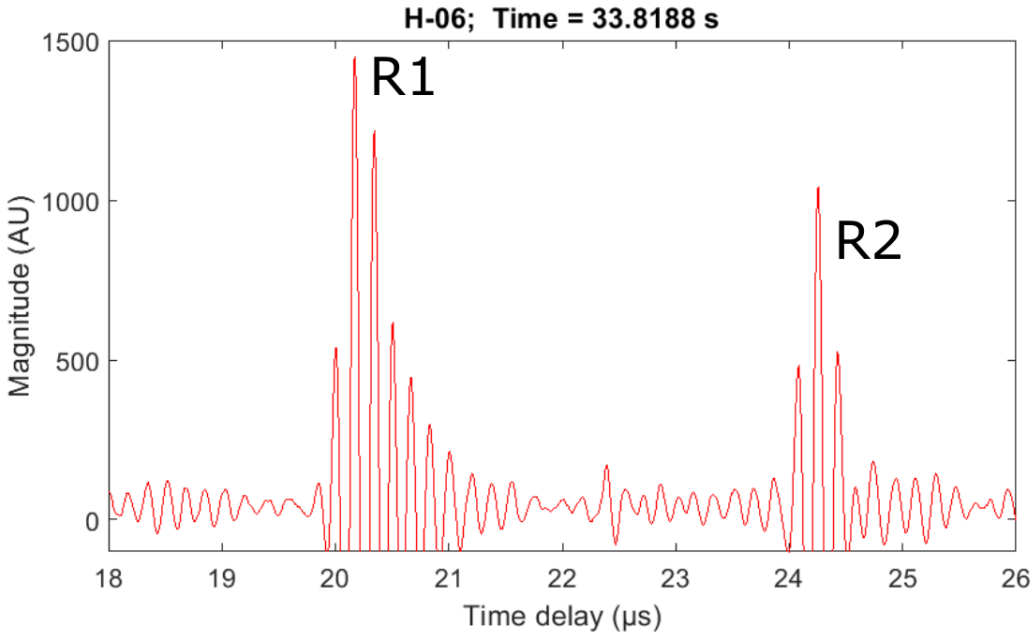

Figure 7.26: Signal from roller-part contact and back face of contact during first spinning pass.

It can be seen that the time from the nose reflection to the back face of the part is approximately 4 µs. This, by Equation 7.2 is a distance of 12 mm. The original part thickness is 12 mm, but some thinning would be expected. The lack of this is explained by the angular difference between the measured and actual thickness. The US waves traverse the roller nose at an angle of α=25 degrees as shown in Figure 7.27. This means that the measured thickness is not the true thickness of the part but the length of the US path. Where the part is fully cylindrical, the angle between the true minimum thickness and the US path, β would be the same as α. But if the part is at an angle (conical in section) as indeed it is known to be, β would be less than α. The measured thickness is actually given by:

$$T_{actual} = T_{measured} cos(\beta) \tag{7.4}$$

Substituting $\alpha = \beta$ gives an actual thickness value of 10.7 mm. However this value is itself contingent on the perfect cylindricity of the part, which in fact is not cylindrical but tends to the conical. So in fact the value for actual thickness must be between 10.7 and 12 mm. Because of the springback when the roller is removed, it is hard to measure the extent of the deviation from the cylindrical while the part is on the machine.

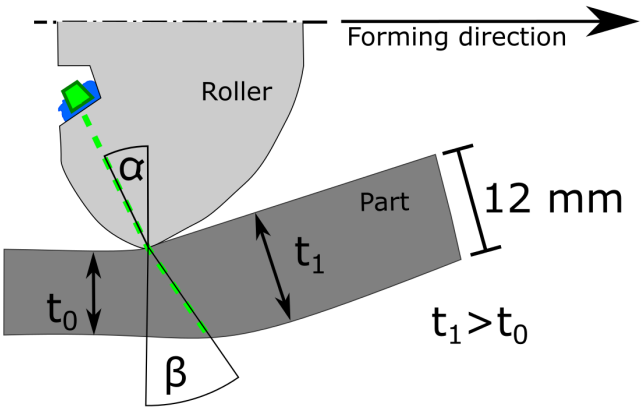

Figure 7.27: Geometric challenges in measuring the spinning part.

Nonetheless, it can be said that the part thickness cannot be greater than the upper

value provided, as there is no possible configuration when the measured distance is less than the actual distance. A further challenge is that the geometry is different again in the second pass. During the second pass, the period of strong signal is longer, lasting for 5 seconds. Figure 7.28 shows the signal captured at the beginning and the end of the second pass. It can be seen that the time delay between the signals is similar to that in the first pass, implying a similar measured thickness. Additionally, there is no reduction in measured thickness from the beginning to end of the part. This is counter-intuitive because the part is known to reduce in thickness during the spinning passes.

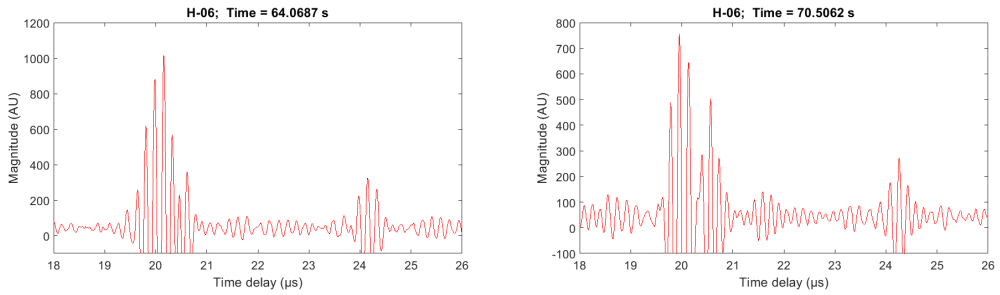

Figure 7.28: Signals at the beginning and the end of the second spinning pass.

There are two possible explanations. Firstly, the cylindricity is increasing through the process (as the part moves from a cone to a cylinder). This will increase the angle of the part to the roller, i.e. β approaches α. So as the process continues, $cos(\beta)$ tends to increase and $T_{measured}$ gets further from T_{actual}. Therefore, while the measured value for thickness in the second pass is the same as in the first pass, the actual value should be trending towards the lower bound of the measure.

Secondly, the angle of the US beam is, in effect, pointing forward into the part. The change in thickness from t_0 to t_1 as shown in Figure 7.27 may largely take place after the UT scans the part, that is, underneath the nose rather than just in front of it. Essentially, the entangled data makes the interpretation challenging.

Conclusions

The difficulty of interpreting these results means that determining thickness is not reliably operable with this system and forming process. The signals are hard to interpret, precisely for the reasons that motivate this project, i.e. that it is difficult to know many of the operational properties while the process is operating. Nonetheless the results are promising and indicative. It is now possible to record signals from the front and back face of a part spinning while covered in sprays of coolant.Extracting thickness information in real time could offer huge benefits for the spinning process. The work that remains now is to refine the system design and process control sufficiently to allow consistent, reliable thickness measurement.

7.6 Conclusions

This chapter has documented the work carried out to test the possibilities for the system. Several avenues have been examined, and some useful results have been recorded.

The trials set out to answer several questions:

1. What insight into forming forces in IRF can US monitoring provide?
2. What insight into contact area in IRF can US monitoring provide?
3. What insight into fracture in IRF can US monitoring provide?
4. What insight into part thickness in IRF can US monitoring provide?

Within the limitations of the work described it is possible to answer the questions as above. It is not possible to use the configuration described in Chapter 6 to measure forming forces because this requires the use of contact area as a proxy for force. The factors (unconnected to force) which alter the contact area are too large to allow force to be determined from the US response. The US response can, however give insight into the contact area of the process, a forming parameter which cannot currently be measured. Cracking can be detected when the cracks are large and parallel to the

material surface as demonstrated. However it is not clear what the lower limits of the detection would be in terms of crack size and aspect. The cracks tested, while they occurred during a real IRF process, were not typical of the process and the results should be considered with this in mind. Finally, it is possible to detect thickness in some very specific circumstances. This process is not robust because to the difficulties in maintaining good SNR and interpreting the results.

The results can be said to have introduced several new possibilities for in-process monitoring of IRF. The potential for real-time detection of contact area, cracking and part thickness present a set of tools for understanding, controlling and improving IRF processes. Future development of the technologies could use these tools to improve operation or to validate modelling of the processes.

The work presented here may be regarded as the launching point for a future area of study. More questions have been raised than answered. By delineating the edges of what may be possible, it is hoped that future work will continue to explore the potential of improved monitoring.

Chapter 8

Discussion and conclusions

The context for this project was the challenging situation for process design and operation in incremental rotary forming (IRF). Despite the significant potential of IRF techniques, they are underutilised in industry. This is principally because of their complexity. The broad aim of the project was to assess the capacity of process monitoring to improve process operation and understanding. Work was carried out to investigate vibration, acoustic and ultrasonic (US) monitoring in varying levels of depth. This chapter reviews the work carried out and assesses the issues, outcomes and next steps.

8.1 Answers to research questions

The project started with the question **What insights can monitoring provideinto an industrial IRF process?** Through the course of the research, different elements of this question emerged and were addressed.

In the research phase (Section 3.6) the following questions were raised and answered:

- How can IRF processes be monitored? *The research shows that vibration, acoustic and US monitoring can all provide insight.*
- What monitoring technologies would be appropriate? *Vibration and acoustic monitoring have been used in similar applications and meet the criterion of*

minimal interference.

- What lessons can be learned from the use of monitoring in other industries? *The complexity of insight is proportionate to the understanding of the system. For a poorly understood system, measurements will likely be coarse.*

After selecting the monitoring technologies for initial investigation, the next question was: **Can vibration and acoustic monitoring detect major process changes in IRF?** Section 5.4.3 explained that this can be answered simply: Major failures (and some minor changes) in the process could be detected. An issue not considered in the question was how practicable this was given current levels of process understanding. The results showed that to gather process insight consistently with this data would require a considerably better process model. Instead, attention was turned to another monitoring technique, one which could gather more detailed information from the point of deformation in the process.

This stage of research addressed the broad question **Can US monitoring provide deeper insight into an industrial IRF process?** Chapters 6 and 7 were focused on answering this question.Through systematic, iterative experimentation, four questions arose and were answered:

1. What insight into forming forces in IRF can US monitoring provide? *It is not possible with the developed geometry to measure force, but the reflection coefficient could be used as a combined measure of force and contact area.*

2. What insight into contact area in IRF can US monitoring provide? *Contact area can be inferred from the machine recorded force information and the contact/force data which is contained in the reflection coefficient.*

3. What insight into fracture in IRF can US monitoring provide? *Fracture detection has been demonstrated under very specific circumstances. It is therefore possible in principle, but would require a system of the correct geometry and sensitivity to detect other types of cracking.*

4. What insight into part thickness in IRF can US monitoring provide? *The theory and results suggest that thickness measurement is possible although it has not been possible to give a calibrated thickness estimate from the US data with the current system geometry.*

The answers above give the answer to the question: **What insight can monitoring provide insight into an industrial IRF process?** It is possible to assert: Acoustic monitoring can detect catastrophic failure of the part. Ultrasonic monitoring can capture information from the DZ to characterise the forming behaviour. With additional work, these could be implemented in an industrial setting.

8.2 Meeting the research aims

The project was carried out as forecast in Section 1.3. In execution, however, the plan in its details. Work on the vibration and acoustic monitoring approaches was carried out in an overlapping fashion. The results from this led to the decision to investigate US monitoring.

The aims, given in Chapter 1, were:

- To broadly explore IRF and process monitoring
- To choose the most appropriate approaches for monitoring IRF
- To establish what capabilities these have for monitoring IRF

These were fulfilled by a process. It started by looking at IRF and monitoring (see Chapters 2 and 3). Next, two monitoring technologies were investigated. This is laid out in Chapter 5 and discussed in Section 8.3. The early trials led to the investigation of US monitoring, which is laid out in Chapters 6 and 7 and discussed in Sections 8.4 and 8.5.

8.3 Review of early investigations

After the literature review stage assessed the state of IRF and the potential input of process monitoring, the downselection (carried out in Section 3.5) led to vibration and acoustic sensing. The early investigations covered in Chapter 5 attempted to consider these technologies for use in IRF in a timely and cost-effective manner. The trials showed that these approaches had some potential, but in the end the research turned to another technology.

Vibration monitoring was attempted because of its low implementation complexity and wide use. Although it was simple to install, the SNR was very poor and the lack of a robust vibration model meant that the results were hard to interpret. Even major, catastrophic failures did not show up on the signal. The results indicate that a working vibration monitoring approach would require a substantial development, which is hard to justify on the limited results shown in this trial.

The acoustic method initially seemed less promising as it is less widely used. But implementation was always likely to be feasible because there was already evidence from the operators that fracture was audible. In operation, it was clear that catastrophic failures did show up in the audio signal. This means that acoustic monitoring has potential for preventing damage to tooling in a major failure. The trials showed little to indicate that acoustic monitoring can detect smaller process changes - it was only possible to elicit a notable response with very large defects. This is largely because of the poor SNR, as with vibration. Further development on acoustic monitoring is limited by the same issues as vibration monitoring.

After these investigations, it was clear that detecting small process changes would be easier with a different approach. Where vibration and acoustic capture information from the whole process, another approach which could scan the site of interest (the deformation zone) directly offered some benefits. The most suitable technology from the earlier downselection was US monitoring, so plans were made to design and test a US system.

8.4 Review of ultrasonic system

The design and operation of the US monitoring system constitutes a major part of this thesis. The process of designing and operating the system gave rise to significant insight. Some of these observations reinforce the correctness of the choices made, and some suggest that other routes would be more profitable in future. The design of the system required a large number of choices to be made. These decisions are discussed in Chapter 6. In the course of the development, a lot of information was suddenly available to assess which aspects of the design worked well, which worked poorly, where the system showed its limitations and how a next-generation system could be improved.

8.4.1 Design successes

Section 8.5 addresses how the main research goals were met. In terms of the design, there are three areas in which it excelled: continuity, non-invasiveness and proximity.

The continuous collection of data was one of the principal aims of the design. In implementation, this proved challenging (see Section 8.4.2), but the challenges were overcome. A continuous stream of data was collected from the DZ. This shows that it is practicable to collect real-time information about the process.

The non-invasiveness requirement for the design was put in place to protect the machine and the process. These aims were clearly met, as forming continued uninterrupted - indeed, the modified roller is still in use as part of a normal toolset. Thus, the primacy of production in an industrial context can be maintained with such a system.

The closesness of the sensor to the area of interest is of great importance. The weakness in the acoustic and vibrometry trials was the long and complex chain connecting the point of interest to the point of data collection. The US design makes a significant step forward in this aspect. The data collected by this system can be clearly related to a small zone on the roller. This makes interpretation far easier than with the broad approach attempted previously. One of the recommendations made below is that this scanned area should become even tighter - i.e. that the design went in the

right direction, but not far enough.

In summary, the implementation of the design proved that the assumptions taken at the outset were valid, and that the design choices made were logical. The priorities for future designs should reflect these successes.

8.4.2 Design limitations

The system had some limitations which became clear during implementation. The design was based in a set of priorities for optimising the monitoring process, while being constrained by limitations of the circumstances of application. That is, the design was based on a series of compromises between an optimal monitoring approach and a practicable industrial one. The limitations, described below, were obvious to varying degrees in operation.

The design uses a single sensor to view the front of the roller nose. Although the sensor presents the most proximate view of the DZ yet achieved, the results suggest that an even closer view would be better. In effect, the sensor is too far from the area of interest and scans too broad an area This large area returns a single point of data, which contributes to poor SNR in two ways. Firstly, the area contains a large amount of signal noise from the effect of coolant on the roller surface. Secondly, the contact area (DZ) makes up only a small part of the area scanned, which decreases the signal strength from the DZ. In addition, it is unclear which exact part of the scanned area is affecting the signal, making it hard to draw insight from the signal.

The choice of continuous fluid coupling was made to give a continuous stream of data recorded in the region of interest. But it came with major challenges in implementation. Maintaining a precise amount of coolant flow between the UT and the roller during the whole process was very difficult. If the coolant flow was too low, air gaps caused signal intermittency. If the coolant flow was too high, or the UT-roller spacing was too large, air bubbles would form with the same result. The weight of the roller meant that a dimensional scan was impossible in the centre. However, manual measurements suggested that the concentricity of the channel manufactured in the back of the roller might be poor. Even a submillimetric variability of the UT-roller spacing is sufficient

to cause signal issues. These challenges meant that experimentation was hampered and limited. A better coupling system would improve the overall system performance, and hence the capacity to collect data.

These limitations in fact represent an important outcome of the research. Without building the system in some form, it would be impossible to begin to refine the design. Section 8.4.3 below describes some of the refinements that can now be made to the UT system.

8.4.3 Insights for future development

As well as the results from experimentation (see Section 8.5), work done with the system gave insight into how US monitoring of IRF could be better accomplished. There are two notable areas of potential improvement: better system design and better data useage.

The limitations of the design (noted in Section 8.4.2 above) are various, but they could all be fixed or improved by changes in a subsequent iteration of the system. These changes could be made to the sensor design, sensor positioning, the number of sensors, and the coupling type. The choice or design of the actual UT was limited in this project by the small number of UTs available with the correct size, frequency range and environmentally resistant properties. But given a wider scope for sensor development, it would benefit the system to use a different, new UT. A UT with a more focused actuator would give a narrower area of scanning. This would have a major benefit - it would mean that the data collected came from a small area around the DZ. This would improve the SNR, as by definition the data would be more signal from the DZ and less noise from the surface around the DZ. In addition, by reducing the scanned area, it would reduce the impact of coolant splashing on the area surrounding the DZ - see Chapter 7 for why this is such an issue. This would further improve the SNR.

The reduction in the area scanned by such a sensor would limit the uses of the set-up. It would exclude some of the applications tested in Chapter 7, notably the spinning work which takes place away from the roller nose and hence out of reach of a narrower-focus sensor. This issue could be countered by using an array of sensors

arranged to scan along the outer surface of the roller profile. Figure 8.1 shows such a design. When the contact patch was in the region covered by each sensor the SNR would be better than the current system because of the smaller area (less noise from surrounding coolant effects) and the other sensors could be disregarded. By locating the nadir of US response across the sensors, such a set-up would make it possible to track the location of contact across the roller surface. The larger material removal needed could be countered by using fixed sensors. These could be installed with less material removal because they do not need access for couplant.

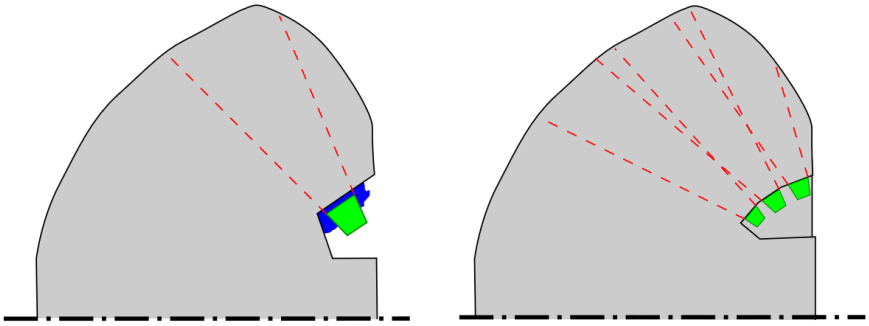

Figure 8.1: Current coverage area from one fluid-coupled sensor (left) and proposed larger coverage from multiple overlapping fixed sensors.

Another area that might be reconsidered in future is the use of fluid coupling. As noted in Section 8.4.2, this set-up gave some advantages but also made for difficult experimentation. After the completion of the experiments, it now seems likely that fixed sensors would have been almost as informative, with a much reduced complexity. Figure 8.2 shows how multiple sensors could be used to capture intermittent data. As long as the speed-to-feed ratio of the process is high enough, the sensor would scan regularly through any developments. Sudden changes would be missed, but this would not be a great loss as the set-up used in this work did not show the capability to detect or predict failure. In addition, the rotation of these sensors with the roller would mean they could effectively scan across the DZ. This would gather more information about the area and shape of the contact patch.

Changes in the electrical hardware driving the UT could also be made. As noted in Chapter 7, the minimum pulsewidth available means that it is challenging to measure

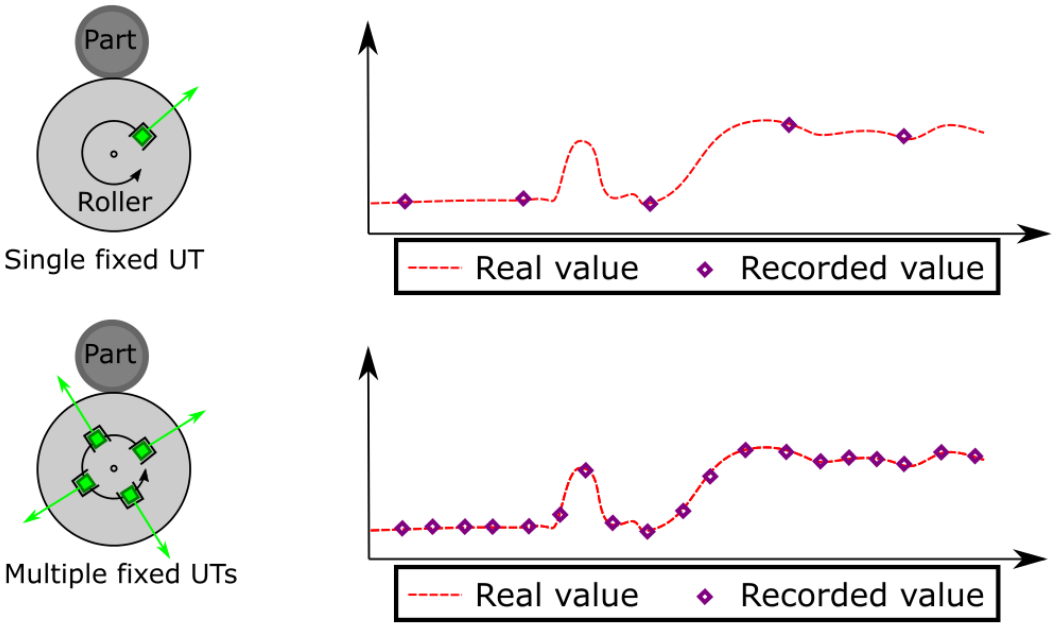

Figure 8.2: Multiple fixed sensors could capture multiple data points per revolution. Cf. Figure 6.4.

between two close points (e.g. the thickness of a thin layer of material). Changes to the US pulsewidth could be given to allow low thickness measurements without the pulses overlapping. If this were combined with the multi-sensor design suggested above, it would be possible to build a system that could sense thickness across all forming paths. This would give a continuous record of contact position and thickness. With calibration, this would give a measurement of springback in spinning (currently impossible).

The suggestions made above would require a total redesign of the system including roller modification, changes in the software to accomodate different pulsewidths and multiple sensors, and possibly the manufacture of bespoke UTs. This would clearly be a major undertaking. But the suggestions are grounded in the results from the project, and are the author's suggestion of the logical next iteration.

8.5 Review of Experimental design and results

This section will review how the experiments were designed and planned, what was prioritised and what was not, and how things might have been done differently.

Suggestions will be made for how future experimentation could strengthen the evidence base for the effectiveness of monitoring IRF.

Section 4 sets out the approach that was taken for the experiments. Initial trials attempted to explore the possibilities of vibration, acoustic and US monitoring with a minimal number of parts. More in depth trials on the US equipment were planned in detail in Chapter 7. This approach was effective as it allowed a flexibility when exploring the new area of IRF monitoring.

Chapter 5 covers the work done in vibration and acoustic monitoring. These approaches were selected because of the directly audible and sensible nature of failures on the machine. They also had the advantages of low cost and simple installation.

In execution, however, a brief examination of vibration was unable to shed light on the flow forming process. In fact, the complexity of the path of vibrations and the many sources of vibration at similar frequencies made interpretation of the signals very challenging. For this reason, attention was shifted to a related technology, acoustic monitoring.

Acoustic monitoring proved to have more mineable potential for insight. It was possible to link rumbling noises to material breakdown in the process. There is therefore potential for an acoustic based emergency shutdown system for FF and similar processes. This could prevent tooling damage and thus make significant savings.

The insight is limited however, as it is not clear that the fine details of the process will ever be measureable by acoustic means. Indeed, it seems likely that acoustic monitoring will be limited to very coarse measurements for the foreseeable future. The consequence of this is that more detailed data relating to the process will need to be gathered by other methods.

In the search for more detailed information about the process behaviour, a method was needed that approached close to the zone of deformation and gathered information about it. US monitoring was selected because of its potential to probe the DZ for data related to force and contact area. Chapter 7 covers the experimental work which aimed to validate the US system. The system was clearly successful under the broad aims given in Section 1.3. The results from the US work bear some discussion. The trials on

FF showed that it is possible to gather more information about the tool-part interface and the behaviour of the part itself.

The work on the force response in FF and SSF shows that information can be gathered from this hitherto unexamined area. The results show that the US system can capture aspects of the forming operation that are partially independent of the forming forces. This means that new information is being captured which has never previously been recorded. The proportion of US signal which is reflected is a result of forming force, contact patch properties and coolant flow. To entirely understand this complex situation, multiple points of data collection are needed. For example, if it was possible to measure the forming force and coolant behaviour, then the size of the contact patch would be measurable.

The data collection demonstrated in this work adds another step towards full understanding of the process behaviour. This source of information contributes to a toolkit for deepening the understanding of IRF. Other elements include laboratory trials, industrial trials, other instrumentation and modelling. As each of these elements find small insights they will feed into each other. For example, knowledge from monitoring could improve modelling accuracy; accurate models aid parameter selection for practical trials, and so on.

The work on thickness and cracking in different parts of the SSF process show that it is possible to collect information from inside the part during the forming process. These results were challenging to interpret, however it is possible to say with confidence that US signals collected from past the DZ contain information about what is happening inside the process. This represents a new capacity for measurement in an area that is currently lacking. The results are indicative, not conclusive. But they show that the thickness could be measured and the presence of cracks detected. The US system, as designed, has design features that limit its ability to scan the parts in this way. Sections 8.4.2 and 8.4.3 discuss how future iterations could be changed to improve this capacity.

8.6 Contribution and utility of the work

The contribution to knowledge of this work can be summarised as follows:

- The first application of acoustic monitoring to FF, which resulted in the demonstration of detection of catastrophic fractures in the process.
- The development of a functional design for an US monitoring system for IRF. This design can form the basis for future work.
- The demonstration of US monitoring capability for gathering information on contact area and fracture.

The utility of this work in the field is likely to be in three areas: process modelling, development and control. The systems developed in this work are not calibrated or ready for industrial use, but more advanced systems which follow on from this work could be. FE models for IRF need to be refined, and they need real world measurements to improve their accuracy. More advanced monitoring systems could give this information. Development of IRF processes is limited by the complex range of parameters. By elucidating the parameter behaviour, these techniques could be used to disentangle the complex parameter effects and interactions. Eventually, fully industrial-ready on-line process monitoring could lead to an area of fully self-controlled IRF machines which adapt reactively to changing designs and materials.

8.7 Future work

The discussion above suggests that the project was successful in its aims. But it also opened many avenues for investigation. Some suggestions may be given for how a future extension of the work might proceed.

In a larger project, it would be possible to look at the problem in its entirety. Initially, the development of a FE process model could be used to design a process suitable for experimentation. The experiments could then be designed using the FE model to create hypotheses for the pressure and contact area behaviour. More detailed

ultrasonic and CAD modelling could be coupled with UT development to create a bespoke transducer array. Such an array, as discussed earlier in this chapter, would allow the collection of more detailed process information.

To fully characterise the behaviour, the new system should first be tested in a simplified scale model. The scale rig could be used to understand how the signal variation relates to specific process behaviour. This would be done by gradually adding complexity in the part geometry, contact shape and coolant regime. These tests are impossible on an industrial machine, for example because it is not possible to use a single roller or to turn off the coolant. The scale model approach would develop the interpretative techniques to be used on the full machine.

Full-scale testing could then be carried out. In a future project, this could be significantly improved with better data handling, processing and interpretation. Data handling could be better if a bespoke front end was developed that integrated the machine signals (force, position, etc.) with the US signals. Processing could see huge benefits with a dedicated signal processing approach, improving the filtering of the data. Interpretation would be improved by the ability to compare with the FE and scaled models.

8.8 Conclusions

The project set out to gain insight into IRF through monitoring. The aims were, firstly, to look at the challenges in the processes and examine the available monitoring solutions. Then, to select some options and attempt to implement them. This was done to learn about the challenges of implementation and the potential for data collection. The overall motivation was to understand how the monitoring could improve process understanding.

Initially, the project looked specifically at identifying and predicting in-process failure. This line of inquiry led first to the minimally disruptive approaches of vibration and acoustic monitoring. These proved limited in scope because the results were hard to interpret for all but the most extreme failures. Small fractures or faults were hard

to identify. But major failure was identifiable (Appleby et al., 2017). This result is valuable because the ability to automatically identify catastrophic failures could allow machine shutdown before damage occurs to the tooling or machine.

One of the key limitations of these methods is that they gather data from the entire process and from surrounding machines. This introduces significant noise, and it is challenging to identify the signal of interest among the noise. Unfortunately, many of the technologies identified for monitoring which had the capacity to gather specific data from a small part of the process had significant implementation challenges. Ultrasonic monitoring had definite potential for looking at the contact between tool and workpiece, and the implementation difficulties seemed surmountable. Work was therefore undertaken to develop a US system that could interrogate the DZ. Difficulties were anticipated where possible, but the commissioning of the system required considerable fine-tuning.

The US showed considerable capacity to collect information about the process. Two significant new capacities were demonstrated - the ability to record information about the size of the DZ, and the ability to identify material fracture in some circumstances. These are both entirely novel in the context of IRF, and have significant potential. Identifying the contact characteristics has potential for validating and improving FE models and theories about deformation behaviour. The ability to detect material fracture could be used to identify forming limits and improve process design - for example to understand why some geometries can be formed and others fracture unexpectedly. In addition, there are indications that it would be possible to measure thickness in spinning, something currently impossible. This would allow a more detailed understanding of forming paths and springback in the process. The experiments show that this technology, and process monitoring in general, has a significant potential to improve the processes, their use and understanding.

The broad, initial research aim was to explore process monitoring technologies and assess their application to IRF. As might be expected, the project has raised more questions than answers - much more development work is needed to gain the full potential of these technologies. But the outlines of process monitoring of IRF have

now been sketched. As IRF processes continue to grow in use in industry, it is to be hoped that interest in process development continues and that monitoring techniques grow in sophistication as the field matures.

Bibliography

Ambhore, N., Kamble, D., Chinchanikar, S., and Wayal, V. (2015). Tool condition monitoring system: A review. *Materials Today: Proceedings*, 2(4-5):3419–3428.

Anderson, D., Jarzynski, J., and Salant, R. (2000). Condition monitoring of mechanical seals: detection of film collapse using reflected ultrasonic waves. *Proceedings of the Institution of Mechanical Engineers, Part C: Journal of Mechanical Engineering Science*, 214(9):1187–1194.

Appleby, A. (2015). A novel acoustic method for improved monitoring of rotary metal forming processes. Master's thesis, University of Strathclyde.

Appleby, A., Conway, A., and Ion, W. (2017). A novel methodology for in-process monitoring of flow forming. In *AIP Conference Proceedings*, volume 1896. AIP Publishing.

Bedekar, V., Pauskar, P., Shivpuri, R., and Howe, J. (2014). Microstructure and texture evolutions in aisi 1050 steel by flow forming. *Procedia Engineering*, 81:2355–2360.

Behrens, A. and Just, H. (2002). Verification of the damage model of effective stresses in cold and warm forging operations by experimental testing and FE simulations. *J. Mater. Process. Technol.*, 125-126:295–301.

Behrens, B.-A., Santangelo, A., and Buse, C. (2013). Acoustic emission technique for online monitoring during cold forging of steel components: a promising approach for online crack detection in metal forming processes. *Prod. Eng.*, 7(4):423–432.

Bhatt, R. J. and Raval, H. K. (2016). Influence of operating variables during flow forming process. *Procedia CIRP*, 55:146–151.

Bhatt, R. J. and Raval, H. K. (2018a). Experimental study on flow forming process and its numerical validation. *Materials Today: Proceedings*, 5(2):7230–7239.

Bhatt, R. J. and Raval, H. K. (2018b). In situ investigations on forces and power consumption during flow forming process. *Journal of Mechanical Science and Technology*, 32(3):1307–1315.

Birosca, S., Ding, R., Ooi, S., Buckingham, R., Coleman, C., and Dicks, K. (2015). Nanostructure characterisation of flow-formed cr–mo–v steel using transmission kikuchi diffraction technique. *Ultramicroscopy*, 153:1–8.

Blessing, L. T. and Chakrabarti, A. (2009). *DRM: A design reseach methodology.* Springer.

Bylya, O. I., Khismatullin, T., Blackwell, P., and Vasin, R. A. (2018). The effect of elasto-plastic properties of materials on their formability by flow forming. *Journal of Materials Processing Technology*, 252:34–44.

D'Annibale, A., Di Ilio, A., Paoletti, A., Paoletti, D., and Sfarra, S. (2017). The combination of advanced tools for parameters investigation and tools maintenance in flow forming process. *Procedia CIRP*, 59:144–149.

Dimla Snr., D. and Lister, P. (2000). Sensor signals for tool-wear monitoring in metal cutting operations - a review of methods. *Int. J. Mach. Tools Manuf.*, 40(8):1073–1098.

DIN (2003a). *DIN 8583-5 Fertigungsverfahren Zugdruckumformen.* Beuth Verlag, Berlin, Germany.

DIN (2003b). *DIN 8584-4 Fertigungsverfahren Zugdruckumformen.* Beuth Verlag, Berlin, Germany.

Ding, S. X. (2008). *Model-based fault diagnosis techniques: design schemes, algorithms, and tools*. Springer Science & Business Media.

Du, F., Li, B., Zhang, J., Zhu, Q. M., and Hong, J. (2015). Ultrasonic measurement of contact stiffness and pressure distribution on spindle–holder taper interfaces. *International Journal of Machine Tools and Manufacture*, 97:18–28.

Dwyer-Joyce, R. (2005). The application of ultrasonic ndt techniques in tribology. *Proceedings of the Institution of Mechanical Engineers, Part J: Journal of Engineering Tribology*, 219(5):347–366.

Dwyer-Joyce, R., Drinkwater, B., and Quinn, A. (2001). The use of ultrasound in the investigation of rough surface interfaces. *Journal of tribology*, 123(1):8–16.

Dwyer-Joyce, R., Reddyhoff, T., and Drinkwater, B. (2004). Operating limits for acoustic measurement of rolling bearing oil film thickness. *Tribology transactions*, 47(3):366–375.

Easterby-Smith, M., Thorpe, R. Y., and Lowe, A. (1991). A.(1991): Management research-an introduction.

El-galy, I. and Behrens, B.-a. (2008). Online Monitoring of Hot Die Forging Processes Using Acoustic Emission (Part I). *Acoustic Emission*, 26:208–219.

El-galy, I. and Behrens, B.-a. (2010). Online Monitoring of Hot Die Forging Processes Using Acoustic Emission (Part II). In *Proc. EWDAE 2010*.

Haghshenas, M. and Klassen, R. (2015). Mechanical characterization of flow formed fcc alloys. *Materials Science and Engineering: A*, 641:249–255.

Hao, S., Ramalingam, S., and Klamecki, B. E. (2000). Acoustic emission monitoring of sheet metal forming: Characterization of the transducer, the work material and the process. *J. Mater. Process. Technol.*, 101(1):124–136.

Havelock, D., Kuwano, S., and Vorländer, M. (2008). *Handbook of signal processing in acoustics*. Springer Science & Business Media.

Hayama, M. and Kudo, H. (1979). Analysis of diametral growth and working forces in tube spinning. *Bulletin of JSME*, 22(167):776–784.

Holdich, T., Hunter, A., Pinna, C., and Dwyer-Joyce, R. (2017). An ultrasonic sensor for the in-process monitoring of strip gauge and lubrication in cold metal rolling. In *IOM3: In-line measurement and control for metals processing 2017*.

Hunter, A., Dwyer-Joyce, R., and Harper, P. (2012). Calibration and validation of ultrasonic reflection methods for thin-film measurement in tribology. *Measurement Science and Technology*, 23(10):105605.

Hwang, S. Y., Kim, N., and Lee, C.-s. (2015). Numerical investigation on the effect of process parameters during aluminum wheel flow-forming. *Strojniški vestnik-Journal of Mechanical Engineering*, 61(7-8):471–476.

Jahazi, M. and Ebrahimi, G. (2000). The influence of flow-forming parameters and microstructure on the quality of a d6ac steel. *Journal of materials processing technology*, 103(3):362–366.

Jayakumar, T., Mukhopadhyay, C. K., Venugopal, S., Mannan, S. L., and Raj, B. (2005). A review of the application of acoustic emission techniques for monitoring forming and grinding processes. *J. Mater. Process. Technol.*, 159(1):48–61.

Jemielniak, K. (2001). Some aspects of acoustic emission signal pre-processing. *J. Mater. Process. Technol.*, 109(3):242–247.

Jemielniak, K., Bombiski, S., and Aristimuno, P. X. (2008). Tool condition monitoring in micromilling based on hierarchical integration of signal measures. *CIRP Ann. - Manuf. Technol.*, 57(1):121–124.

Jolly, S. S. and Bedi, D. (2010). Analysis of power and forces in the making of long tubes in hard-to-work materials. *Proc. W. Congr. Eng*, 2.

Kendall, K. and Tabor, D. (1971). An utrasonic study of the area of contact between stationary and sliding surfaces. *Proc. R. Soc. Lond. A*, 323(1554):321–340.

Kong, L. X. and Nahavandi, S. (2002). On-line tool condition monitoring and control system in forging processes. *J. Mater. Process. Technol.*, 125-126:464–470.

Kuljanic, E., Totis, G., and Sortino, M. (2009). Development of an intelligent multisensor chatter detection system in milling. *Mechanical Systems and Signal Processing*, 23(5):1704–1718.

Lee, D. E., Hwang, I., Valente, C. M. O., Oliveira, J. F. G., and Dornfeld, D. a. (2006). Precision manufacturing process monitoring with acoustic emission. *Int. J. Mach. Tools Manuf.*, 46(2):176–188.

Lei, Y., Lin, J., Zuo, M. J., and He, Z. (2014). Condition monitoring and fault diagnosis of planetary gearboxes: A review. *Measurement*, 48:292–305.

Lloyd, E. (1986). An introduction to some metal-forming theory, principles and practice. *Portcullis Press*.

Lu, M.-C. and Kannatey-Asibu, E. (2002). Analysis of sound signal generation due to flank wear in turning. *Journal of Manufacturing Science and Engineering*.

Lynch, C. T. (2019). *Handbook of Materials Science: Volume 1 General Properties*, volume 1. CRC Press.

Makhdum, F., Conway, A., and Blackwell, P. (2016). Experimental investigation on shape evolution in metal forming hybrid process. In *Key Engineering Materials*, volume 716, pages 420–427. Trans Tech Publ.

Marinescu, I. and Axinte, D. A. (2008). A critical analysis of effectiveness of acoustic emission signals to detect tool and workpiece malfunctions in milling operations. *International Journal of Machine Tools and Manufacture*, 48(10):1148–1160.

Marini, D., Cunningham, D., and Corney, J. (2015). A review of flow forming processes and mechanisms. *Key Engineering Materials*, 651-653:750–758.

Mark, W. D., Lee, H., Patrick, R., and Coker, J. D. (2010). A simple frequency-domain algorithm for early detection of damaged gear teeth. *Mechanical Systems and Signal Processing*, 24(8):2807–2823.

Meijer, C. (2006). "Snell's law" - a Wikimedia Commons image in the public domain. URL: https://commons.wikimedia.org/wiki/File:Snells_law.svg, accessed 01-09-2019.

Miscandlon, J., Tuffs, M., Halliday, S. T., and Conway, A. (2018). Effects of flow forming parameters on dimensional accuracy in cr-mo-v steel tubes. *Procedia Manufacturing*, 15:1215–1223.

Molladavoudi, H. R. and Djavanroodi, F. (2011). Experimental study of thickness reduction effects on mechanical properties and spinning accuracy of aluminum 7075-o, during flow forming. *The International Journal of Advanced Manufacturing Technology*, 52(9-12):949–957.

Mulvihill, D. M., Kartal, M. E., Nowell, D., and Hills, D. A. (2011). An elastic–plastic asperity interaction model for sliding friction. *Tribology international*, 44(12):1679–1694.

Muñoz, J. L. A., Blanco, J. L. Y., and Capuz-Rizo, S. F. (2017). *Project Management and Engineering Research*. Springer.

Nie, M. and Wang, L. (2013). Review of condition monitoring and fault diagnosis technologies for wind turbine gearbox. *Procedia CIRP*, 11(Cm):287–290.

Pai, P. S. and Rao, P. K. R. (2002). Acoustic emission analysis for tool wear monitoring in face milling. *Int. J. Prod. Res.*, 40(5):1081–1093.

Parsa, M., Pazooki, A., and Ahmadabadi, M. N. (2009). Flow-forming and flow formability simulation. *The International Journal of Advanced Manufacturing Technology*, 42(5-6):463–473.

Pau, M., Aymerich, F., and Ginesu, F. (2000). Ultrasonic measurements of nominal contact area and contact pressure in a wheel-rail system. *Proceedings of the Institution of Mechanical Engineers, Part F: Journal of Rail and Rapid Transit*, 214(4):231–243.

Pau, M., Aymerich, F., and Ginesu, F. (2002). Distribution of contact pressure in wheel–rail contact area. *Wear*, 253(1-2):265–274.

Pedaste, M., Mäeots, M., Siiman, L. A., De Jong, T., Van Riesen, S. A., Kamp, E. T., Manoli, C. C., Zacharia, Z. C., and Tsourlidaki, E. (2015). Phases of inquiry-based learning: Definitions and the inquiry cycle. *Educational research review*, 14:47–61.

Podder, B., Banerjee, P., Ramesh Kumar, K., and Hui, N. B. (2018). Flow forming of thin-walled precision shells. *Sādhanā*, 43(12):208.

Pollitt, D. (1995). Metal spinning in the automotive industry. *Sheet Metal Industries*, 72(4):31.

Polyblank, J. A., Allwood, J. M., and Duncan, S. R. (2014). Closed-loop control of product properties in metal forming: A review and prospectus. *Journal of Materials Processing Technology*, 214(11):2333–2348.

Quigley, E. and Monaghan, J. (2000). Metal forming: an analysis of spinning processes. *Journal of Materials Processing Technology*, 103(1):114–119.

Rajan, K. and Narasimhan, K. (2001). An investigation of the development of defects during flow forming of high strength thin wall steel tubes. *Practical Failure Analysis*, 1(5):69–76.

Razani, N., Aghchai, A. J., and Dariani, B. M. (2014). Flow-forming optimization based on hardness of flow-formed aisi321 tube using response surface method. *The International Journal of Advanced Manufacturing Technology*, 70(5-8):1463–1471.

Razani, N., Jalali Aghchai, A., and Mollaei Dariani, B. (2011). Experimental study on flow forming process of aisi 321 steel tube using the taguchi method. *Proceedings of the Institution of Mechanical Engineers, Part B: Journal of Engineering Manufacture*, 225(11):2024–2031.

Ren, Q., Balazinski, M., Baron, L., Jemielniak, K., Botez, R., and Achiche, S. (2014). Type-2 fuzzy tool condition monitoring system based on acoustic emission in micromilling. *Information Sciences*, 255:121–134.

Rizal, M., Ghani, J. A., Nuawi, M. Z., and Haron, C. H. C. (2013). The application of i-kaztm-based method for tool wear monitoring using cutting force signal. *Procedia Engineering*, 68:461–468.

Rose, J. L. (2014). *Ultrasonic guided waves in solid media*. Cambridge university press.

Roy, M., Maijer, D., Klassen, R. J., Wood, J., and Schost, E. (2010). Analytical solution of the tooling/workpiece contact interface shape during a flow forming operation. *Journal of Materials Processing Technology*, 210(14):1976–1985.

Salgado, D. R. and Alonso, F. J. (2007). An approach based on current and sound signals for in-process tool wear monitoring. *Int. J. Mach. Tool Manu.*, 47:2140–2152.

Saravanan, S., Yadava, G. S., and Rao, P. (2006). Condition monitoring studies on spindle bearing of a lathe. *Int J Adv Manuf Technol*.

Scheffer, C. and Heyns, P. S. (2004). An industrial tool wear monitoring system for interrupted turning. *Mech. Syst. Signal Process.*, 18(5):1219–1242.

Schmerr, L. W. and Song, J.-S. (2007). *Ultrasonic nondestructive evaluation systems*. Springer.

Schneider, V., Hirt, G., Brethfeld, a., Lehmann, G., and Diener, U. (2007). Ermittlung von Umformgrenzen beim Freiformschmieden. *Materwiss. Werksttech.*, 38(4):274–287.

Seemuang, N., Mcleay, T., and Slatter, T. (2016). Using spindle noise to monitor tool wear in a turning process. *Int. J. Adv. Manuf. Tech.*

Shinde, H., Mahajan, P., Singh, A. K., Singh, R., and Narasimhan, K. (2016). Process modeling and optimization of the staggered backward flow forming process of maraging steel via finite element simulations. *The International Journal of Advanced Manufacturing Technology*, 87(5-8):1851–1864.

Singhal, R., Saxena, P., and Prakash, R. (1990). Estimation of power in the shear spinning of long tubes in hard-to-work materials. *Journal of materials processing technology*, 23(1):29–40.

Skåre, T. and Krantz, F. (2003). Wear and frictional behaviour of high strength steel in stamping monitored by acoustic emission technique. *Wear*, 255(7-12):1471–1479.

Song, X., Fong, K., Oon, S., Tiong, W., Li, P., Korsunsky, A. M., and Danno, A. (2014). Diametrical growth in the forward flow forming process: simulation, validation, and prediction. *The International Journal of Advanced Manufacturing Technology*, 71(1-4):207–217.

Talluri, S. and Sarkis, J. (2002). A methodology for monitoring system performance. *International Journal of Production Research*, 40(7):1567–1582.

Tekıner, Z. and Yeşılyurt, S. (2004). Investigation of the cutting parameters depending on process sound during turning of aisi 304 austenitic stainless steel. *Materials & Design*, 25(6):507–513.

Teti, R., Jemielniak, K., O'Donnell, G., and Dornfeld, D. (2010). Advanced monitoring of machining operations. *CIRP Ann. - Manuf. Technol.*, 59(2):717–739.

Tsivoulas, D., da Fonseca, J. Q., Tuffs, M., and Preuss, M. (2015). Effects of flow forming parameters on the development of residual stresses in cr–mo–v steel tubes. *Materials Science and Engineering: A*, 624:193–202.

Wang, X., Zhan, M., Fu, M., Guo, J., Xu, R., and Lei, X. (2017). A unique spinning method for grain refinement: repetitive shear spinning. *Procedia Engineering*, 207:1725–1730.

Weingaertner, W. L., Schroeter, R. B., Polli, M. L., and Gomes, J. d. O. (2006). Evaluation of high-speed end-milling dynamic stability through audio signal measurements. *J. Mater. Process. Technol.*

Weller, E., Schrier, H. M., and Weichbrodt, B. (1969). What sound can be expected from a worn tool? *Journal of Engineering for Industry*, 91(3):525–534.

Wong, C. C. (2004). Incremental forming of solid cylindrical components using flow forming principles. *J. Mater. Process. Technol.*, 153-154(1-3):60–66.

Wong, C. C., Dean, T. A., and Lin, J. (2003). A review of spinning, shear forming and flow forming processes. *Int. J. Mach. Tools Manuf.*, 43(14):1419–1435.

Wymore, M. L., Dam, J. E. V., Ceylan, H., and Qiao, D. (2015). A survey of health monitoring systems for wind turbines. *Renew. Sustainable Energy Rev.*, 52(1069283):976–990.

Xu, W., Zhao, X., Ma, H., Shan, D., and Lin, H. (2016). Influence of roller distribution modes on spinning force during tube spinning. *International Journal of Mechanical Sciences*, 113:10–25.

Xu, Y., Zhang, S., Li, P., Yang, K., Shan, D., and Lu, Y. (2001). 3D rigid–plastic FEM numerical simulation on tube spinning. *Journal of Materials Processing Technology*, 113(1-3):710–713.

Appendix A

Gantt chart of project

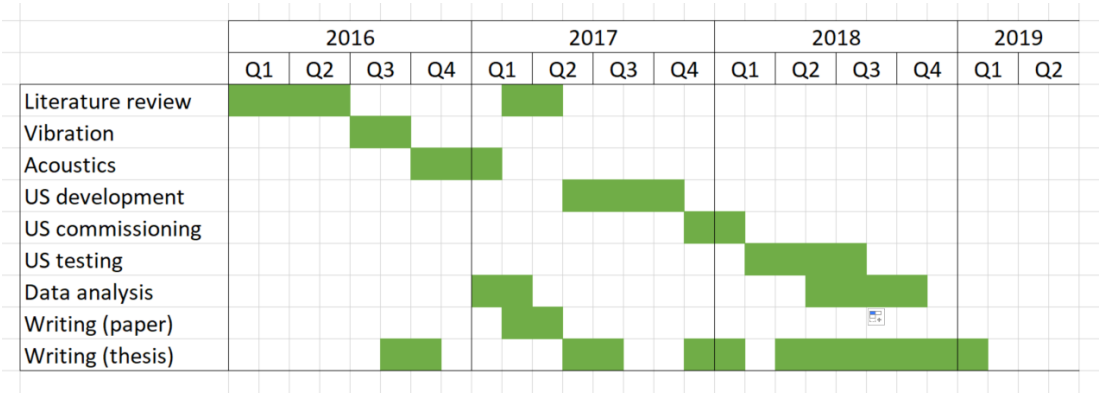

Figure A.1: Gantt chart of project activities.

Appendix B

Drawings and models

B.1 Roller modification

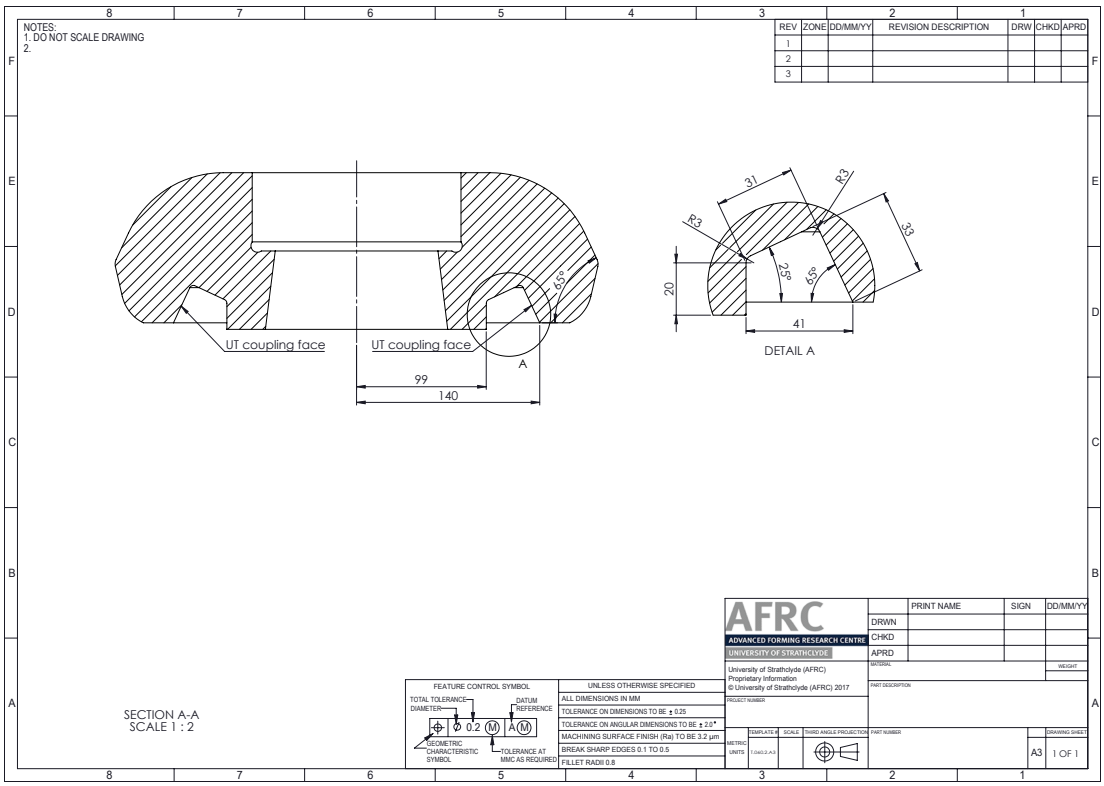

Figure B.1: Roller modification drawing.

B.2 Mounting bracket

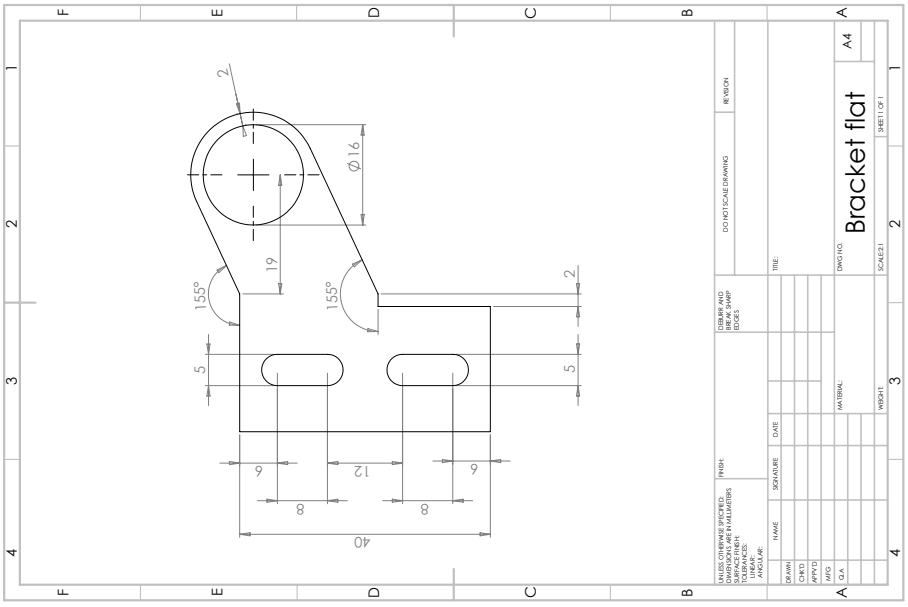

Figure B.2: Drawing of bracket for manufacture from plate. The angle was put in on the press brake.

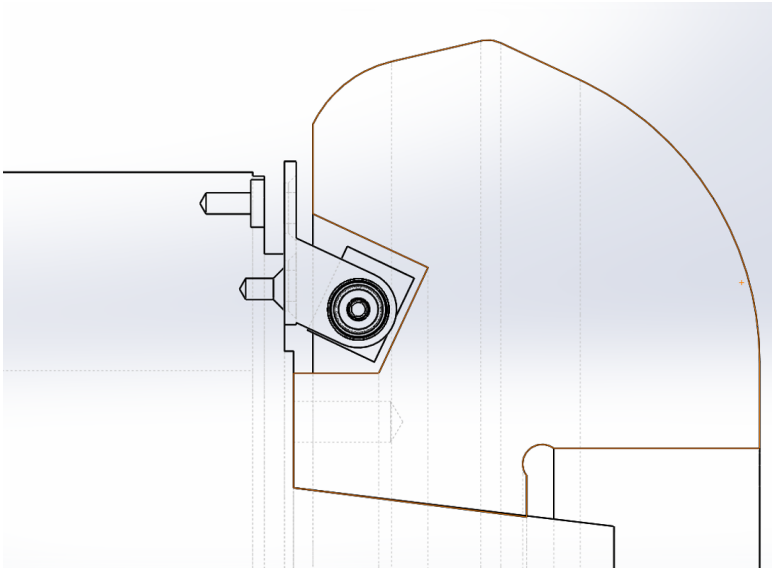

Figure B.3: Bracket in situ.

B.3 Flow forming preform

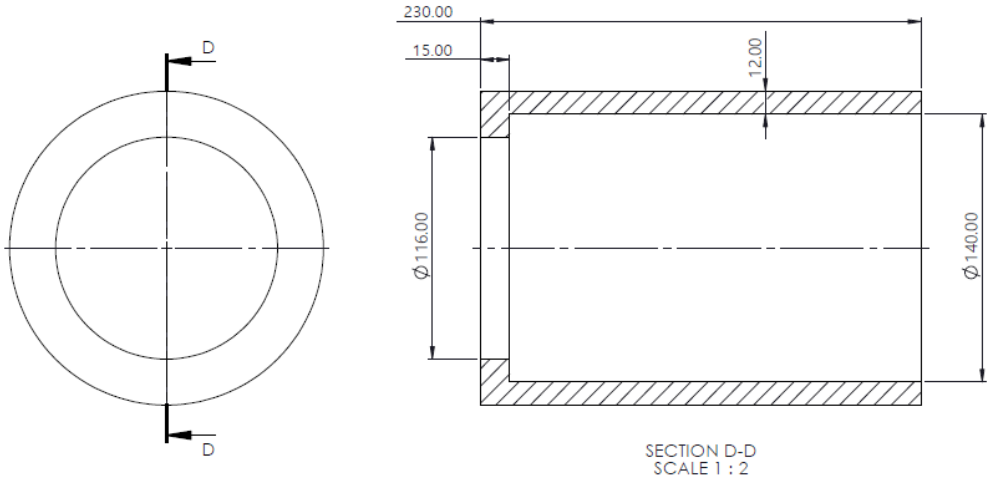

Figure B.4: 12 mm wall thickness preform geometry

B.4 Flow form part geometry

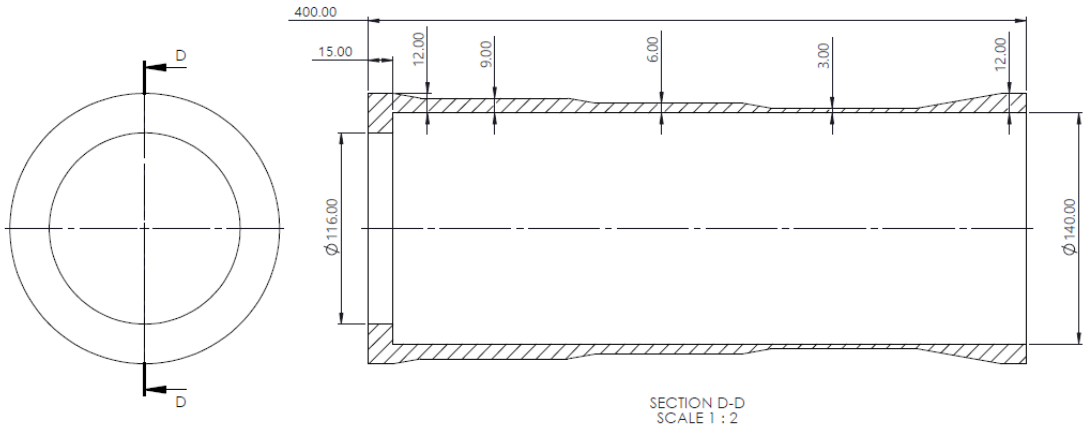

Figure B.5: 25-50-75 reduction of 12 mm preform

B.5 Flow form part geometry

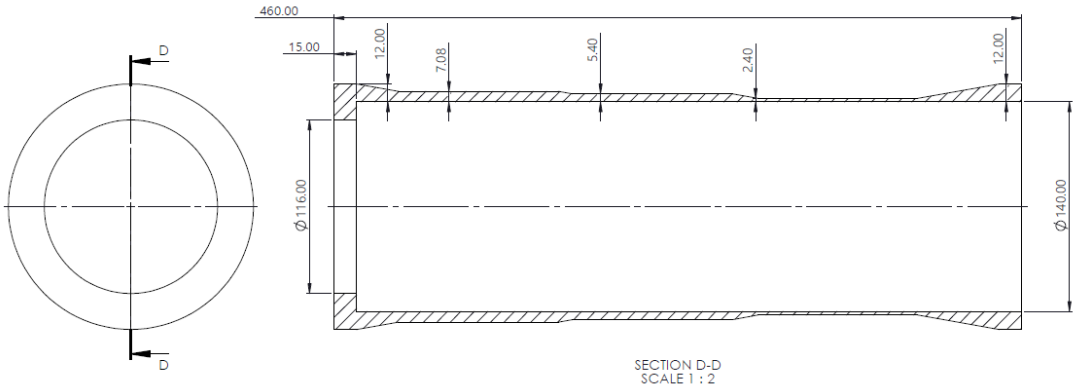

Figure B.6: 31-55-80 reduction of 12 mm preform

B.6 SSF preform

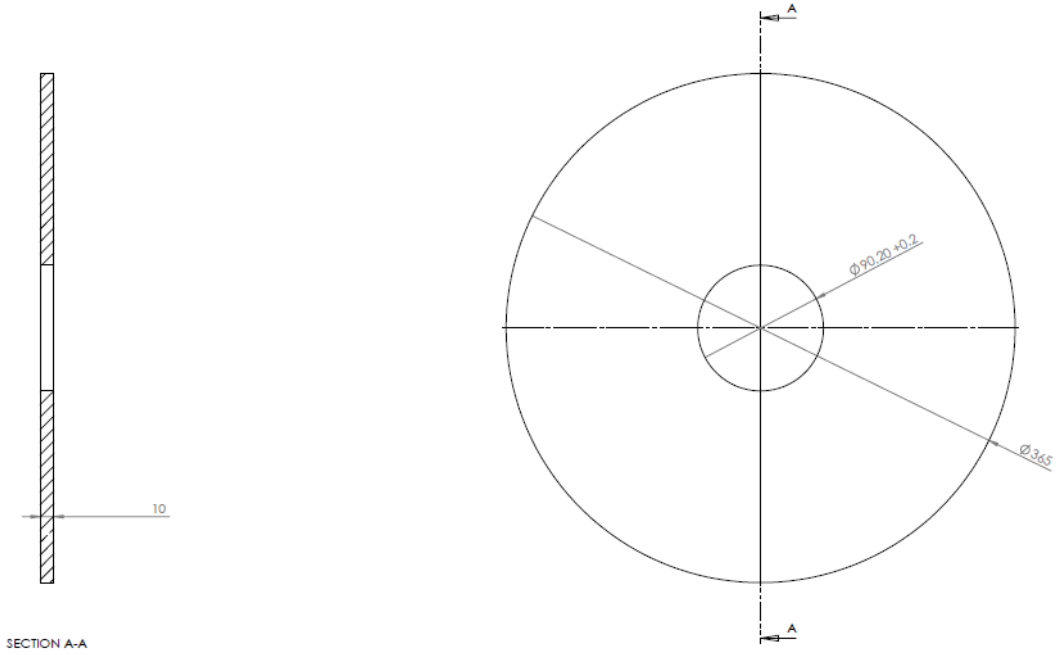

B.7 AISI D2 tool steel data

Industeel

ArcelorMittal

D2

D2: A cold work tool steel

D2 is a high chromium tool steel specifically designed to provide a high abrasive wear resistance and a high hardenability.
The grade is delivered in annealed condition to keep a good machinability. After machining it requires a hardening to achieve its service properties. The adjustment of hardness should be done to get the best compromise between touhness and wear resistance.

This grade can be used for cutting and deformation tools submitted to high abrasive wear. It can be used when 2% carbon steels (D3 type) shows an excessive sensivity to cracking or chipping.
Main applications are stamping tools, punches and dies, forming dies, shear blades and cutters, ceramic molds, ...

PROPERTIES

STANDARDS

> EURONORM	X153 CrMoV12
> Werkstoff Nb	W1.2379
> AISI	D2

CHEMICAL ANALYSIS -% WEIGHT

Typical values

C	S max	P max	Si	Mn	Cr	Mo	V
1.55	0.005	0.020	0.30	0.35	11.75	0.75	0.75

MECHANICAL PROPERTIES

D2 is delivered in annealed condition with hardness ≤ 250 HB

Hardness in annealed condition (HB)	Hardness in heat treated condition (HRC)	Young modulus (GPA)	Compression strength (MPA)	KV* J
250 max	56	205	2000	18
	60	205	2190	12

* unnotched specimen. Typical values.

PROPERTIES

PHYSICAL PROPERTIES

Thermal conductivity W m^{-1} K^{-1}	Thermal expansion coefficient 10^{-6} °C^{-1}/10^{-6} °K^{-1}			
20°C 68°F	20-100°C 68-212°F	20-200°C 68-392°F	20-300°C 68-572°F	20-400°C 68-752°F
18	11.7	11.96	12.2	12.7

Specific heat (J.kg^{-1} °C^{-1})	Density 20 °C
460	7.8

ABRASIVE WEAR RESISTANCE

D2 has a very good wear resistance based on high carbon and chromium contents.

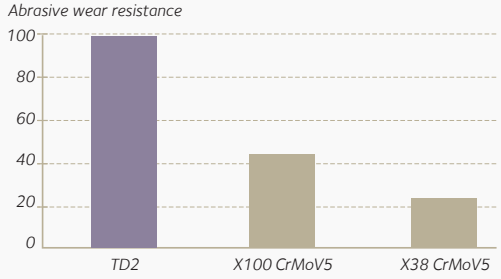

METALLURGIC PROPERTIES

D2 is delivered in annealed condition to make machining easier. Its structure is made of primary carbides inserted in a soft ferritic matrix in which there is also a distribution of secondary carbides of chromium and vanadium.

Metallurgical transformation points

AC_1		AC_3		Ms	
°C	°F	°C	°F	°C	°F
820	1508	860	1580	200	390

CCT Diagram

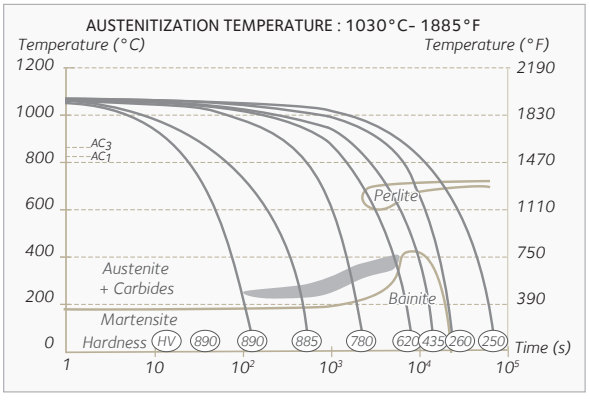

TTT Diagram

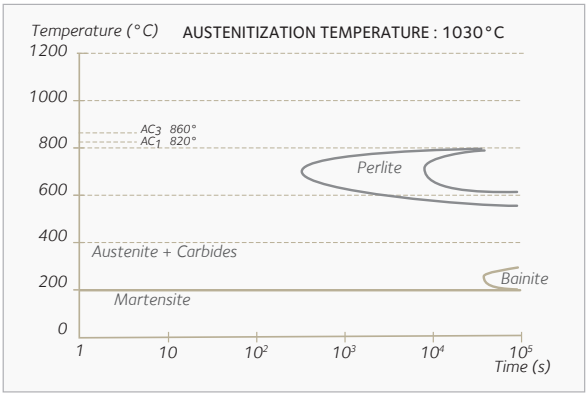

DELIVERY CONDITIONS

DIMENSIONAL PROGRAM

Thickness	Width
15 - 100 mm (.59" - 3.9")	1500 - 2000 mm (59" - 78.7")

For specific sizes, please consult

®Industeel Trademark - D2 - 10/2017

MACHINING

Milling with carbide tips

Cutting parameters	Roughing	Finishing
Cutting speed (Vc) m/min	100-130	120-150
Feed (Fz) - mm/tooth	0.15 - 0.4	0.1 - 0.23
Cutting depth (ap) / mm	2 - 5	≤ 2

Drilling with naked HSS drill

Cutting parameters	Ø ≤ 10	Ø 10-20
Cutting speed (Vc) m/min	10	10
Feed (Fz) - mm/rotation	0.08 - 0.3	0.3 - 0.4

HEAT TREATMENT

After machining, service properties of D2 should be restored by hardening. Generally, heat treatment consist in made of **a quenching operation and at least two temperings.** It is recommended to perform heat treatments in vacuum furnaces or under protective atmospheres to avoid decarburization or oxidation of surfaces.

Austenitization

> To minimize deformations and cracking risks, slow heating rates should be used with an homogenization at 750°C -1380°F (holding time ½ hour per 25 mm thickness). After homogenization, final heating shall be done also slowly.

> Austenitization temperature shall be high enough to ensure a complete dissolution of secondary carbides. On an other hand, a too high austenitization temperature will induce an important grain coarsening detrimental for toughness, it will also induce a high content of retained austenite. The best optimized temperature range is 1020 / 1050°C.

> Generally holding time at austenitization temperature shall be 1min/mm. The final holding time is left to the heat treating company, according to the size and shape of the piece, and according to furnace characteristics and to the constitution of the furnace load.

Quenching

> Quenching process shall be selected in order to:
1. Obtain the best microstructure (martensite),
2. Reduce cracking risks,
3. Ensure the smallest deformation possible.

> Cooling speed shall be sufficient to avoid formation of unacceptable components such as bainite or pearlite. Selection of quenching media shall take into account the size of the piece (see CCT diagram).

> On an other hand, a high cooling speed can cause strong distortions, because of important temperature gradients between mid-thickness and surface of the piece.

> High stress levels induced by fast cooling rates can also eventually generate cracking when pieces have complex shapes.

> When possible, cooling under over pressed gases (nitrogen) shall be preferred to more efficient media such as oil quenching. Oil quenching should be limited to high sections and simple shapes.

Tempering

> Service hardness will be obtained by the adjustment of tempering temperature (see softening curve below).

It is highly recommended to perform several successive tempering, at least two, to reduce as much as possible the quantity of retained austenite. Destabilization of retained austenite will be more efficient when tempering is done at high temperature (500°C-930°F and over). It is not advised to perform tempering at low temperature (200°C-392°F), which may induce a weakening of the tools.

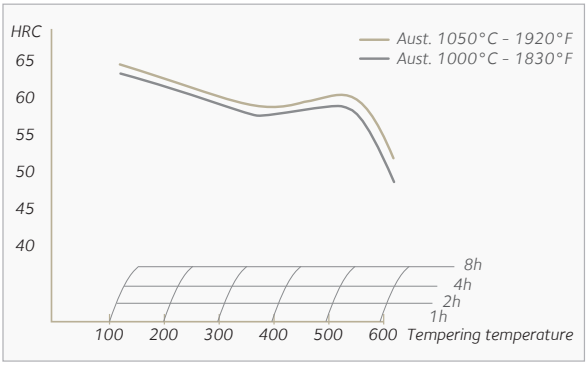

D2-Softening curve for a plate th 80 mm (3.1") oil quenched

Heat treatment chart

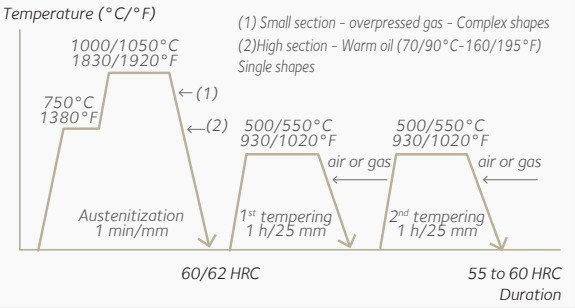

Vacuum furnaces or heat treatment under protective atmosphere

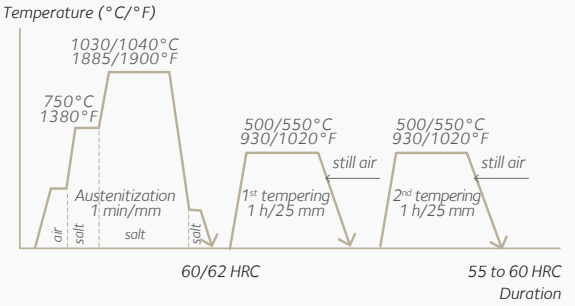

Salt bath heat treatment

Stress relieving

In case of complex shape or heavy machining, it may be necessary to perform a stress relieving before hardening to avoid distortion during heat treatment.
Stress relieving shall be conducted as follow:

> Heating 650/700°C (1200/1300°F) - vacuum furnace to avoid decarburization,

> Holding time ½ hour per 25 mm,

> Slow cooling in furnace.

Annealing

When necessary, it is possible to perform an annealing to soften (250 HB max) a piece which is already hardened.
Thermal cycle to apply is:

> Heating 860°C ±10°C (1580°F ±50°F),

> Holding ½ hour per 25 mm,

> Cooling 60°C/H max down to 780°C (1435°F),

> Cooling 20°C/H max within 780/700°C (1430/1290°F)

> Still air-cooling.

YOUR CONTACTS

Perrine Lavalley
Tel. +33 3 85 80 52 56
perrine.lavalley@arcelormittal.com

http://industeel.arcelormittal.com

Industeel France
Le Creusot Plant
56 rue Clemenceau
F-71202 Le Creusot Cedex

Technical data and information are to the best of our knowledge at the time of printing. However, they may be subject to some slight variations due to our ongoing research programme on steels.Therefore, we suggest that information be verified at time of enquiry or order.Furthermore, in service, real conditions are specific for each application. The data presented here are only for the purpose of description, and considered as guarantees when written formal approval has been delivered by our company.Further information may be obtained from the address opposite.

Appendix C

Data

The data for the trials is held in two datasets:

- https://doi.org/10.15129/e1236424-3131-471f-a13b-25980424ca8d
- https://doi.org/10.15129/dcf1b66c-0b1d-4cca-867f-cb90e30d5560

Appendix D

Experimental information

D.1 Accelerometer positioning

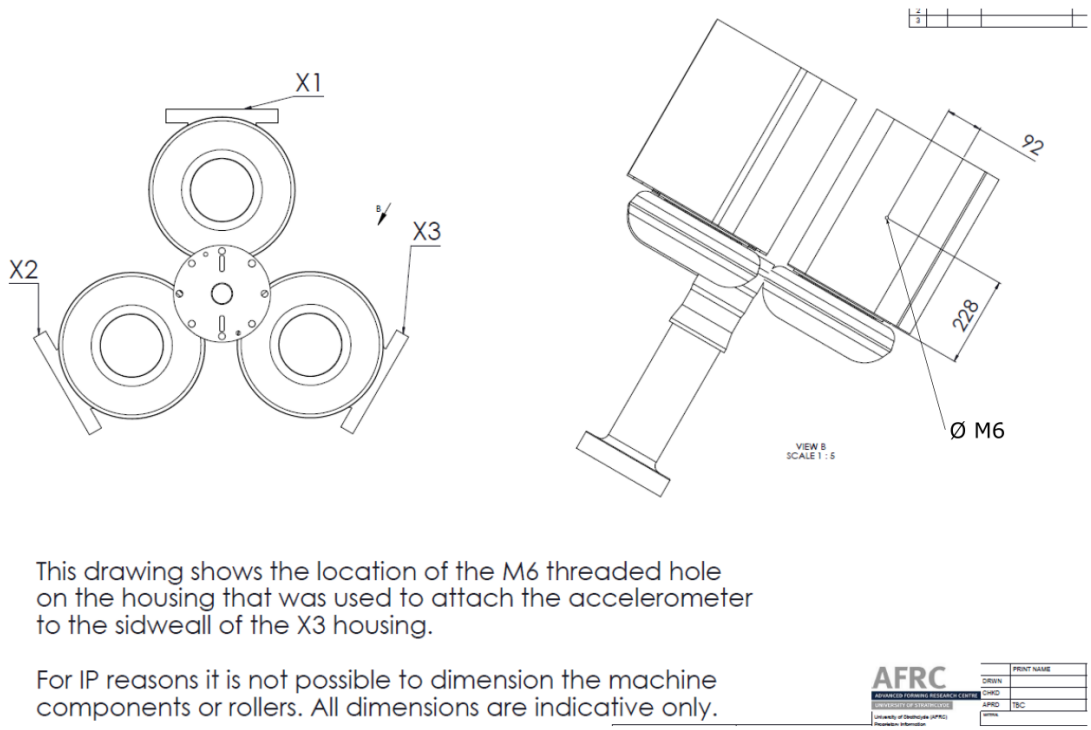

Figure D.1: Vibration monitoring equipment positional schematic.

D.2 Microphone positioning

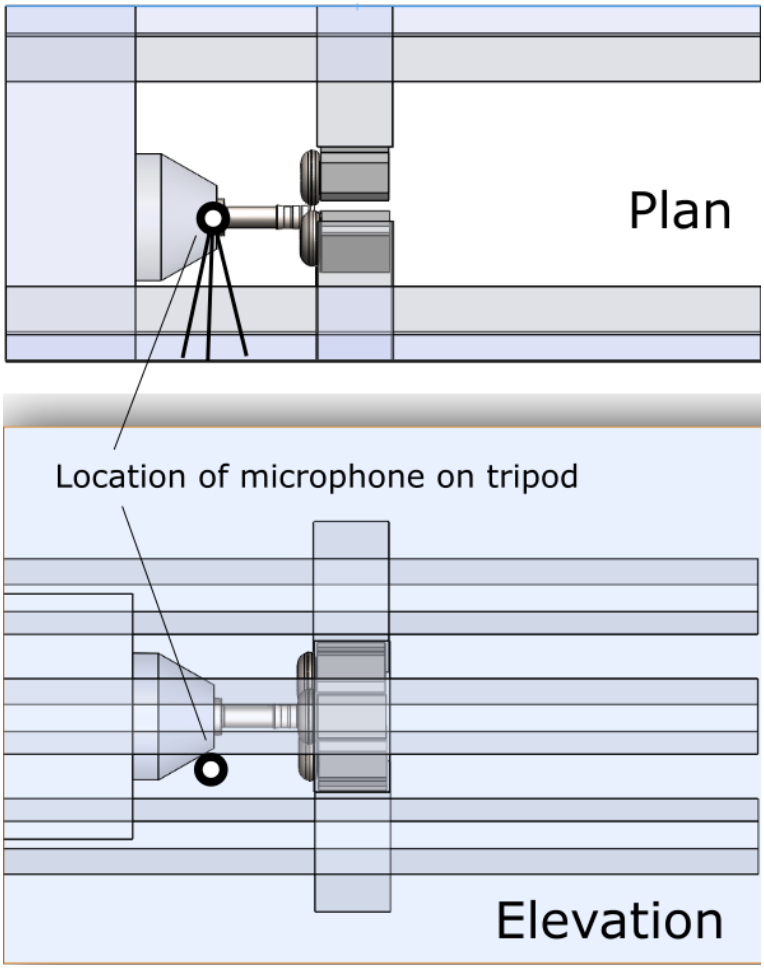

Figure D.2: Acoustic monitoring equipment positional schematic.

D.3 Plan of experiments for operational parameter testing

Table D.1: Parameter values for testing

Trial	Voltage	Filter	Pulsewidth
1	L	4	L
2	L	4	M
3	L	4	H
4	H	4	L
5	H	4	M
6	H	4	H
7	L	5	L
8	L	5	M
9	L	5	H
10	H	5	L
11	H	5	M
12	H	5	H
13	L	6	L
14	L	6	M
15	L	6	H
16	H	6	L
17	H	6	M
18	H	6	H

D.4 Interaction plot of parameter experiments

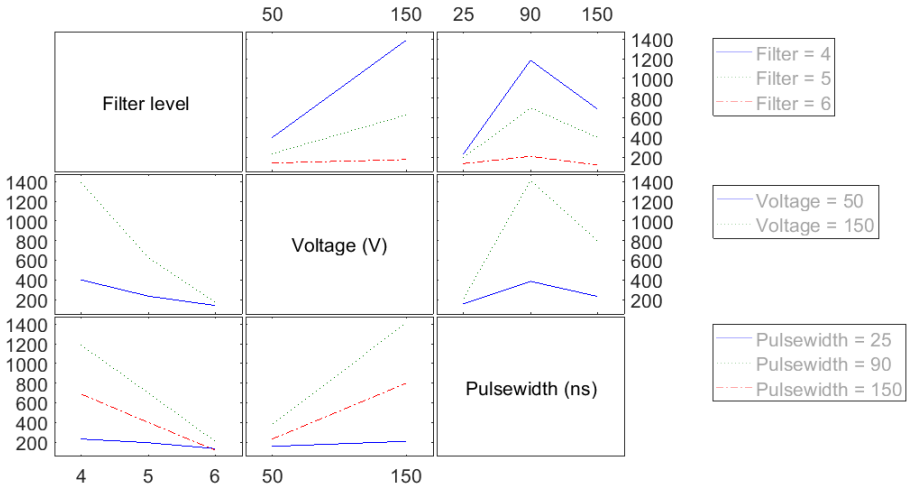

Figure D.3: Interaction plot of parameter experiments

D.5 Plan of experiments for force response testing

Table D.2: DOE for testing force response

Trial	Thickness	Order	Feed Rate
1	L	0	L
2	H	0	L
3	L	0	L
4	H	0	L
5	L	0	H
6	H	0	H
7	L	0	H
8	H	0	H
9	L	1	L
10	H	1	L
11	L	1	L
12	H	1	L
13	L	1	H
14	H	1	H
15	L	1	H
16	H	1	H

Appendix E

MATLAB code

E.1 Master Reader File

This is the general implementation file for handling the data.

```
%% ============================ %%
%% MASTER DATA MANAGEMENT FILE %%
%% ============================ %%
clc; clearvars -except dat
 tic
counter = 0;
%% Select trial

series   = 'H';     % Series letter
for trial    = 6;       % Trial number

if series == 'G';
    SinXnum  = 3;        % Roller number of interest
elseif series == 'D';
    SinXnum  = 3;        % Roller number of interest
elseif series == 'H';
```

```
    SinXnum  = 1;       % Roller number of interest
elseif series == 'I';
    SinXnum  = 1;       % Roller number of interest
elseif series == 'F';
    SinXnum  = 0;       % Roller number of interest
elseif series == 'EP';
    SinXnum  = 0;       % Roller number of interest
elseif series == 'EN';
    SinXnum  = 0;       % Roller number of interest

else
    disp('No roller number data')
end

if counter ~= 0
    clearvars loc
end


%% Switches
LOADDAT =   1;
TDMStoMAT = 0; % Convert
MATtoDAT =  0; % Process and import .mat data
PEAKFIND =  0;
PLAYBACK =  1; % Option to playback and graph US record
SETOFFSET = 0;
SAVEDAT =   0;

strial = num2str(trial);
    if trial<10
```

```
        strial = strcat('0',num2str(trial));
    end
Xdat = (strcat(series,'-',strial)); disp(Xdat)

loc = strcat('H:\My Documents\03 Trials Documentation\01
   All dat files\',Xdat,'.mat');

%% Load dat file
if LOADDAT ==1
    disp('Loading dat file')
    load(loc)
end

%% TDMS to MATLAB .dat
if TDMStoMAT == 1
    disp('Converting .TDMS to .MAT ...')
    fn = strcat('H:\My Documents\03 Trials Documentation\',
       series,' Series\',Xdat,'.tdms');
    simpleConvertTDMS(1, fn);
    disp('TDMStoMAT done')
end
%% Import US data
if MATtoDAT == 1;
    disp('Formatting to dat ...')
    singledouble = 2;
    dat = fnMAT2DAT(series, trial, SinXnum, singledouble);
    disp('MATtoDAT done')
end

%% Process and import US data
```

```
if PEAKFIND == 1
    disp('Finding peak values ...')
    playspeed = 1; % display 1 of every n frames. POSITIVE
       INTEGER VALUE
    downsample = 1;
    UrecT = dat{18,2};
    dat = fnPEAKFINDER(dat, playspeed, UrecT);
    disp('Peak values found')
end

%% playback of US file
if PLAYBACK == 1
    disp('Displaying ...')
    win = [dat{4,2} dat{4,2}+dat{5,2}];
    win = [18 26]; % Window to look at in microseconds
    perint = [60  dat{18,2}]; % Period of time in seconds
       from recording start INTEGER ONLY
    playspeed = 10; % display 1 of every n frames. POSITIVE
        INTEGER VALUE
%     downsample = 100;

    info = dat(:,:); % cell of information
    data = dat{2,2}; % matrix of recorded values
    winind = [((win(1) - info{4,2})*100)+1 ((win(2) - info
       {4,2})*100)-1];
    range = 100*info{5,2}; % number of data points in each
       pulse snapshot
    pct = length(dat)/range; % Count of total number of
       pulses
    srt = info{9,2}; % snapshot sampling rate in Hz
```

```
    time = floor(pct/srt); % time of whole recordingload
       PN1t
    Soff = floor(info{17,2}/.3); % Sinucom offset
    tdat = linspace(win(1),win(2),winind(2)-winind(1)+1);

%     peaktN1 = dat{19,2};
%     peakmN1 = dat{20,2};
%
%     peaktB1 = dat{23,2};
%     peakmB1 = dat{24,2};
%
%     peaktN2 = dat{21,2};
%     peakmN2 = dat{22,2};
%
%     peaktB2 = dat{25,2};
%     peakmB2 = dat{26,2};

    for i = (perint(1))*info{9,2}+1:playspeed:perint(2)*
       info{9,2}
        datc = data(range*i - range + 1 : range*i); % full
           snapshot
        datc = datc(winind(1) : winind(2)); % windowed
           snapshot around time of interest (win)
        plot(tdat,datc,'r')
        title([Xdat ';  Time = ' num2str(i/info{9,2}) ' s'
           ])
        axis([win(1) win(2) -100 800])
        xlabel('Time delay (microseconds)','FontSize',20)
        ylabel('Magnitude (AU)','FontSize',20)
        hold on
```

```
%          plot(peaktN2(i),peakmN2(i)-  mean(datc),'ko')%
   Plot peaks found
%          plot(peaktB2(i),peakmB2(i)-  mean(datc),'kx')%
   Plot peaks found

         if 1==0
             rulht1 = 300;
             rulht = 490;
             for ruler = 54:2:88
%                  th = cos((15/180)*pi)*2000*ruler/5900; %
   Mult. by cosine of angle of sensor to mandrel axis
%                  text(th,rulht1,[' ' num2str(ruler)])
%                  plot([th th],[rulht1 rulht1-100],'b')
                 th = 2000*ruler/5900; %
                 text(th,rulht,[' ' num2str(ruler)])
                 plot([th th],[rulht rulht-50],'k')

             end

             text(win(2)-2,rulht - 100,['Estimated distance
                \newline from sensor (mm) '])
         end

         hold off
         pause
     end
end


%% Add offsets
```

```
if SETOFFSET ==1
    if series == 'G';
        Tstart = [1 2 3; 40 8 12];
        Hoffs = [1 2 3; 8.5 31.7 16];
        dat{17,2} = [Hoffs(2,find(Hoffs(1,:)==trial))
           Tstart(2,find(Tstart(1,:)==trial))];
    elseif series == 'H';
        Hoffs = [1 2 3 4 5 6 7 10; 72 18 5 15 8 101 74 83];
        dat{17,2} = Hoffs(2,find(Hoffs(1,:)==trial));
    elseif series == 'F';
        Tstart = [1 2 3 4 5 6 7 8 9; 0 0 0 0 0 0 0 0 0 ];
        Hoffs = [1 2 3 4 5 6 7 8 9; 0 0 0 0 0 0 0 0 0 ];
        dat{17,2} = Hoffs(2,find(Hoffs(1,:)==trial));
    elseif series == 'I';
        Tstart = [1 2 3 4 5 6 7 8 9 10 11 12 13 14 15 16
           17;...
                7 3 12.5 6 0 0 0 0 2 7 6 5 0 0 0 0 0];
        Hoffs = [1 2 3 4 5 6 7 8 9 10 11 12 13 14 15 16 17;
           ...
                216 198 151 193 191 0 197 184 198 199 198
                   196 237 203 206 207 0];
        dat{17,2} = [Hoffs(2,find(Hoffs(1,:)==trial))
           Tstart(2,find(Tstart(1,:)==trial))];
    else
        disp('No offset data')
    end
end


%% Strip out full data and save dat to Xdat
```

```
if SAVEDAT == 1
    disp('Saving dat file ...')
    save(loc,'dat', '-v7.3')
    disp('Dat file saved')
end
disp('Master reader execution finished')
counter = counter+1
toc
end
```

E.2 Sinucom Plotter

This implementation code is for presenting the data in graphs after processing.

```
clc; clearvars -except dat; close all
loopcount = 0;
% figure
series = 'H';
for trial = 6%
loopcount = loopcount+1;
strial = num2str(trial);
if trial<10
    strial = strcat('0',num2str(trial));
end
Xdat = (strcat(series,'-',strial));
loc = strcat('H:\My Documents\03 Trials Documentation\01
   All dat files\',Xdat,'.mat');
load(loc)

% dat(27,1:2) = {'B1-N1 time' dat{23,2}-dat{19,2}}; Done in
    peakfinder
```

```
% dat(28,1:2) = {'SXF/1NRM' dat{25,2}-dat{21,2}};

varswitch = [... % switch these on to plot specific
   variables
    0 ...       % Sinucom X Posit.
    0 ...       % Sinucom Z Posit.
    0 ...       % Sinucom X Force
    0 ...       % Sinucom Z Load
    0 ...       % US 1st nose reflection  timestamp
    1 ...       % US 1st nose reflection  magnitude
    0 ...       % US 2nd nose reflection  timestamp
    0 ...       % US 2nd nose reflection  magnitude
    1 ...       % US 1st back reflection  timestamp
    0 ...       % US 1st back reflection  magnitude
    0 ...       % US 2nd back reflection  timestamp
    0 ...        % US 2nd back reflection  magnitude
    0 ...       % B1-N1 Time
    ];

varlocs = [13 14 15 16 19 20 21 22 23 24 25 26 27 ];
Stime = dat{11,2}; % Sinucom time
Utime = linspace(1,dat{18,2},dat{18,2}*dat{9,2});
if isnumeric(dat{17,2})
    offs = dat{17,2};
    offset = offs(1);% offset in seconds
    start = 0;%offs(2);
else
    offset = 0;
    disp('Offset undefined')
end
```

```
ds = 100; % Downsampling rate


%% Pick Vars
vars = varswitch.*varlocs; vars(vars==0) = [];

%% Implement time offset
Utime = Utime - start;% + offset;
Utimeds = decimate(Utime,ds);
Stime = Stime - offset -start;


%% Select variables to plot
figure
% subplot(2,1,loopcount)
% subplot(4,4,loopcount)
hold on
legs = cell(length(vars),1);
for i = 1:length(vars)
    var = vars(i);
        plotvar = dat{var,2};
    if var < 19
        yyaxis left
        plotvar = interp1(Stime, plotvar, Utimeds)';
        plot(Utimeds, plotvar,'LineWidth',2);
        varSC = plotvar;
        ylim([-20 160])
    else
        yyaxis right
```

```
        plot(Utimeds, decimate(plotvar,ds),'-.','LineWidth'
            ,2)
        varUS = decimate(plotvar,ds);
        ylim([0 1400])

    end
    legs{i} = dat{var,1};
end
% legend(legs,'Location','SouthWest')
tit = strcat('Trial: ',dat{1,2});
title(tit)
xlabel('Time (s)')
ylabel('US nose reflection magnitude')
yyaxis left
ylabel('Force on X axis (kN)')
xlim([0 (max(Utime)+10)])
% xlim([0 35])


% %%%%%%%%%%%%%%%%%%%%%%%%%%%%%%%%%%%%%%%%%%%%%%%%%%%%%%%%
% % Find correlations
% %%%%%%%%%%%%%%%%%%%%%%%%%%%%%%%%%%%%%%%%%%%%%%%%%%%%%%%%
% corvars = [Utimeds; varUS'; varSC'];
% timeset = [6 35];
% ind1 = max(find(Utimeds<timeset(1)));
% ind2 = max(find(Utimeds<timeset(2)));
% corrtest = corvars(:,ind1:ind2);
% R = corrcoef(corrtest(2,:),corrtest(3,:)); R(2); %
   correlation
% %text(0,0,['CorrCoef (t=5:t=30) = ' num2str(R(2))])
```

```
% % figure
% % subplot(2,1,2)
% % % subplot(4,4,loopcount+8)
% % plot(varSC(ind1:ind2),varUS(ind1:ind2),'.')
% % title(tit)
% % xlabel(['CorrCoef (t=' num2str(timeset(1)) ':t='
   num2str(timeset(2)) ') = ' num2str(R(2))])
% % timeset(1)


% UT = decimate(dat{20,2},ds); %
% SF = dat{15,2}; % Sinucom force
% SFst = find(Stime > 0);
% SF = SF(SFst); Stimet = Stime(SFst);% trim to length
% SFi = interp1(Stimet,SF,Utimeds); %
% R = corrcoef(UT,SFi); R(2) % correlation



% % %% Calculate cross-correlation

%
% %% Curve fitting
% UTf = -.01*UT+15;
% figure
% plot(Utimeds, UTf, Stimet, SFst)
% tit = strcat('Trial ',Xdat,': UT data fitted to Sinucom
   Force recording');
% title(tit)
% xlabel('Time (s) into IRF process')
```

```
% ylabel('Magnitude')



%


%
%
% SC = timeseries(varSCi,Utime);
% US = timeseries(varUS,Utime);
% x1=squeeze(SC.data);
% y1=squeeze(US.data);
% plot(x1,y1,'*')

end
```

E.3 fnPEAKFINDER

A function for extracting peak values.

```
function dat = fnPEAKFINDER(dat, playspeed, UrecT)
%% Checks
% strial = num2str(trial);
% if trial<10
%     strial = strcat('0',num2str(trial));
% end

%% Select windowing
wins = [19 21; 38 41; 22 29; 43 45]; % Window to look at in
    microseconds
```

```
% % loc = strcat('H:\My Documents\80 MATLAB\
   Master_Reader_and_Functions\',Xdat);
% % load(loc)

for  i = 1:4
    win = wins(i,:);
    %
       ================================================================

    %% Establish the...
    %
       ================================================================

    perint = [0 UrecT]; % Period of time in seconds from
       recording start INTEGER ONLY
    data = dat{2,2}; % matrix of recorded values
    winind = [((win(1) - dat{4,2})*100)+1 ((win(2) - dat
       {4,2})*100)-1];
    range = 100*dat{5,2}; % number of data points in each
       pulse snapshot
    pct = length(dat{2,2})/range; % Count of total number
       of pulses
    srt = dat{9,2}; % snapshot sampling rate in Hz
    time = floor(pct/srt); % time of whole recording
    Soff = floor(dat{17,2}/.3); % Sinucom offset
    tdat = linspace(win(1),win(2),winind(2)-winind(1)+1);

disp(strcat('Searching window from ',num2str(win(1)),' to '
   ,num2str(win(2)),'microseconds'))
```

```
%
%% CHECKS
if win(1) < dat{4,2}
    disp('Error: Delay range starts before captured
       window')
    return
end
if win(2) > (dat{4,2}+dat{5,2})
    disp('Error: Delay range ends after captured window
       ')
    return
end
if perint(2) > time
    disp('Error: Time period extends beyond recording
       length')
    return
end

%% Find magnitude of peak
for j = (perint(1))*dat{9,2}+1:playspeed:perint(2)*dat
   {9,2}
    datc = data(range*j - range + 1 : range*j); % full
       snapshot
    datc = datc(winind(1) : winind(2)); % windowed
       snapshot around time of interest (win)
    [peak peakloc] = max(datc + mean(datc));
    %          plot(tdat,datc)
    %          hold on
    %          plot(tdat(find(datc==max(datc))),peak -
       mean(datc),'ko')
```

```
        %           hold off
        %           pause
        pr(j,1:2) = [tdat(peakloc) peak]; % peak reflection
    end


    %% Save peaks
    if i == 1
        dat(19,1:2) = {'Peak Nose 1: timestamp (us)' pr
            (:,1)};
        dat(20,1:2) = {'Peak Nose 1: magnitude' pr(:,2)};
    elseif i==2
        % % second peak
        dat(21,1:2) = {'Peak Nose 2: timestamp (us)' pr
            (:,1)};
        dat(22,1:2) = {'Peak Nose 2: magnitude' pr(:,2)};
    elseif i==3
        dat(23,1:2) = {'Peak Back 1: timestamp (us)' pr
            (:,1)};
        dat(24,1:2) = {'Peak Back 1: magnitude' pr(:,2)};
    elseif i==4
        dat(25,1:2) = {'Peak Back 2: timestamp (us)' pr
            (:,1)};
        dat(26,1:2) = {'Peak Back 2: magnitude' pr(:,2)};
    end
end

dat(27,1:2) = {'B1-N1 time' dat{23,2}-dat{19,2}};

% save dat datfull '-v7.3'
```

E.4 fnMAT2DAT

A function for converting the data format.

```
function dat = fnMAT2DAT(series, trial, SinXnum,
   singledouble)
%% Checks
if ~ischar(series)
    error('"Series" must be a character')
end
if ~isnumeric(trial)
    error('"trial" must be a number')
end

strial = num2str(trial);
    if trial<10
        strial = strcat('0',num2str(trial));
    end
Xdat = (strcat(series,'-',strial));


dat = cell(22,2);% datcell is an x by 2 by 18 cell of the
   data from the trial series
st = num2str(trial);
if trial<10
    st = strcat('0',st); %st{1} = strcat('0',st{1});
end

filename = strcat('H:\My Documents\03 Trials Documentation\
   ',series,' Series\',Xdat,'.mat');%{1},'-',st{2},'.mat');
```

```
%% Unpick data from TDMS import
dat1 = load(filename);
dat2 = struct2cell(dat1); % A 3x1 cell array:  [1x1 struct
   ]; '1.99'; {1x1 cell}
dat3a = struct2cell(dat2{3});% Struct from dat2, containing
    dat4
dat4e = dat3a(5); dat4e = struct2cell(dat4e{1}); % A cell
   array containing dat5
dat5a = dat4e{2}; %1x8 struct array with fields:    Name
      Data    Total_Samples    Property
dat6 = struct2cell(dat5a); % 4x1x8 cell array
dat7a = dat6(:,:,1); % Containing struct with fields:  Name
   : 'Root'  Value: {'e01p02'}
dat7c = dat6(:,:,3); % DATA + INFO
dat8a = dat7c(1); %data name
dat8b = dat7c(2); dat8b = dat8b{1}; datx = dat8b; % DATA
dat8c = dat7c(3); % Data file length
dat8d = struct2cell(dat7c{4}); % File info
% name = dat6(:,:,1);    name = name{4};    name = char(
   getfield(name, 'Value'));
name = {'Filename' Xdat };
%% Cell approach
dat(1,:) = name;
data = dat7c(1:2)';
dat(2,:) = data;

for j = 1:8
    %     info = dat8d(:,:,j)'
%     dat(j+2,:,pass) = dat8d(:,:,j)';
dat(j+2,:,1) = dat8d(:,:,j)';
```

```
end

range = 100*dat{5,2}; % number of data points in each pulse
    snapshot
pct = length(dat{2,2})/range; % Count of total number of
   pulses
srt = dat{9,2}; % snapshot sampling rate in Hz
time = floor(pct/srt); % time of whole recording
dat(18,1:2) = {'Total US recording time' time};

%% Struct approach
% fieldnames = name;
% fieldvals = data;
% names = {'fred' 'sam' 'al'};
% for index = 1 : length(fieldnames)
%     struc.(fieldnames{index}) = index;  % Assign index to
    s.fred, s.sam, and s.al
% end
%% Add sinucom data to datcell
if SinXnum ~= 0
    sinfilename = strcat('H:\My Documents\03 Trials
       Documentation\',series,' Series\',Xdat,'.csv'); %
       sinfilename = strcat(['H:\My Documents\03 Trials
       Documentation\' series ' Series\' series '-' num2str
       (trial) '-1.csv']);
    SinDat = csvread(sinfilename,16,0);
    dat(11,1:2) = {'Sinucom Time' SinDat(:,1)}; % Time
       starts at (r,c): 17 1
    dat(12,1:2) = {'Sinucom Spindle speed (RPM) [Sinucom]'
       SinDat(:,6)}; % Spindle starts at (r,c): 17 6
```

```
dat(17,1:2) = {'Sinucom to UT offset (s) and SN to
   start (s)' 'ADD ME LATER'}; % Sinucom starts n
   seconds earlier than UT. Found from (Sin delay to
   200rpm - UT delay to noisiness)
if SinXnum == 3
    dat(13,1:2) = {'X3 Position [Sinucom]' SinDat(:,2)
       }; % x3 position starts at (r,c): 17 2
    dat(14,1:2) = {'Z3 Position [Sinucom]' SinDat(:,5)
       }; % z3 position starts at (r,c): 17 5
    dat(15,1:2) = {'X3 Force [Sinucom]' SinDat(:,3)}; %
        x3 force starts at (r,c): 17 3
    dat(16,1:2) = {'Z3 Load [Sinucom]' SinDat(:,4)}; %
       z3 force starts at (r,c): 17 4
elseif SinXnum == 2
    dat(13,1:2) = {'X2 Position [Sinucom]' SinDat(:,11)
       }; % x2 position starts at (r,c): 17
    dat(14,1:2) = {'Z2 Position [Sinucom]' SinDat(:,12)
       }; % z2 position starts at (r,c): 17
    dat(15,1:2) = {'X2 Force [Sinucom]'    SinDat(:,9)
       }; % x2 force starts at (r,c): 17
    dat(16,1:2) = {'Z2 Load [Sinucom]'    SinDat(:,7)};
        % z2 force starts at (r,c): 17
elseif SinXnum == 1
    dat(13,1:2) = {'X1 Position [Sinucom]' SinDat(:,13)
       }; % x2 position starts at (r,c): 17
    dat(14,1:2) = {'Z1 Position [Sinucom]' SinDat(:,14)
       }; % z2 position starts at (r,c): 17
    dat(15,1:2) = {'X1 Force [Sinucom]'    SinDat(:,10)
       }; % x2 force starts at (r,c): 17
```

```
        dat(16,1:2) = {'Z1 Load [Sinucom]'     SinDat(:,8)};
            % z2 force starts at (r,c): 17


    end
else
    disp('No Sinucom data')
end
if singledouble == 1
    disp('Single precision output')
    dat{2,2} = single(dat{2,2});
elseif singledouble ==2
    disp('Double precision output')
else
    disp('Select 1 (single precision) or 2 (double)')
end

%     dat = dat;
    clearvars -except dat
    % save dat '-v7.3'
```